Plk1 regulates PICH, a centromere-associated SNF2 family translocase that is required for the spindle checkpoint

Dissertation
zur Erlangung des Doktorgrades der Naturwissenschaften
(Dr. rer. nat.)
der Fakultät für Biologie der Ludwig-Maximilian Universität München

Vorgelegt von

Christoph Baumann

München 09.02.2007

Datum der mündlichen Prüfung: 30.03.2007

Erstgutachter: Prof. Dr. Erich A. Nigg

Zweitgutachter: Prof. Dr. Peter B. Becker

Ehrenwörtliche Erklärung und Erklärung über frühere Promotionsversuche

Hiermit erkläre ich, dass ich, Christoph Baumann, die vorliegende Dissertation selbständig und ohne unerlaubte Hilfe angefertigt habe. Sämtliche Experimente sind von mir selbst durchgeführt, ausser wenn explizit auf Dritte verwiesen wird. Ich habe weder anderweitig versucht, eine Dissertation einzureichen oder eine Doktorprüfung durchzuführen, noch habe ich diese Dissertation oder Teile derselben einer anderen Prüfungskommission vorgelegt.

München, den 06. Februar 2007

Table of contents

Acknowledgements

I would like to thank Prof. Erich Nigg for the possibility to work in his lab on that wonderful subject and for all his support.

I am thankful to Prof. Peter Becker for reviewing this manuscript.

I am grateful to Prof. Matthias Wabl for his continuous support, for being a mentor and friend over the recent years.

I would like to thank Francis Barr, Thomas Mayer, Herman Sillje and Olaf Stemmann for their support and many helpful discussions. Thanks to Susan Gasser, Ulrike Grüneberg, Anja Hanisch, Kay Hofmann, Karl-Peter Hopfner, Andrea Musacchio, Rüdiger Neef and Frank Uhlmann for discussion and/or reagents.

Thanks to my colleagues and friends: Sabine Elowe, Tom and Louise Gaitanos, Stefan Hümmer (thanks man!), Mikael LeClech, Anna Santamaria, Andreas Schmidt and Volker Stucke for support, reagents, discussions and a good time. I am happy that Lily Wang and Manuel Kaulich (the new “PICH folks”) are following up on my project.

Having mentioned the perfect organization of the lab I want to highlight that the permanent warm atmosphere and perfect setup of the lab is largely achieved by Alicja Baskaja, Alison Dalfovo, Elena Nigg, Lidia Pinto, Albert Ries, Marianne Siebert and Klaus Weber. Thank you!

Thanks to Roman Körner not only for excellent MS-data but also for all the Caipirinha.

Thank you Ulla (Ulf Klein) for your friendship and the countless discussions!

Big thanks to my “non-lab friends” Michael Tillich, Lilli Neumann, Ingvar Ferby, Tim Holmström, Thomas Wechsler and Arno Alpi.

I am very grateful to my beautiful wife Marina for sharing her life with me.

My deepest gratitude goes to my parents, Heidi and Leo Baumann and to my brother Gilbert for all their support, for believing in me and for their patience over so many years.

Zusammenfassung

Um die Rolle Kinetochor-assoziierter Proteine in der humanen Zellteilung zu studieren, haben wir die Funktion einer strukturellen Kernkomponente des Kinetochores analysiert, den Ndc80 Komplex. In diesem Komplex interagieren die Proteine Hec1 und Nuf2 über ihre N-termini und Hec1 interagiert darüberhinaus über Spc25 mit dem Spc24/Spc25 Unterkomplex. Der Proteinkomplex ist essentiell für die Chromosomensegregation und für das Rekrutieren mehrerer Proteine, darunter die mitotische Kinase Plk1.

In Immunopräzipitationsexperimenten mit Plk1 Antikörpern konnte eine Kinetochor / Zentromer-assoziierte DNA-Translokase (PICH) als direkter Interaktor von Plk1 identifiziert werden. Die subzelluläre Lokalisierung von PICH an Kinetochoren und Zentromeren wird durch Plk1 reguliert. Plk1 inhibiert die Chromatin-Assoziation von PICH durch Phosphorylierung. PICH assoziiert mit auffallenden Fäden, die bis in die Anaphase bestehen und von Topoisomerase II aufgelöst werden. Darüberhinaus ist PICH eine neue, essentielle Komponente des Spindelkontrollpunktes (spindle assembly checkpoint), und das PICH Kontroll-Signal wird wahrscheinlich über Regulierung der Kinetochor-Lokalisierung des Kontrollpunkt-Proteins Mad2 weitergeleitet.

Diese Arbeit stellt Fragen über das Verhalten zentromerischer DNA bei der Teilung von Schwesterchromatiden in der Mitose und den zeitlichen Ablauf von Dekatenation von Schwesterchromatiden. Wir vermuten, daß diese ATPase angehend in Prometaphase mit katenierter, zentromerischer DNA assoziiert, wo sie möglicherweise benötigt wird um die Spannung zwischen Schwesterkinetochoren zu messen.

Summary

To investigate the requirements of mitotic, kinetochore-associated proteins for human chromosome segregation we analyzed the human Ndc80 complex, a core structural component of the outer kinetochore. The Ndc80 complex contains Hec1 and Nuf2 that interact via their N-termini and a smaller subcomplex of Spc24 and Spc25 is linked to Hec1. The complex is required for faithful chromosome congression and the recruitment of several proteins of the outer kinetochore, including the mitotic regulatory kinase Plk1.

Pull down experiments with Plk1 identified a novel kinetochore/centromere associated DNA translocase, which we termed PICH, as an interactor of Plk1. The localization of PICH to kinetochores and centromeres is controlled by Plk1; and moreover, Plk1 phosphorylation on PICH negatively regulates its localization / chromatin association. PICH associates with conspicuous threads that persist into anaphase where Topoisomerase II causes their resolution. Moreover, PICH is a novel component of the spindle assembly checkpoint and PICH-dependent checkpoint signaling is likely to be mediated via kinetochore associated Mad2. This study raises questions as to the fate of centromeric DNA in sister chromatid separation and its timing of decatenation. We speculate that this enzyme associates with catenated, centromeric DNA from prometaphase where it may be required to sense the tension between sister kinetochores.

Introduction

Cell division

In 1885 Rudolf Virchow published the doctrine “omnis cellula ex cellula”: every cell originates from another cell. This turned out to be a basic principle of cell biology and hence the mechanism how cells duplicate is still one of the key questions of modern biology.

The purpose of cell division is to produce two genetically identical daughter cells. Therefore, the DNA of eukaryotes has to be faithfully replicated, and the genetic material must then be accurately distributed into the two daughter cells so that each cell receives an identical copy of the parental genome. Walther Flemming was the first cytologist to describe in detail how chromosomes move during mitosis, or cell division (Figure 1). He observed cell division in salamander embryos where cells divide at fixed intervals and developed a method to stain chromosomes to observe this process.

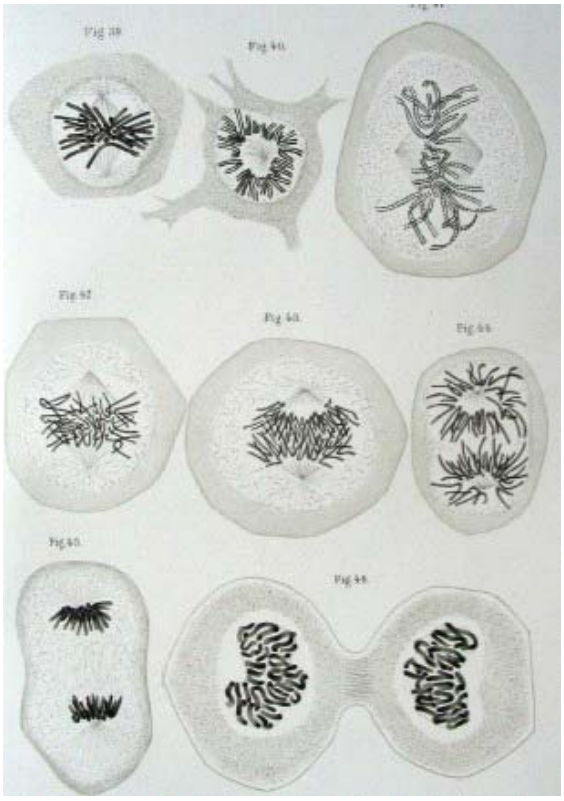

Figure 1. Illustration of the book “Zell-substanz, Kern und Zelltheilung”, 1882, by the german discoverer of chromatin and chromosomes, Walther Flemming

Ultimately, Flemming described in a book published in 1882 the whole process of mitosis, from chromosome doubling to their even partitioning into the two resulting cells. The terms he coined, like prophase (chromosome condensation), metaphase (alignment of chromosomes at a plate before separation), anaphase (separation of chromatids) and telophase (formation of daughter nuclei) are still used to describe the steps of cell division, today.

The spindle assembly checkpoint

In 1991 the spindle assembly checkpoint and several of its signalling components were first discovered by two parallel screens in yeast (Hoyt et al., 1991; Li and Murray, 1991). This mitotic checkpoint is conserved in eukaryotes and monitors the correct bipolar attachment of chromosomes to microtubules to ensure that replicated sister chromatids are distributed equally to daughter cells (Cleveland et al., 2003; Li and Nicklas, 1995; Musacchio and Hardwick, 2002; Pinsky and Biggins, 2005; Stern and Murray, 2001). Therefore anaphase onset is only triggered when all the chromosomes are properly attached and aligned at the metaphase plate (Figure 2 and 3). This allows the equal separation of sister chromatids and their accurate delivery to each spindle pole.

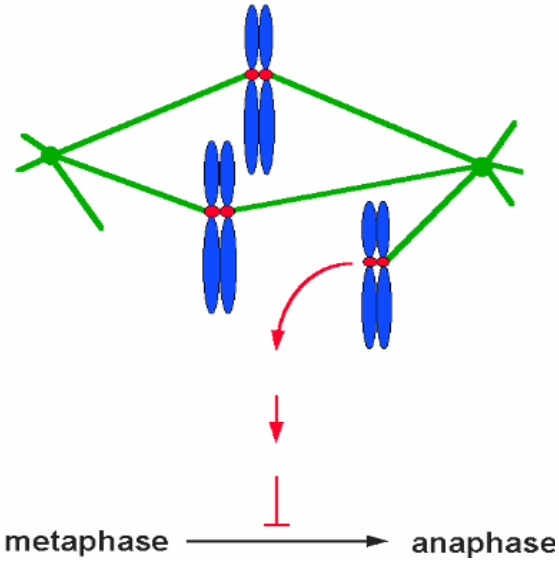

Figure 2. Simplified illustration of spindle assembly checkpoint (SAC) function: The checkpoint inhibits mitotic progression to anaphase by inhibitory signalling until the last pair of sister chromatids is attached to microtubules and aligned at the metaphase plate. Silencing of the SAC allows progression into anaphase.

Elegant cell-biological studies have shown that a single unattached kinetochore is sufficient to inhibit the onset of anaphase throughout the cell. Laser ablation of this unattached kinetochore relieves this mitotic delay (Rieder et al., 1995). Although changes in the phosphorylation state of kinetochore-associated proteins have been correlated with checkpoint activity status (Ahonen et al., 2005; Nicklas et al., 1995), the molecular source of the inhibitory spindle checkpoint signal remains unknown. There are several lines of evidence that the spindle checkpoint somehow ‘senses’ the tension that develops between sister kinetochores upon bipolar attachment (Figure 4), reflecting an equilibrium between poleward and anti-poleward forces acting on the sister chromatids (Nicklas et al., 1995; Rieder et al., 1994). Manipulations of chromosomes in insect spermatocytes showed that tension exerted across kinetochores during mitosis was enough to satisfy the spindle checkpoint (Li and Nicklas, 1995). However, to what extent lack of microtubule attachment and tension on kinetochores contribute to checkpoint activation in metazoan cells and where and how tension is monitored remains to be clarified (Musacchio and Hardwick, 2002).

The prevention of anaphase onset is achieved by inhibition (Figure 2) of the Anaphase promoting complex (APC/C), a multiprotein ubiquitin ligase, which is the target of the spindle checkpoint (Figure 3). APC/C activation by spindle checkpoint silencing leads to the destruction of Securin and CyclinB, which in turn permits progression into anaphase (Peters, 2002; Pines, 2006). Genetic and biochemical data concur to demonstrate essential functions for several proteins, notably Mad1, Mad2, Bub3 and the protein kinases Bub1, BubR1 and Mps1, in spindle checkpoint signalling (Figure 3). How these proteins cooperate to inhibit the APC/C remains to be fully understood, but most models emphasize a key role of Mad2 in the inhibition of the APC/C-accessory and activating protein Cdc20 (Mapelli et al., 2006; Yu, 2006).

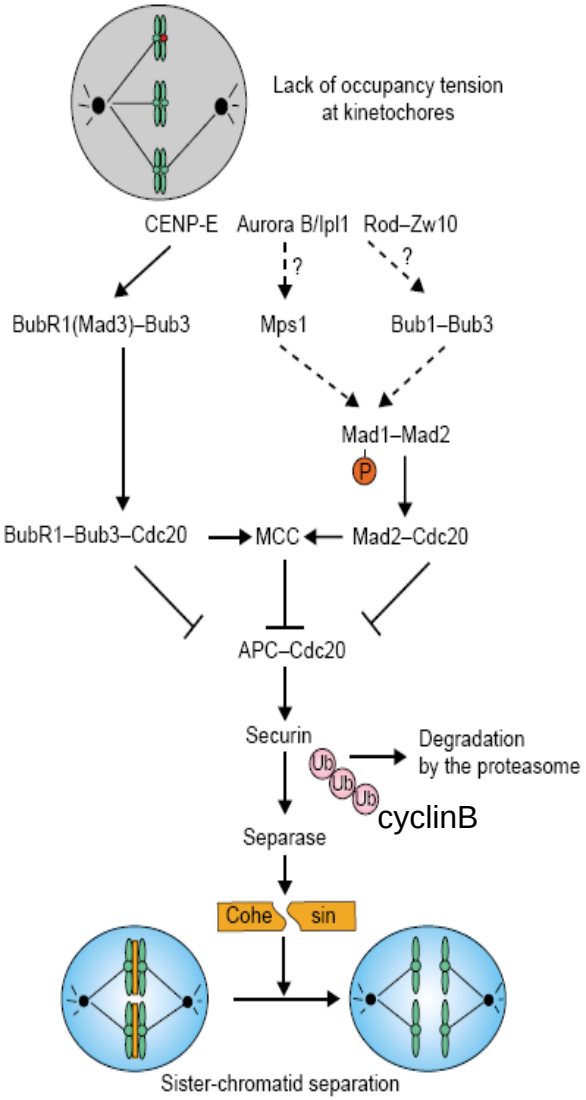

from Yu, CurrOpinionCellBiol 2002

Figure 3. Model of spindle checkpoint signalling: Upon lack of microtubule occupancy or tension at kinetochores several proteins at kinetochores and centromeres contribute to establish an inhibitory "wait anaphase" signal. Downstream effector proteins (BubR1, Bub3 and Mad2) directly prevent the activation of the anaphase promoting complex (APC/C) by binding to its activator Cdc20, either alone or in a multiprotein complex (MCC: mitotic checkpoint complex). When the APC/C is no longer inhibited, this E3 ubiquitin ligase ubiquitylates the substrates Securin and the Cdk1 activating subunit CyclinB, leading to their degradation by the proteasome. Subsequently Cdk1 activity drops and the protease Separase is no longer inhibited by Securin, allowing the proteolytic removal of cohesins - the glue that holds sister chromatids together – resulting in chromatid separation and the onset of anaphase.

Recently, the role of Mad2 in spindle checkpoint signalling has been described by two prevailing models, the "template model" from the lab of Andrea Musacchio (DeAntoni et al., 2005) and the "exchange model" by Hongtao Yu (Yu, 2006). Both models are based on the observation that Mad2 can adopt two conformational states and that spindle checkpoint signalling requires a conformational change from inactive Mad2 (O-Mad2; N1-Mad2) to active Mad2 (C-Mad2; N2-Mad2). C-Mad2 is more potent in Cdc20 binding and subsequent APC/C inhibition. The activation reaction is proposed to be catalyzed via a Mad1-Mad2 interaction/intermediary complex formation at the kinetochore.

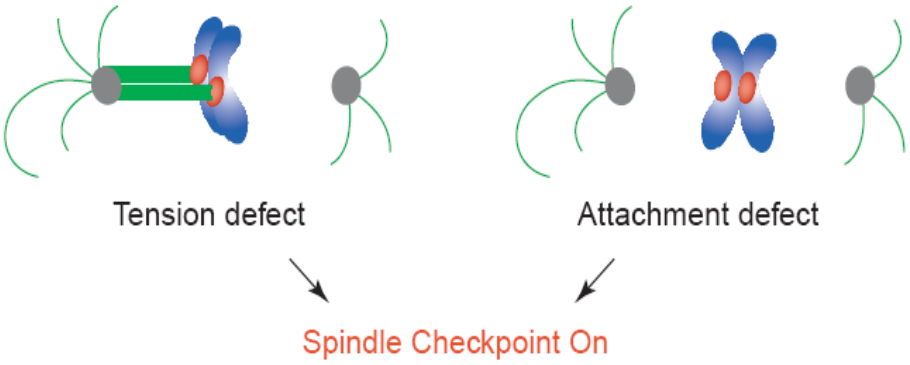

from Pinsky and Biggins, Trends in Cell Biology

Figure 4. The spindle assembly checkpoint senses the lack of microtubule attachment at kinetochores and the presence/absence of tension between sister chromatids. Until today it remains elusive how and where exactly these signals are sensed and created. While the list of kinetochore and centromere associated proteins is growing, a clear mechanism still needs to be understood.

Regulation of sister chromatid separation

On a protein level sister chromatid separation is largely regulated by two posttranslational mechanisms: by protein phosphorylation and protein degradation.

a) Protein phosphorylation: The most prominent mitotic kinases are the Cyclin-dependent kinases (Cdks) as well as members of the Polo-like kinase family (Plks) and the Aurora family (Barr et al., 2004; Nigg, 2001; Vagnarelli and Earnshaw, 2004). These enzymes contribute to the regulation of cell division via phosphorylation of numerous key substrates, including components of the cohesin complex, that holds sister chromatids together until the onset of anaphase. Sister chromatid separation requires the removal of cohesin proteins (Haering and Nasmyth, 2003) as well as decatenation of DNA by Topoisomerase II (Shamu and Murray, 1992; Yanagida, 1995) at the onset of anaphase. In vertebrates, cohesin proteins are removed from chromosome arms already during prophase, as a result of their phosphorylation by Polo-like kinase (Losada et al., 2002; Sumara et al., 2002) (Figure 5). However, centromere-associated cohesin is protected from phosphorylation by a type 2 phosphatase (PP2A) in complex with Shugoshin (Sgo1) (Kitajima et al., 2006; Riedel et al., 2006; Tang et al., 2006) so that its

removal depends on proteolytic cleavage by the protease Separase, a process initially described in yeast (Uhlmann et al., 2000).

b) Proteolysis: Mitotic proteolysis is triggered primarily by the anaphase promoting complex/cyclosome (APC/C). This multiprotein complex functions as an ubiquitin ligase that initiates protein degradation via ubiquitylation of target proteins that are then degraded by the proteasome (Peters, 2002; Pines, 2006). Most importantly the APC/C controls the destruction of both CyclinB, whose presence is required for Cdk1 kinase activity and Securin, the degradation of which is needed for liberating Separase proteolytic activity.

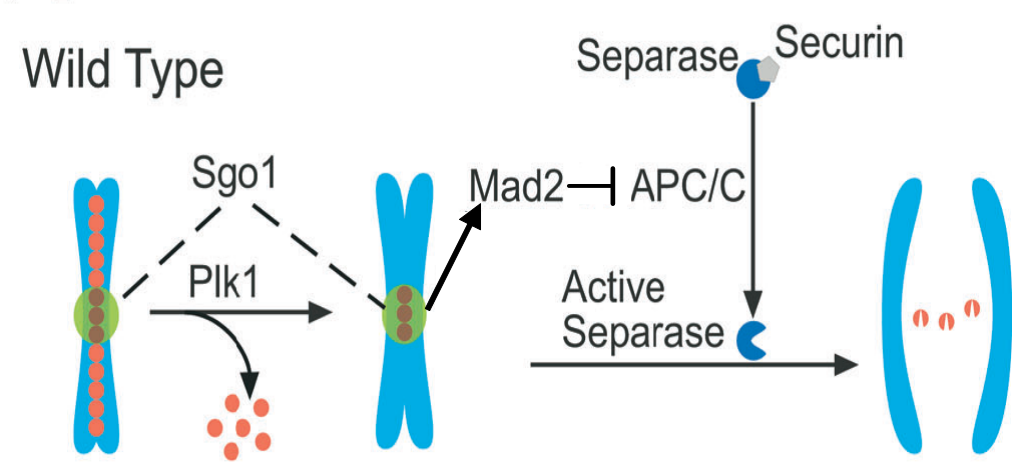

adapted from McGuinness et al. PLOS Biology 2005

Figure 5. During vertebrate mitosis, cohesins (red circles) are removed from chromosome arms via phosphorylation by Plk1 during prophase/prometaphase. The centromeric cohesins (brown circles) are protected by Sgo1 (Shugoshin) until the metaphase-anaphase transition. Once all chromosomes have successfully bi-oriented on the metaphase plate, inhibitory spindle checkpoint signalling by Mad2 to the APC/C is relieved, allowing Separase activation. Separase in turn removes cohesin remaining at centromeres through cleavage of the Scc1 subunit, allowing the cell to enter anaphase. In the absence of Sgo1 (Sgo1 depletion), cohesin is removed from the chromosome arms and the centromere during prophase/prometaphase before chromosomes have properly bi-oriented and been attached to their full complement of spindle microtubules.

Polo-like kinase 1 (Plk1)

In recent years Polo-like kinases have demanded an increasing amount of attention as key enzymes required in cooperation with Cyclin dependent kinase (Cdk) to regulate cell division. The most well-characterized member of this group, Plk1 (Figure 6), is a serine-threonine kinase that has been described in eukaryotes from yeast to human (Barr et al., 2004). In vertebrates, Polo-like kinase1 performs several important functions throughout mitosis, including the regulation of centrosome maturation and spindle assembly, the removal of cohesins from chromosome arms, the inactivation of APC/C inhibitors, and the regulation of mitotic exit and cytokinesis (Barr et al., 2004). Concomitantly, Plk1 localizes to centrosomes and spindle poles, kinetochores, the central spindle and the postmitotic bridge. These dynamic localizations depend on the C-terminal non-catalytic region of Plk1 (Jang et al., 2002; Seong et al., 2002), referred to as the Polo-box domain (PBD)(Elia et al., 2003b).

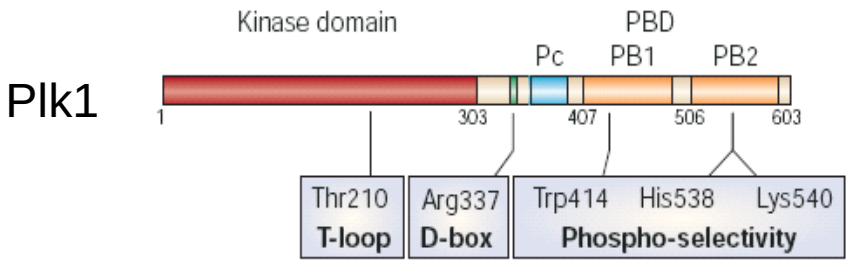

from Barr et al., Nat. Rev. MCB 2004

Figure 6. Schematic illustration of Plk1. Plk1 consists of an N-terminal kinase domain and a C-terminal Polo-box-domain (PBD). The PBD of Plk1 consists of two polo boxes (PBs), joined by a linker region, and a small region known as the polo-box cap (Pc). Highlighted are residues Trp414, His538 and Lys540, that are implicated in phosphopeptide binding. Also indicated are a conserved, activating phosphorylation site in the T-loop (Thr210) and the D-box motif that is required for degradation by the APC/C–Cdh1.

The PBD mediates the recruitment of Plk1 to proteins that have been 'primed' by phosphorylation at appropriate residues, notably at sites that conform to a consensus S-pS/pT-P/X (Elia et al., 2003a)(Figure 7 and 8). This docking mechanism constitutes an effective device for controlling Plk1 in time and space

(Hanisch et al., 2006; Jang et al., 2002; Lowery et al., 2005; Seong et al., 2002). The identification of the PBD as an interaction domain for phosphopeptide motifs prompts important questions as to the nature of the priming kinases as well as the identity of the docking proteins. Current evidence points to Cdk1-Cyclin B (Elia et al., 2003a) and the MAP kinase Erk2 (Fabbro et al., 2005) as prominent priming kinases. In addition, Calmodulin dependent kinase II (CaMKII) (Rauh et al., 2005) as well as Plk1 itself (Neef et al., 2003) have been identified as priming kinases. Several candidate docking proteins for Plk1 have also been described (Fabbro et al., 2005; Goto et al., 2005; Hanisch et al., 2006; Kang et al., 2006; Lowery et al., 2005; Nishino et al., 2006; Qi et al., 2006), but additional Plk1 interaction partners undoubtedly await discovery.

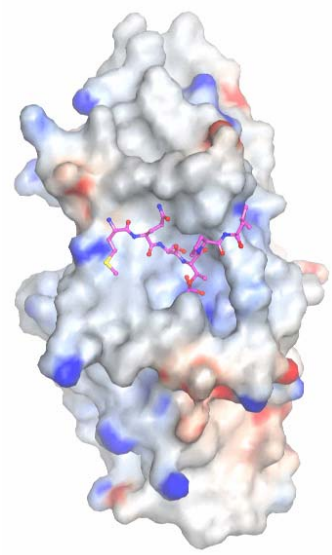

from Cheng et al (2003), EMBO J.

Figure 7. Crystal structure of the polo-box domain (PBD) of Plk1. The PBD binds to target proteins after their phosphorylation by a priming kinase. Shown is a phospho-threonine (peptide (MQS(pT)PL)) in the phosphopeptide binding pocket of the PBD. Phosphopeptide binding also results in increased Plk1 kinase activity, due to a relief of autoinhibition by the PBD on the Plk kinase domain.

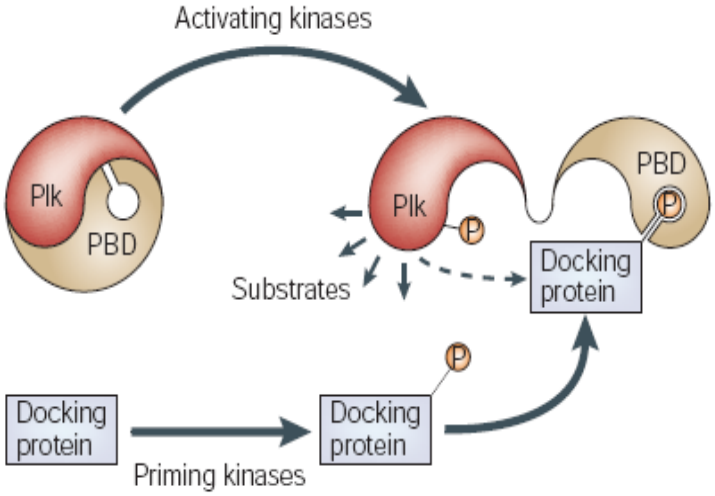

from Barr et al., Nat. Rev. MCB 2004

Figure 8. Plk1 activation and PBD-mediated targeting. Plk1 kinase activity can be activated by phosphorylation through an activating kinase on Thr210 (T-Loop activation). A docking site for Plk1 substrate binding can be created by phosphorylation through a priming kinase or Plk1 itself. Plk1 phosphopeptide binding occurs via its PBD.

The centromere, the kinetochore and the Ndc80 complex

Every chromatid has a centromere, a specialized chromatin region consisting of a series of α-satellite DNA repeats that provide a structural and functional foundation for the kinetochore. Specialized centromeric protein components are the histone H3 variants CenP-A, H3K4 and H3K9 (histone H3 methylated on Lysine 4 or 9) (Cleveland et al., 2003; Sullivan and Karpen, 2004), as well as further *cen*tromeric *P*roteins (CenPs) (Foltz et al., 2006). At the onset of mitosis the centromere builds up a proteinaceous structure, termed the kinetochore (Figure 9). The kinetochore hosts proteins that are required for microtubule attachment, such as the Ndc80 complex, that consists of the highly conserved, SMC-domain carrying proteins, Nuf2 (Nuclear Filamentous 2, 52kD) and Ndc80/Hec1 (Highly Expressed in Cancer 1, 78kD) and the subunits Spc24 and Spc25 (Spindle Pole Component, 24kD and 25kD). The Ndc80 complex plays a crucial role in the assembly of the outer kinetochore, the recruitment of other proteins and the establishment of microtubule attachment (DeLuca et al., 2005; McCleland et al., 2003). Recent studies suggest how the individual subunits might interact at the kinetochore (see Figure 66) and propose that Hec1 and Nuf2 have a shared and direct function in microtubule attachment, whereas the sub-complex of Spc24 and Spc25 might be

required for anchorage to the centromere (Ciferri et al., 2005; Wei et al., 2007; Wei et al., 2005). A higher order complex around Ndc80 has been described to contain the proteins Af15q14, Zwint, Q9H410, D31, PMF1 and Mis12 (Cheeseman et al., 2004). In addition, kinetochore proteins recruit checkpoint signalling proteins, including Mad2, BubR1 and Mps1 to kinetochores, supporting the idea that the spindle checkpoint signal originates from where spindle microtubule attachment and/or tension between sister chromatids is generated. A more detailed list of centromere and kinetochore associated proteins is reviewed by (Maiato et al., 2004; Vos et al., 2006).

While the chromatin of vertebrates at chromosome arms is separated already during prophase by the removal of cohesin ring complexes and decatenation, centromeric DNA seems to still connect sister kinetochores in metaphase (Hirano, 2000). This bridging can be visualized by immunofluorescence for centromeric proteins such as the chromosomal passenger complex (Vagnarelli and Earnshaw, 2004), CenP-B, CenP-A or other Histone H3 variants (Sullivan and Karpen, 2004) or the human centromeric autoimmunesera CREST or ANA. However, the exact path of centromeric DNA in mitosis, its timely resolution and its regulation by cohesion regulating enzymes like Plk1, Sgo1 and Topoisomerase IIa remain to be understood.

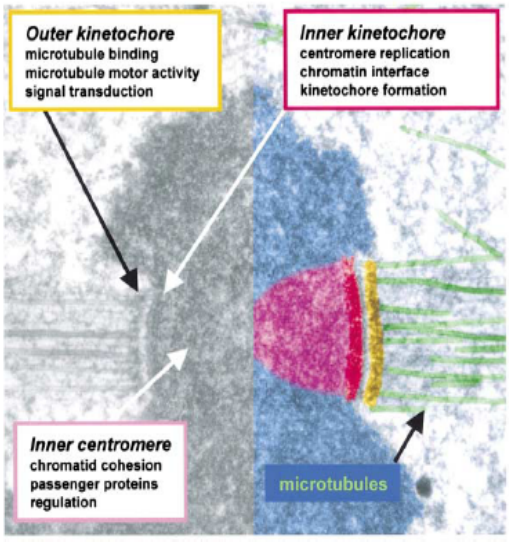

from Cleveland and Sullivan, Cell 2003

Figure 9. Organization of the kinetochore/centromere. Colors represent microtubules (green), the outer kinetochore (yellow), the inner kinetochore (red) and the centromere (violet).

SNF2 type helicases

The protein (PICH), which is the main subject of this study, provides a link between chromosome segregation and DNA decatenation, the mitotic spindle assembly checkpoint and chromatin remodelling by DNA translocating enzymes. Therefore, this chapter provides a short introduction into the field of helicases and translocases.

The central roles of DNA and RNA in transcription, recombination, genome replication, repair, expression and epigenetics place high demands on their structure, compaction and accessibility. Thus, a vast number of proteins and enzymes are required to spacially and temporally modulate DNA and RNA depending on the specific requirements of the cell.

Helicases, and their traditional characteristic of enzymatic unwinding of DNA, were first described in bacteria (*Escherichia coli)* in 1976 (Abdel-Monem et al., 1976; Abdel-Monem and Hoffmann-Berling, 1976). Since then, RNA and DNA helicases with diverse functions have been found in all organisms. Generally helicases harness the chemical energy of NTP binding and hydrolysis to execute their various functions. Processes which require helicase functions include the separation of complementary strands of double-stranded nucleic acids; the translocation along dsDNA; the removal of nucleic acid-associated proteins; and the catalysis of homologous DNA recombination (Singleton and Wigley, 2002; Singleton and Wigley, 2003). Although single helicase enzymes display these activities *in vitro*, most of them work efficiently as part of larger protein complexes.

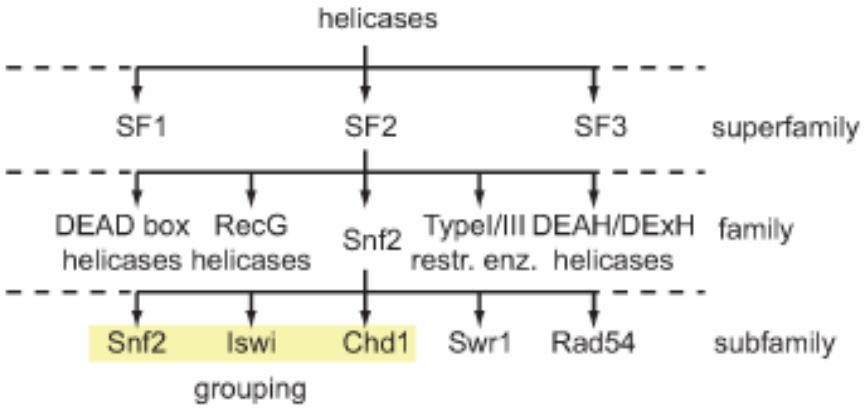

from Flaus et al. NucleicAcidResearch, 2006

Figure 10. Schematic illustration of the hierarchy of helicase superfamilies (SF), families and subfamilies. E.g. Rad54 belongs to the Rad54 subfamily of SNF2 type family ATPases which belong to helicase superfamily II (SF2).

Gorbalenya and Koonin (Gorbalenya and Koonin, 1993) classified a large group of proteins sharing a series of short ordered amino acid motifs. The majority of members with known function were nucleic-acid-strand separating helicases, so the sequences became known as helicase motifs and were labelled sequentially I, Ia, II, III, IV, V and VI. These helicase motifs also include the so-called Walker A and B sequences required for nucleotide binding. Proteins containing these motifs are subdivided into superfamilies on the basis of similarity (Figure 10). Structural characterizations have revealed that helicase-like superfamilies 1 and 2 (SF1 and SF2) are related by a common core of two recA-like domains (Subramanya et al., 1996), whereas predicted SF3 type helicases share only three conserved motifs. Proteins with a helicase-like region of similar primary sequence to *Saccharomyces cerevisiae* Snf2p belong to the SNF2 family within SF2. The SNF2 family of SF2 helicases can be further subdivided into several sub-families such as SNF2-like itself, SSO1653-like, ISWI-like and Rad54-like ((Flaus et al., 2006), Figure 10).

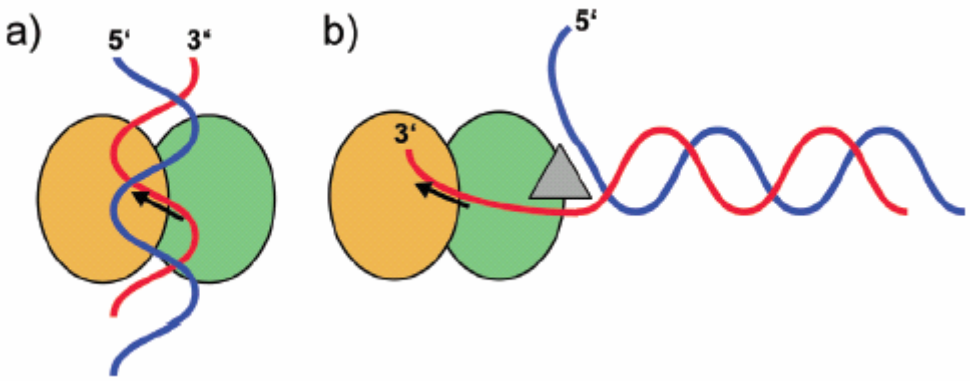

from Dürr et al., Nucleic Acids Research, 2006

Figure 11. Simplified illustration of the mode of action of Snf2 family ATPases and "classical" helicases. Schematic comparison of (A) dsDNA translocases (e.g. Snf2) and (B) ssDNA translocases. Both enzyme families contain a conserved RecA-like domain core (orange/green), but differ in other subunits (data not shown). Helicases move along ssDNA and often contain an upstream DNA unwinding element (grey triangle). In contrast, Snf2 family enzymes also recognize the 5`–3` strand (blue) and track along the minor groove. Despite many functional differences, however, both enzyme families bind the 3`–5` strands at an equivalent site across the two RecA-like domains, indicating that ATP-driven conformational changes transport DNA substrates via the 3`–5` strands in analogous ways (arrows).

The whole SNF2 family comprises a large group of ATP-hydrolysing proteins that are ubiquitous in eukaryotes, but also present in eubacteria and archaea. Rather than acting as processive helicases, members of the SNF2 family generally use ATP hydrolysis to displace proteins from chromatin (Becker and Horz, 2002), translocate on double stranded DNA (Durr et al., 2006; Svejstrup, 2003)(Figure 11), or generate superhelical torsion (Beerens et al., 2005; Havas et al., 2001; Lia et al., 2006). Accordingly, SNF2 family members have been implicated in chromatin remodeling, DNA recombination and DNA repair (Becker and Horz, 2002). Moreover, many of these SNF2 family members are ATPases within chromatin remodelling complexes such as the RSC complex (Saha et al., 2002) and the BAF complexes (Liu et al., 2001). Hence, it is thought that the presence of a SNF2-like core protein might be a defining property of ATP-dependent chromatin remodelling complexes (Becker and Horz, 2002). Interestingly, recent studies suggest that the ATPase and DNA translocation activity of SNF2 type enzymes (RSC;SWI/SNF2) depends on the template DNA conformation and applied tension (Lia et al., 2006; Zhang et al., 2006).

Topoisomerase II

DNA Topoisomerases play an essential role by altering the structure of double-stranded DNA. There are two major types of Topoisomerases: Topoisomerase I and II, the distinction being based on the mode of their enzymatic activity. Only Topoisomerase II can work bidirectionally to remove positive or negative supercoils and to catenate or decatenate DNA duplexes (Cozzarelli, 1980) (Figure 12). Due to its ATP dependent and DNA strand passing activity, Topoisomerase II plays a role in a variety of processes involving double-stranded DNA and functions at multiple steps in the assembly of mitotic chromosomes and the onset of mitosis. In vertebrates it is required for the separation of individual chromosomes, which occurs mainly in G2. In collaboration with the condensin complex Topoisomerase II is also believed to play a role in chromosome condensation (Uemura et al., 1987).

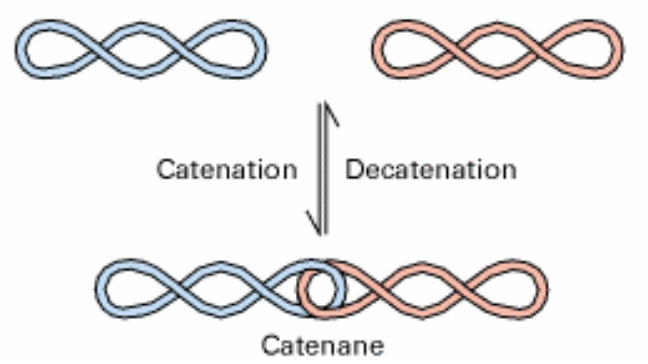

from Lodish, Molecular Cell Biology

Figure 12. Catenation and decatenation of two different DNA duplexes. Both prokaryotic and eukaryotic Topoisomerase II enzymes can catalyze this reaction.

The decatenation activity of Topoisomerase II is required for sister chromatid resolution in prometaphase. The predominant phenotype when Topoisomerase II function is deficient is the impaired separation of sister chromatids in anaphase (Downes et al., 1991; Gorbsky, 1994; Holm et al., 1985; Shamu and Murray, 1992; Skoufias et al., 2004).

Topoisomerase II accumulates at mitotic centromeres in prometaphase and remains there until early anaphase (Christensen et al., 2002; Rattner et al., 1996; Taagepera et al., 1993). A number of studies have suggested that Topoisomerase II may have a role in regulating kinetochore structure (Rattner et al., 1996) or centromeric cohesion (Bachant et al., 2002) and this view has been strengthened by molecular studies on human centromeric regions, where major sites of Topoisomerase II cleavage activity have been identified (Floridia et al., 2000; Spence et al., 2002).

Aims of this work

Beginning with the identification of human Hec1 (Martin-Lluesma et al., 2002), the vertebrate Ndc80 complex, consisting of its four subunits Nuf2, Hec1, Spc24 and Spc25, has been proposed to function as a structural core component of the kinetochore, required for the recruitment of several proteins, chromosome congression and microtubule attachment (DeLuca et al., 2005; DeLuca et al., 2003; McCleland et al., 2003; Wei et al., 2007; Wei et al., 2005). This work aimed first to study the composition of the Ndc80 complex and its function in mitotic kinetochore assembly and mitotic progression.

The mitotic kinase Plk1 is required for the regulation of several mitotic stages and its function is often reflected by its localization (Barr et al., 2004). In prometaphase, when the spindle assembly checkpoint is active, Plk1 localizes primarily to centrosomes and kinetochores. At this mitotic stage Plk1 is crucial for the removal of cohesins from chromatid arms to allow faithful segregation of sister chromatids (Hauf et al., 2005). However, even though an increasing number of Plk1 interactors at the kinetochore is being described (Goto et al., 2005; Kang et al., 2006; Qi et al., 2006), the function of Plk1 at the kinetochore remains to be fully understood. The discovery of the Plk1-PBD substrate docking mechanism (Elia et al., 2003a; Lowery et al., 2005) and our finding that the kinetochore association of Plk1 depends on the Ndc80 complex prompted us in the second part of this work to search for novel Plk1 interacting proteins at the kinetochore, and then study their functions in sister chromatid separation and the spindle assembly checkpoint.

Results part I

Studies on the Ndc80 complex

Based on the identification of human Hec1 (Martin-Lluesma et al., 2002) the original goal of this study was a functional and biochemical characterization of the human Ndc80 complex and the investigation of its role in kinetochore assembly, mitotic progression and the spindle assembly checkpoint.

Assembly of the Ndc80 complex, a structural component of the kinetochore

To understand the functional importance of the Ndc80 complex at kinetochores, HeLa cells were subjected to Nuf2 siRNA (Figure 13). It has previously been reported that depletion of one component of the Ndc80 complex results in the mislocalization of all other complex members (Bharadwaj et al., 2004). Therefore, efficient depletion of Nuf2 and complex dissociation were monitored by the levels of Hec1 protein at kinetochores. As a result of a 48h Nuf2 siRNA treatment, cells showed severely reduced Hec1 association with kinetochores and underwent a prometaphase-like mitotic arrest (Martin-Lluesma et al., 2002).

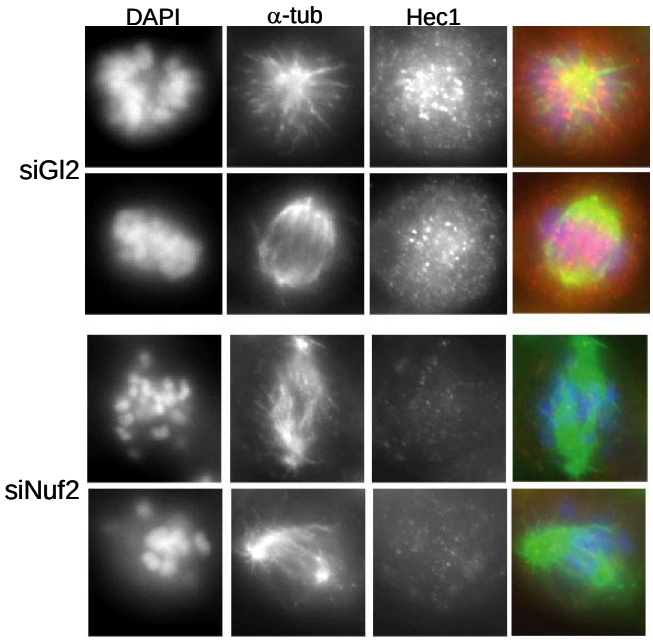

Figure 13. HeLaS3 cells were treated for 48h with siRNA oligos targeting Nuf2 or GL2 control, respectively. Then cells were permeabilized, fixed, and labeled for α-tubulin (green), Hec1 (red) and DNA (DAPI).

Interestingly, Nuf2 siRNA treated cells frequently showed elongated spindles with a greater distance between their poles (Figure 13, lower panel) compared to controls. Taken together these data suggest that depletion of Nuf2 results in a Hec1 depletion phenotype and confirms that the Ndc80 complex is a crucial component of the kinetochore required for mitotic microtubule organization and chromosome congression.

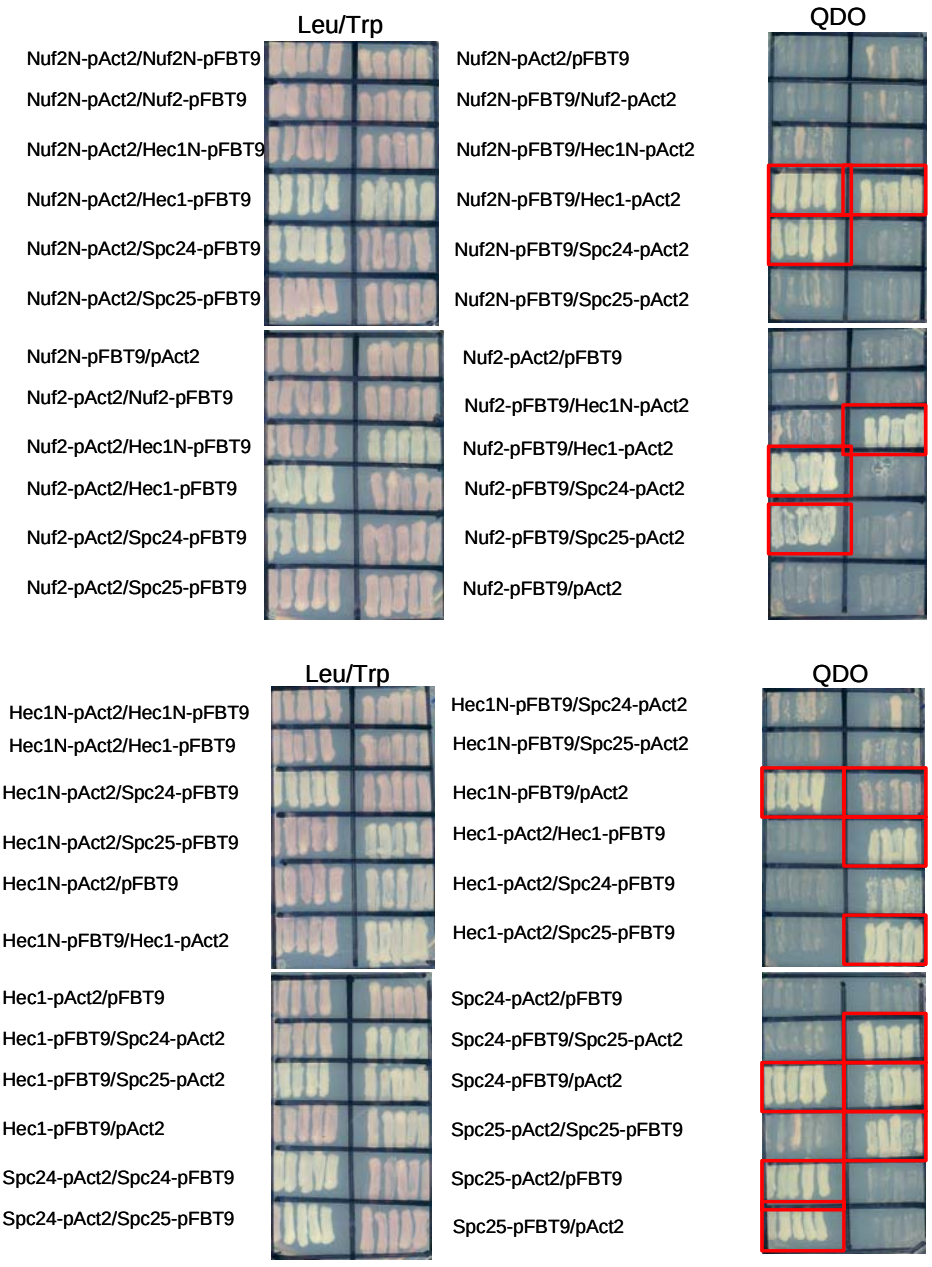

Figure 14. All four Ndc80 complex members and N-terminal domains of Hec1 and Nuf2 (Nuf2$^{f.l.}$, Nuf2$^{1-208}$, Hec1 $^{f.l.}$, Hec1$^{1-250}$, Spc24 $^{f.l.}$, Spc25 $^{f.l.}$) were cloned in both the pFBT9 yeast-2-hybrid bait domain and the pACT2 activation domain carrying vectors. Each fragment was assayed against all other in a directed yeast-2-hybrid analysis. Positives on QDO (Quadruple Drop Out: Leu$^-$/Trp$^-$/His$^-$/Ade$^-$) selection plates (right panels) are marked in red.

To gain structural insight into the molecular organization of the Ndc80 complex a directed yeast-2-hybrid approach was used with its members Hec1, Nuf2, Spc24 and Spc25. To this end, cDNAs coding for the four known components Spc24, Spc25, Hec1, Nuf2 (McCleland et al., 2004) as well as N-terminal fragments of Hec1 (aa1-250) and Nuf2 (1-208) were amplified and cloned into both the yeast-2-hybrid bait vector pFBT9, and the pACT2 library vector carrying the GAL4 activation domain. A directed yeast-2-hybrid screen probing all proteins against each other was carried out (Figure 14) to test which components and domains interact with each other and allow complex formation. The observed interactions are summarized in Figure 15A. A scheme of our data for the Hec1-Nuf2 interaction obtained from the directed yeast-2-hybrid assay is shown in Figure 15B. A model proposing interactions between Nuf2 and Hec1 via their N-termini, as well as Spc25 interaction with Hec1 and, furthermore, Spc25 interaction with Spc24 is presented in Figure 15C.

A

bait \ AD	Nuf2 1-208	Nuf2	Hec1 1-250	Hec1	Spc24	Spc25
Nuf2 1-208	-	-	-	+	-	-
Nuf2	-	-	-	+	-	-
Hec1 1-250	SA	SA	SA	SA	SA	SA
Hec1	+	+	-	-	-	+
Spc24	SA	SA	SA	SA	SA	SA
Spc25	-	-	-	+	+	+

B

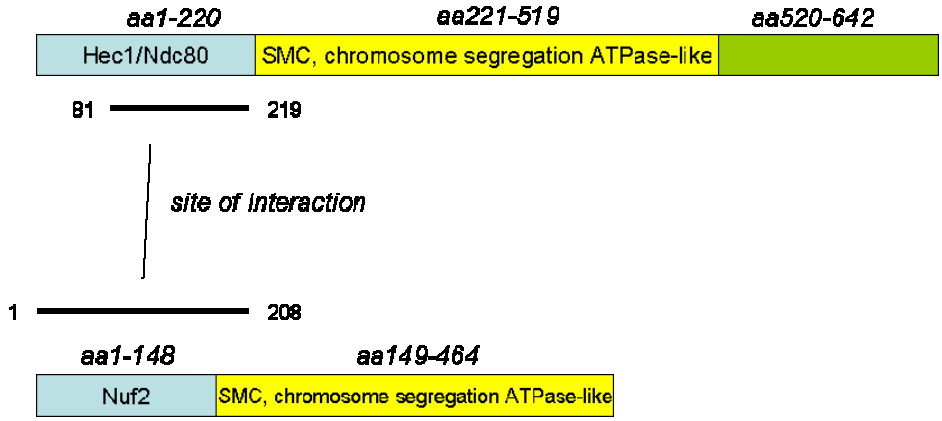

C

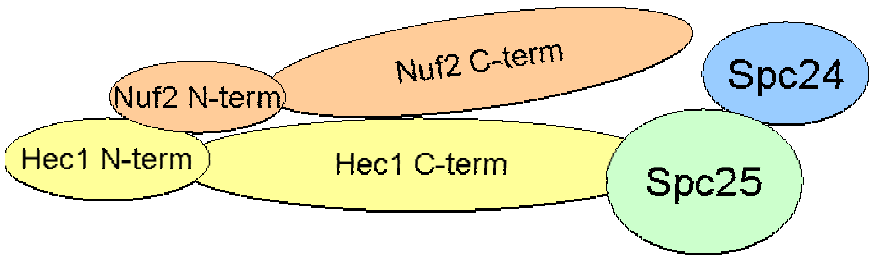

Figure 15. Model of Ndc80 complex formation derived from the Yeast-2-hybrid data: Table summarizing the observed interactions (Figure 14) with +: interaction, -: no interaction, SA: no data due to self activation of the bait-protein (A). Direct interactions observed between the N-termini of Nuf2 and Hec1 suggest that Hec1$^{81-219}$ and Nuf2 $^{1-208}$ are sufficient for binding (B). A model consistent with the Ndc80 interaction data above is shown in C).

Interaction partners of the Ndc80 complex

To answer the question of how the Ndc80 complex is functionally involved in the structure and/or spindle checkpoint function at the outer plate of the kinetochore, we searched for interaction partners. Two yeast-2-hybrid screens were carried out using Spc25 (Figure 16) or Nuf2$^{1-208}$ (Figure 18) as a bait. For both screens a pACT2 testis cDNA library (kindly provided by Evelyn Fuchs, MPI of Biochemistry, Martinsried) was used with approximately 500 000 transformands in the Spc25 screen and approx. 1.2 million transformands in the Nuf2$^{1-208}$ screen. Positives were put in three categories: strong interactors (with colony growth on QDO selective plates within 4 days), moderate interactors (growth within 7 days) and weak interactors (growth within 10 days). In the Spc25 screen 4 potentially significant single hits were obtained: Nek2B, Zwint, Hec1 and Apc7; and, moreover three proteins appeared twice: HCR (Rod-homologue), TRAF4 (Tumor necrosis factor receptor-associated factor 4), and the sarcoma antigen NY-SAR-48. For a detailed list of all the yeast-2-hybrid results see below (Figure 16).

STRONG INTERACTORS	MODERATE INTERACTORS	WEAK INTERACTORS
Nek2B	HCR (Rod-homologue)	Spata11
ZWINT	TRAF4 associated factor	SDHB
HEC1	PSME3 Makropain	Clusterin isoform2
APC7	BAC clone CIT987SK-384D8	Calmodulin 2/CAMK2
HCR (Rod-homologue)	PER1	KIAA 1443
TRAF4 associated factor 1	p34SEI1(cdk4 interactor)	
AKAP350	CDK5 regulatory subunit associated protein 3	
AKAP82	PIAS 1	
BICD1	ANKRD7	
SNX4	HSFY	
MTX2	hypothetical protein LOC283871	
Olfactomedin 1	Integrin alpha 5	
Nrg1		
NY-SAR-48		
NY-SAR-48		
UXT		
NADE		

Figure 16. Results of the Y-2-H screen using Spc25 as a bait. Proteins are categorized into strong/moderate/weak interactors, dependent on the yeast colony growth on QDO selective plates. Known kinetochore/mitotic proteins are printed in bold, proteins appearing twice in the screen are shown in blue.

Sequence analysis of the pACT2 cDNA library insert revealed that the NIMA kinase Nek2B was interacting with Spc25 in the yeast-2-hybrid assay, via a C-terminal fragment that is alternatively spliced and thus not present in the endogenous Nek2A protein, suggesting that this interaction with Spc25 might be specific for Nek2B. This kinase had previously been proposed to function at the centrosome (Twomey et al., 2004). The observation of Hec1 as an interactor indicated that the assay was functional and further confirmed data from the directed screen shown above (Figure 14-15). The protein Zwint had previously been suggested to be required for the recruitment of Rod/ZW10 and the dynein/dynactin complex to kinetochores (Cheeseman et al., 2004; Lin et al., 2006; Starr et al., 2000).

To verify potential interactions between Spc25 and Nek2B or Zwint, the full length proteins were amplified from a marathon cDNA library (Clontech) by nested PCR and tested against Spc25 in a directed yeast-2-hybrid screen (Figure 17).

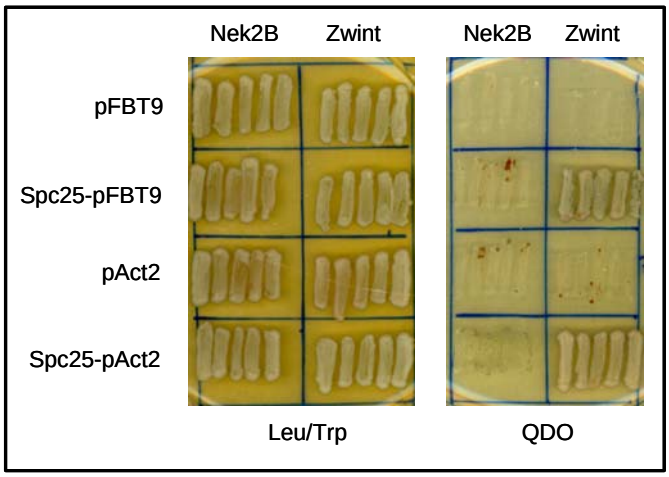

Figure 17. Directed interaction assay to test the obtained potential Spc25 interactors Nek2B and Zwint as full length clones in both pFBT9 and pACT2 vectors.

Only full length Zwint but not the full length kinase Nek2B showed growth on QDO selective medium when cotransfected with Spc25 constructs in pACT2 or pFBT9. With regard to Nek2B this questioned the specificity of the interaction or, alternatively, indicated that the folding of the full length protein did not allow for efficient binding in this approach. With regard to Zwint, these experiments confirmed work from other laboratories, indicating that Zwint is associated with the Ndc80 complex (Cheeseman et al., 2004; Kops et al., 2005a). Moreover, our data further show that Zwint directly interacts with Spc25. Thus, these results provide a link between the structural basis of the outer kinetochore and the microtubule interface at the outer corona.

None of the three proteins appearing as double hits (HCR, NY-SAR-48 and Traf4 associated factor 1 (Tumor necrosis factor receptor-associated factor associated factor 1) have previously been described to either localize to kinetochores or to be required for mitotic progression. Therefore, these proteins have not been analyzed so far and remain interesting candidates that could be further pursued.

STRONG INTERACTORS	MODERATE INTERACTORS	WEAK INTERACTORS
Hec1 (3x)	MGC40107 (3x)	PHD finger protein 8
C10Orf94 (3x)	hypothetical protein XP_499286	hypothetical protein LOC286333
CSDA	DC12 protein	hypothetical protein FLJ38101
	FLJ90706 fis	ISYNA1
	hypothetical protein FLJ38101	RPL37
	NIPSNAP	Rho-GTPase interacting protein 19
	FLJ35785 (SMC)	BAC RP11-335I12
		HES1
		UQCRB
		chromosome 5 clone CTC-286C20

Figure 18. Results of the Yeast-2-Hybrid screen using Nuf2$^{1-208}$ as a bait. Proteins are categorized into strong/moderate/weak interactors, dependent on the yeast colony growth on QDO selective plates. Known kinetochore/mitotic proteins are printed in bold, proteins appearing twice ore more often in the screen are shown in blue.

The second screen with Nuf2$^{1-208}$ as bait identified Hec1 as an interaction partner three times, confirming our previous findings that Hec1 is able to interact with the N-terminus of Nuf2 (summarized in Figure 15A). Moreover, a so far uncharacterized protein, C10Orf94 (Hypothetical telomeric protein, synaptonemal complex central element protein 1, RP11-108K14.6, LOC93426), carrying an SMC domain in its N-terminus, also appeared as a strong interaction partner of Nuf2 three times. Full length C10Orf94 was amplified from a HeLa marathon cDNA library, cloned into myc-expression vectors and yeast-2-hybrid plasmids and awaits further study.

A monoclonal antibody specific for human Nuf2

For further investigations of the role of Nuf2 and the Ndc80 complex in kinetochore structure and assembly, we generated monoclonal α-Nuf2 antibodies (see methods). A summary of the properties of three hybridoma cell lines tested in western blots on recombinant protein and cell extracts, in immunofluorescence, and in immunoprecipitation is listed below (Table 1).

Hybridoma	rec. Protein (WB)	endogenous Protein (WB)	Immunofluores-cence	Immuno-precipitation	Isotype
27-123-1	+++	-	++	++	IgG1
28-37-1/3	++	+	+	++	IgG1
28-241-1	+++	-	-	?	IgG2b

Table 1. Results of the characterization of 3 different hybridoma clones derived after immunization of 2 mice with full length His-Nuf2 (see methods).

Colocalization analyses by immunofluorescence of the clones 27-123 and 28-37 in HeLa cells showed that both hybridoma clones decorate kinetochores (Figure 19). That the antibodies decorate kinetochores was confirmed by co-staining with BubR1.

To test for the specificity of the Nuf2 monoclonal antibody, clone 28-37 was used for immunofluorescence on siRNA depleted HeLa cells (Figure 20). Following 48h treatment with Nuf2 siRNA the Nuf2 positive kinetochore signal readily disappeared, confirming the specificity of the monoclonal antibody.

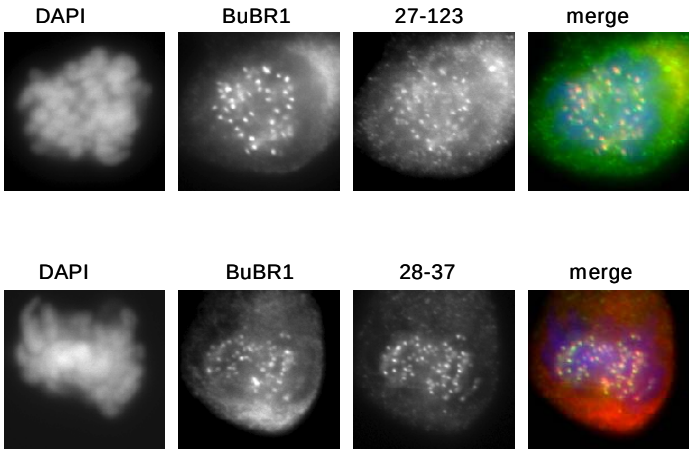

Figure 19. Testing of two Nuf2 hybridoma clones (27-123 and 28-37) in immunofluorescence. HeLaS3 cells were fixed and labelled for Nuf2 (green), BubR1 (red) and DNA (blue; DAPI).

Staining with a Mps1 monoclonal antibody (Stucke et al., 2004; Stucke et al., 2002) showed significant reduction of the Mps1 kinetochore signal in Nuf2 depletion compared to control cells, indicating a dependency of Mps1 on Nuf2 and the Ndc80 complex (Figure 20). These data are in line with a previous study, showing that the depletion of Hec1 results in the loss of Mps1 and Mad1/Mad2 from kinetochores (Martin-Lluesma et al., 2002).

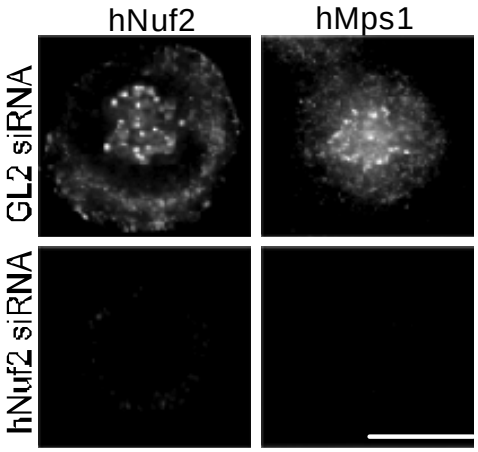

Figure 20. HeLaS3 cells were treated for 48h with siRNA oligos for Nuf2 or GL2 control respectively. Cells were fixed and labelled for Nuf2 and Mps1. Note that Mps1 is mislocalized in Nuf2 depletion.

The Ndc80 complex is required for Plk1 kinetochore localization

The Ndc80 complex is not only a structural component of the outer kinetochore but is also required for the kinetochore assembly and functionality of checkpoint components such as Mps1, Mad1 and Mad2 (Martin-Lluesma et al., 2002). Using siRNA mediated depletion of Nuf2, the localization of fourteen structural and/or signalling proteins of the kinetochore and the inner centromere (Maiato et al., 2004) were analyzed by immunofluorescence.

Hec1	Mps1	Mad1	Mad2	Plk1	Cdc20	Bub1	AuroraB	InCenP	CenP-B	CenP-E	CenP-F	BubR1	Survivin
-	-	-	-	-	-	-	+	+	+	+	+	+	+

Table 2. Summary of immunofluorescence analyses for protein localization in Nuf2 depletion. – indicates mislocalization of the indicated protein, + indicates that the localization is unaltered compared to GL2 control.

Interestingly Nuf2 was neither required for the proper localization of the outer kinetochore components CenP-E, CenP-F and BubR1 (Abrieu et al., 2000; Ditchfield et al., 2003; Maiato et al., 2004) nor for the centromere association of the chromosomal passenger complex, including AuroraB, Incenp and Survivin (Ditchfield et al., 2003; Vagnarelli and Earnshaw, 2004). However, the proteins Mad1, Mad2, Bub1 and Cdc20, all of which are involved in spindle checkpoint signalling (Musacchio and Hardwick, 2002; Pinsky and Biggins, 2005; Tang et al., 2004), required the proper association of Nuf2 to the kinetochores for their wild type localization (Table 2). These results indicates that these proteins all belong to a kinetochore assembly branch dependent on the Ndc80 complex (see also (Vigneron et al., 2004)). Moreover, the mitotic kinase Plk1 was lost from kinetochores in Nuf2 depleted cells. As Plk1 is involved in a variety of mitotic events at different cellular structures as the centrosomes, the midzone/central spindle, the postmitotic bridge and the kinetochore (Barr et al., 2004), a sole dependency on the Ndc80 complex for its kinetochore localization might allow further studies that focus on the mitotic role of Plk1 at kinetochores in Ndc80 depletion experiments.

To corroborate this effect of Nuf2 knockdown on Plk1 localization, further siRNA experiments were carried out. Using HeLa and U2OS cell lines, Hec1, Nuf2, CenP-F, BubR1, CenP-E, AuroraB, Sgo1 and Mad2 were depleted by siRNA and Plk1 localization was examined. The data indicate that not only Hec1 and Nuf2, but also the centromeric proteins AuroraB and Sgo1 all contribute to proper Plk1 kinetochore localization (see also (Ahonen et al., 2005; Goto et al., 2005)) and Table 3).

siRNA	Hec1	Nuf2	Plk1	CenP-F	CenP-E	BubR1	Mad2	Bub1	AuroraB	Sgo1
Plk1 at the kinetochore	-	-	-	+	+	+	+	+	-	-

Table 3. Summary of immunofluorescence analyses for Plk1 kinetochore localization in various depletion background. – indicates mislocalization of Plk1, + indicates that Plk1 localization is unaltered compared to GL2 control.

Conclusions I

In this first part of our study we analyzed the composition of the human Ndc80 complex and its requirement for kinetochore assembly and chromosome congression. We found that the N-terminal amino acid residues 81-219 of Hec1 and 1-208 of Nuf2 are sufficient for their interaction. Furthermore, Hec1 interacts with the complex subunit Spc25, which binds Spc24. In line with previous studies depletion of Nuf2 abrogates kinetochore association of Hec1 and results in a prometaphase-like arrest with elongated spindles, indicating defects in chromosome congression and microtubule attachment (DeLuca et al., 2005; Martin-Lluesma et al., 2002; McCleland et al., 2003). Screening for interacting proteins by using the yeast-2-hybrid assay identified several potential complex binding proteins, amongst them Zwint (Kops et al., 2005a) as an interactor of Spc25, and C10Orf94, an SMC domain carrying, so far uncharacterized open reading frame, as an interactor of Nuf2. We analyzed the effect of Nuf2 depletion by siRNA and subsequent disruption of the Ndc80 complex on 14 centromeric / kinetochore associated proteins. While centromere association of the chromosomal passenger complex and CenP-B, as well as the kinetochore localization of CenP-E, CenP-F and BubR1 were unaltered, the spindle checkpoint signalling components Mps1, Mad1, Mad2, Cdc20 and Bub1 were mislocalized from kinetochores, suggesting a specific assembly pathway of these mitotic regulators dependent on the Ndc80 complex. Moreover, Polo-like kinase (Plk1) was lost from kinetochores in Nuf2 depleted cells. Further testing in different siRNA backgrounds showed that the localization of Plk1 requires the Ndc80 complex as well as Sgo1 and AuroraB, but not CenP-E, CenP-F, BubR1 and Mad2, suggesting that Plk1 kinetochore association does not only depend on a single interaction partner (Goto et al., 2005; Kang et al., 2006; Nishino et al., 2006; Qi et al., 2006).

Results part II

Studies on Plk1

The appearance of several publications on the Ndc80 complex (Bharadwaj et al., 2004; Ciferri et al., 2005; DeLuca et al., 2005; Deluca et al., 2006; DeLuca et al., 2003; McCleland et al., 2003; McCleland et al., 2004; Wei et al., 2005) together with the discovery of the Plk1 substrate binding mechanism (Elia et al., 2003a) prompted us to use the Polo-box domain of Plk1 to search for novel substrates and interactors and to characterize their role in mitosis.

Identification of PICH, a novel Plk1 interacting protein

Previous reports identified a number of interactors, substrates and kinetochore recruiting factors of Plk1, for example NudC (Nishino et al., 2006), Incenp (Goto et al., 2005), PBIP1 (Kang et al., 2006), Bub1 (Qi et al., 2006), Mklp2 (Neef et al., 2003) and XErp1 (Rauh et al., 2005). To search for further mitotic proteins, that interact with Plk1 and are regulated through recruitment of Plk1, HeLa cell lysates were prepared by arresting cells in mitosis via treatment with nocodazole. Plk1 was immunoprecipitated from these mitotic lysates using two different monoclonal Plk1 antibodies (36-298 and 36-206) and the efficient recovery of Plk1 was tested by Western blotting (Figure 21 lower panel). These immunoprecipitates were then examined for the presence of Plk1-binding proteins, using a recombinant C-terminal polo-box domain (GST-PBD) of Plk1, in a Far Western ligand-blotting assay (Figure 21, upper panel), (Neef et al., 2003).

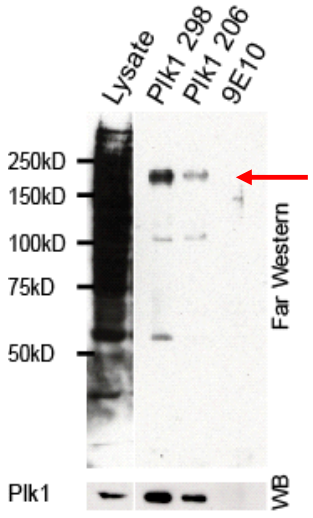

Figure 21. To search for Plk1-PBD binding proteins, HeLa cells were arrested in mitosis by treatment with nocodazole. Plk1 was immunoprecipitated using two different monoclonal antibodies (298 and 206) and efficient recovery of Plk1 was assessed by Western blotting (lower panel). Immunoprecipitates were then examined for the presence of Plk1-binding proteins, using a recombinant C-terminal polo-box domain (PBD) in a ligand-blotting (Far Western) assay (upper panel). The whole cell lysate (left), as well as a control immunoprecipitate prepared with an unrelated antibody (anti-myc; 9E10) were analyzed in parallel (upper panel) and support the specificity of the experiment.

Specifically, immunoprecipitates were used for western blotting followed by partial renaturing on the membrane. The blots were then incubated with recombinant GST-PBD, and the GST-Tag was assessed by primary / secondary antibody detection. The most prominent potential PBD-interacting protein migrated at about 220 kD, whereas two weaker bands could be observed at 100 kD and 60 kD, respectively. Aliquots of the same immunoprecipitates were loaded on a preparative SDS-page minigel and coomassie bands migrating at approximately 220kD were cut out and used for analysis by LC-MS/MS (MS analyses were carried out by Dr Roman Körner, MPI of Biochemistry, Munich).

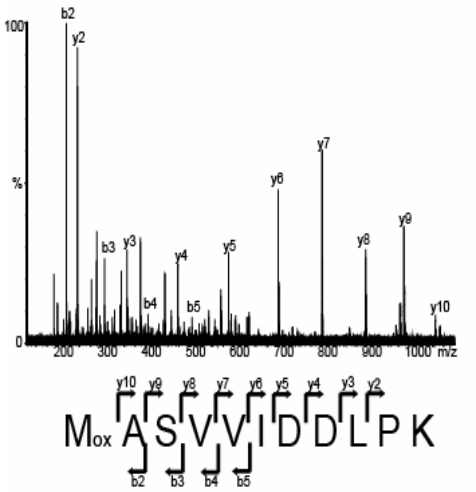

Figure 22. Samples were prepared as described in Figure 21 but were resolved by preparative gel electrophoresis. Gel slices corresponding to the 220 kD mass range were analyzed by mass spectrometry (LC-MS/MS, using a quadrupole time-of-flight mass spectrometer). This approach identified several peptides that were present in both anti-Plk1 immunoprecipitates but absent in the control. They matched ORF FLJ20105 encoded on chromosome Xq13.1 (Acc. No. BC111486 in the NCBI database). The mass spectrum shown was obtained by collision induced dissociation (CID) of the ORF FLJ20105-derived peptide M_{ox}ASVVIDDLPK.

Figure kindly provided by Dr Roman Körner

This approach identified the ORFs FLJ90238, FLJ31932 and FLJ20105 (all representing parts of the same unpublished open reading frame), encoded on chromosome Xq13.1, as a candidate binding partner of human Plk1 (Figures 21, 22, 23).

To assemble the sequence of the full length ORF a combined bioinformatic and experimental approach was used: the information derived from peptides gained from MS analysis by Dr Roman Körner indicated the minimum length of the PICH sequence. Bioinformatical sequence alignments of truncated PICH versions at NCBI (FLJ31932, FJL90238, FLJ20105) together with PICH-related ESTs and additional sequence information obtained through 5` RACE PCRs suggested, that FLJ20105 (Acc. No. BC111486) represents the full length ORF. This is supported

by the presence of a Kozak consensus sequence for translation initiation (Kozak, 1987) upstream of the ATG start codon. The whole ORF could be amplified by nested PCR from a HeLa marathon cDNA library, providing additional evidence that this cDNA/ORF does exist in human cells. Thus, the sequence shown in Figure 23 represents the full length protein.

MEASRRFPEAEALSPEQAAHYLRYVKEAKEATKNGDLEEAFKLFNLAKDIFPNEKVLSRIQKIQEALEELAEQ
GDDEFTDVCNSGLLLYRELHNQLFEHQKEGIAFLYSLYRDGRKGGILADDMGLGKTVQIIAFLSGMFDASLVN
HVLLIMPTNLINTWVKEFIKWTPGMRVKTFHGPSKDERTRNLNRIQQRNGVIITTYQMLINNWQQLSSFRGQE
FVWDYVILDEAHKIKTSSTKSAICARAIPASNRLLLTGTPIQNNLQELWSLFDFACQGSLLGTLKTFKMEYENPI
TRAREKDATPGEKALGFKISENLMAIIKPYFLRRTKEDVQKKKSSNPEARLNEKNPDVDAICEMPSLSRKNDLI
IWIRLVPLQEEIYRKFVSLDHIKELLMETRSPLAELGVLKKLCDHPRLLSARACCLLNLGTFSAQDGNEGEDSP
DVDHIDQVTDDTLMEESGKMIFLMDLLKRLRDEGHQTLVFSQSRQILNIIERLLKNRHFKTLRIDGTVTHLLERE
KRINLFQQNKDYSVFLLTTQVGGVGLTLTAATRVVIFDPSWNPATDAQAVDRVYRIGQKENVVVYRLITCGTVE
EKIYRRQVFKDSLIRQTTGEKKNPFRYFSKQELRELFTIEDLQNSVTQLQLQSLHAAQRKSDIKLDEHIAYLQSL
GIAGISDHDLMYTCDLSVKEELDVVEESHYIQQRVQKAQFLVEFESQNKEFLMEQQRTRNEGAWLREPVFPS
STKKKCPKLNKPQPQPSPLLSTHHTQEEDISSKMASVVIDDLPKEGEKQDLSSIKVNVTTLQDGKGTGSADSI
ATLPKGFGSVEELCTNSSLGMEKSFATKNEAVQKETLQEGPKQEALQEDPLESFNYVLSKSTKADIGPNLDQL
KDDEILRHCNPWPIISITNESQNAESNVSIIEIADDLSASHSALQDAQASEAKLEEEPSASSPQYACDFNLFLED
SADNRQNFSSQSLEHVEKENSLCGSAPNSRAGFVHSKTCLSWEFSEKDDEPEEVVVKAKIRSKARRIVSDGE
DEDDSFKDTSSINPFNTSLFQFSSVKQFDASTPKNDISPPGRFFSSQIPSSVNKSMNSRRSLASRRSLINMVLD
HVEDMEERLDDSSEAKGPEDYPEEGVEESSGEASKYTEEDPSGETLSSENKSSWLMTSKPSALAQETSLGA
PEPLSGEQLVGSPQDKAAEATNDYETLVKRGKELKECGKIQEALNCLVKALDIKSADPEVMLLTLSLYKQLNNN

Figure 23. Predicted amino acid sequence of ORF FLJ20105. The approximate positions of various motifs are indicated in colour, as used in Figure 24.

Analysis of the domain structure of ORF FLJ20105 at NCBI and SMART databases revealed that this protein carries several domains (Figure 23 and 24): The N-terminus harbours a SNF2-like helicase domain accompanied by a C-terminal HELICc extension, which has high homology to the human SNF2 family members CSB/Ercc6 and Rad54. This SNF2 helicase domain is further characterized by the presence of a DEXH domain (Walker B motif) and a GKT sequence (Walker A motif), both of which are required for nucleotide binding and hydrolysis. This clearly suggests that FLJ20105 belongs to the subfamilies of Rad54-like or SSO-1653-like helicases of the SNF2 family of helicase superfamily 2 (Eisen et al., 1995; Flaus et al., 2006).

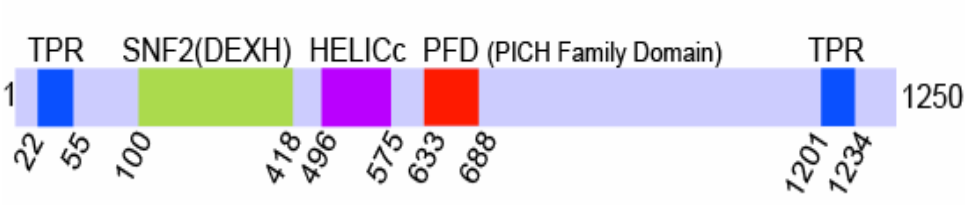

Figure 24. Schematic illustration of subdomains within ORF FLJ20105 (PICH), as predicted by Scansite and Blast analyses on NCBI databases. Numbers refer to amino acid residues.

At the very N- and C-termini of ORF FLJ20105 single tetratricopeptide repeats (TPR motifs) were found. These motifs have been shown to mediate protein-protein interactions (Lamb et al., 1995).

Because the described ORF carries a helicase domain, it interacts with the mitotic kinase Plk1, and is required for the spindle assembly checkpoint (see below), we named it PICH: **P**lk1 **I**nteracting **C**heckpoint '**H**elicase'.

In cooperation with Dr Kay Hofmann (Miltenyi Biotech, Cologne) the PICH amino acid sequence was analyzed for orthologs in other species. Using comparative sequence analyses, Dr Hofmann found a novel, conserved motif C-terminal of the 'helicase' domain of PICH (Figure 25) that appears to be specific for PICH orthologs. This highly conserved region can be used as a signature motif for PICH in other species and thus we call it the PICH family domain (PFD) (Figure 24 and 25).

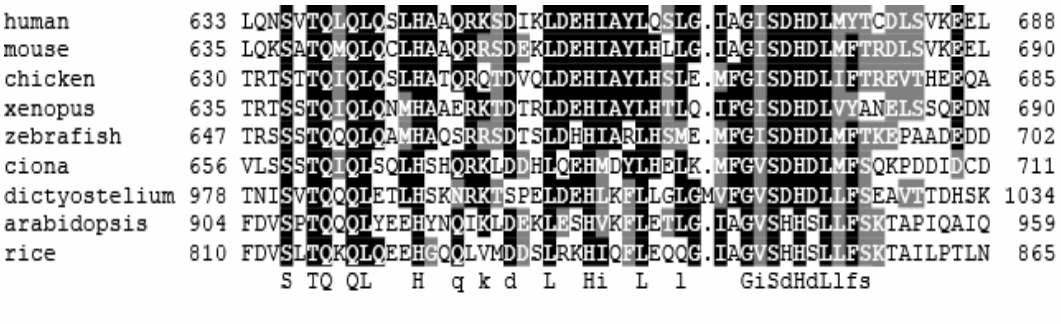

Figure kindly provided by Dr Kay Hofmann

Figure 25. Evolutionary conservation of the PICH family domain (PFD). Amino acid residues are indicated using single-letter code and numbers refer to their positions. Dark and light gray indicate conservation and conservative substitutions, respectively. A putative consensus is indicated below the alignment.

Database searches by Dr Hofmann focused on the PFD revealed PICH orthologs in vertebrates and plants as well as in a non-vertebrate chordate, in *Dictyostelium,* and in the single cell eukaryotic parasite Entamoeba, but (so far) not in yeast or the typical invertebrate model organisms *Drosophila melanogaster* or *Caenorhabditis elegans*.

Detection of endogenous PICH

Full length, bacterially expressed MBP-PICH was used for immunizations of two rats and two rabbits. The sera of all four animals (rabbits: F95-antibody and G95-antibody; rats: rat I and rat II) showed crossreactivity with human PICH in immunofluorescence. Both rabbit antibodies were affinity purified and successfully used for western blotting analysis of PICH (Figure 26A).

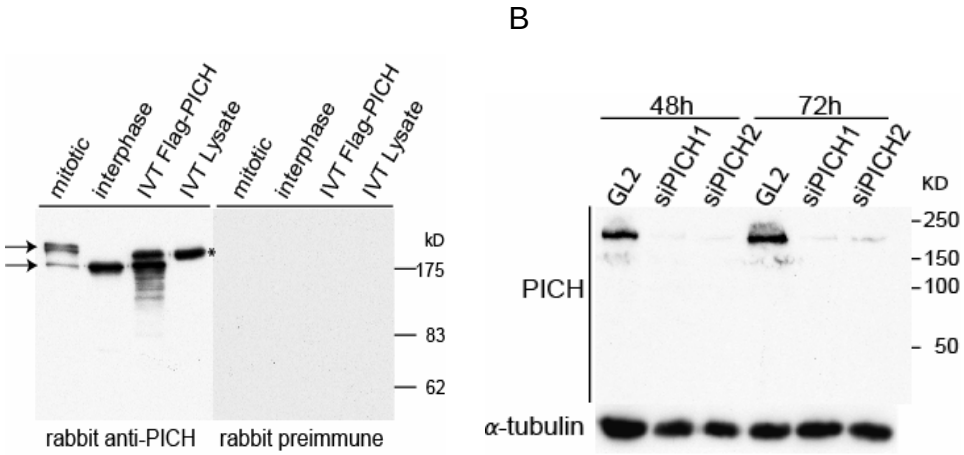

Figure 26. The rabbit G anti-PICH antibody (A, left panel) and the corresponding pre-immune serum (A, right panel) were used for Western blotting. Lysates were prepared from mitotic (nocodazole-arrested) and interphase HeLa cell extracts or from rabbit reticulocyte lysates that were primed for in vitro transcription by addition of a Flag-PICH transcription vector. Reticulocyte lysate alone was used as a control. Arrows indicate the two distinctly migrating forms of PICH; the asterisk marks a crossreacting band in the control lysate. When used for Western blotting on extracts prepared from asynchronously growing HeLa cells, an affinity-purified rabbit anti-PICH antibody recognized a single protein migrating at 180 kD. Attesting to antibody specificity, this immunoreactivity was almost completely abolished upon siRNA-mediated knock-down of PICH for 48 or 72 h, using either one of two different oligonucleotide duplexes (B). The duplex GL2 was used for control, and α-tubulin levels (lower panel) were determined to show equal loading.

Western blot analysis with rabbit α-PICH antibodies identified a protein of ~180kD in interphase lysates (Figure 26A), whereas, in the mitotic lysate an additional band migrating at approximately 220kD was recognized (arrows). This 220kD band likely corresponds to the PBD-interacting protein identified in mitotically arrested cells (Figure 21). PICH is composed of 1250 amino acids with a predicted molecular weight of approximately 140kD, in contrast to the observed molecular weight in interphase extracts of 180kD. Analysis of the isoelectric point using the bioinformatics website www.expasy.org revealed an acidic pI of 5.2, which might account for the retarded migration behaviour of PICH. To corroborate that non-modified PICH migrates at 180kD, recombinant PICH was produced by in vitro translation. This Flag-PICH construct co-migrated with PICH from interphase extracts (Figure 26A, lanes 2 and 3), whereas, an additional slower migrating band (asterisk) appeared also in control IVT rabbit reticulocyte lysates (Figure 26A, lanes 3 and 4), showing that this band is not related to human in vitro translated PICH, even though it could reflect crossreactivity of the antibody with the rabbit ortholog of PICH from the reticulocyte lysate (Figure 26A).

To further analyze the specificity of the antibody, siRNA transfections were carried out and analyzed by western blotting and immunofluorescence. Using two different siRNA oligo duplexes designed to target PICH on asynchronously growing Hela cells, PICH levels could be significantly reduced after at least 48h of incubation (Figures 26B). Depletion of PICH could also be confirmed by immunofluorescence microscopy (see below).

The Plk1-PICH interaction is mediated by Polo-box binding to phosphorylated threonine 1063

To confirm the interaction between Plk1 and PICH, nocodazole arrested cells were used to test for coprecipitation of Plk1 in immunoprecipitations of endogenous PICH and vice versa. As shown by Western blotting, endogenous PICH could readily be detected in Plk1 immunoprecipitates (Figure 27A, see also Figure 21) and endogenous Plk1 was present in PICH precipitates (Figure 27B). These two proteins were not precipitated by control antibodies. In addition, other mitotic proteins such as Hec1 and BubR1 were not detected in Plk1 or PICH

immunoprecipitates respectively, supporting the specificity of the PICH-Plk1 interaction (Figure 27).

A B

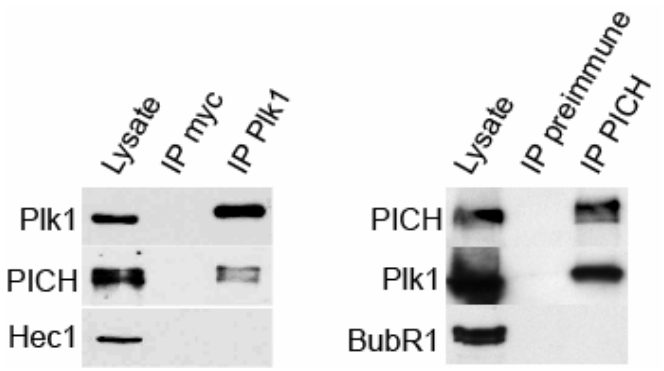

Figure 27. Immunoprecipitations with mouse anti-Plk1 or 9E10 anti-myc antibodies were performed from nocodazole arrested HeLa cells and probed by Western blotting with antibodies against the indicated proteins (left panel). Reciprokal immunoprecipitations with rabbit anti-PICH or preimmune antibodies were performed from nocodazole arrested HeLa cells and probed by Western blotting with antibodies against the indicated proteins (right panel).

To study the cell cycle regulation of the PICH-Plk1 interaction, myc-PICH and flag-Plk1 were co-expressed in HEK293T cells and reciprocal co-immunoprecipitation / Western blotting experiments were performed on asynchronously growing and nocodazole arrested cells. Plk1-PICH complex formation could be observed in mitotic cells but not in interphase samples (Figure 28), suggesting a requirement for a mitosis specific modification of PICH, most likely a priming phosphorylation (Elia et al., 2003a; Lowery et al., 2005).

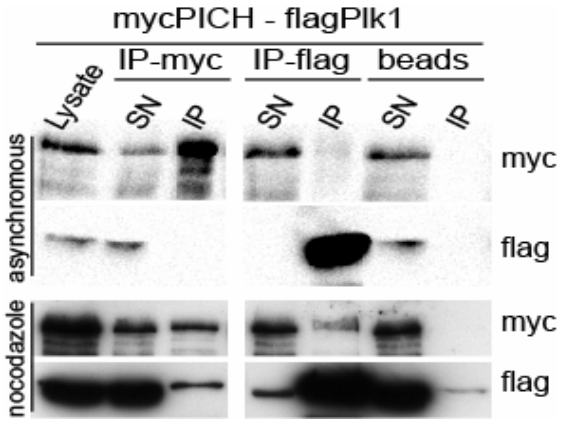

Figure 28. mycPICH and flagPlk1 were co-expressed for 48 hrs in HEK293T cells before immunoprecipitations were performed, using anti-flag or anti-myc antibodies (or beads for control), from asynchronously growing cells (upper panel) or from cells that had been arrested for 16 hrs in nocodazole (lower panel). All samples were then probed by Western blotting with anti-myc and anti-flag antibodies. Note that Plk1 and PICH only co-immunoprecipitate from mitotic extracts.

Supporting the idea that PICH is phosphorylated a progressive increase in PICH mobility was seen upon release of HeLa cells from a nocodazole arrest (Figure 29). This PICH upshift on SDS-gels disappeared concomitantly with Cyclin B, suggesting that it is mitosis specific.

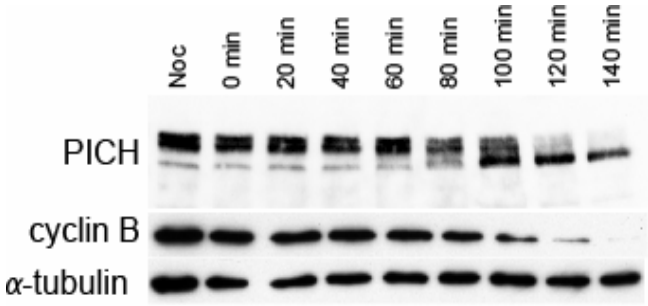

Figure 29. HeLa cells were released from a nocodazole-induced mitotic arrest, samples were collected every 20 min and probed by Western blotting, using the antibodies indicated. Cyclin B levels indicate exit from mitosis and α-tubulin levels serve as a loading control.

Moreover, when mitotic (nocodazole arrested) lysates were treated with CIP (calf intestine phosphatases) for 30 min., PICH displayed a phosphatase-sensitive

retardation in electrophoretic mobility (Figure 30), comparable to the migration of the protein in interphase (aphidicoline) lysates. Thus, PICH is phosphorylated during mitosis as long as Cdk1 activity persists but undergoes dephosphorylation as cells exit mitosis.

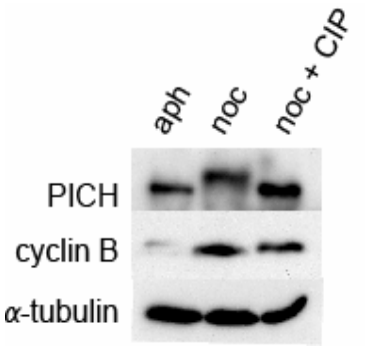

Figure 30. The electrophoretic mobility of PICH in SDS-PAGE was assayed by Western blotting performed on interphase (aph; aphidicoline arrested) or mitotic (noc; nocodazole arrested) lysates. The latter lysates were pretreated for 30min with or without calf intestinal phosphatase (CIP). The mitotic status was assayed by monitoring Cyclin B levels. Equal loading is shown by detection of α-tubulin.

Potentially important, evolutionarily conserved phosphorylation and Plk1 docking sites were then analyzed using sequence alignments of PICH orthologs. Indeed, a STPK amino acid sequence highly conserved in vertebrates could be identified at positions aa1062-1065 (Figure 31). This threonine site may constitute a Plk1-PBD docking site after being primed via phosphorylation by a proline directed serine/threonine kinase (Elia et al., 2003a).

Xenopus tropicalis	svkgitastpklnks
Homo sapiens	svkqfdastpkndis
Mus musculus	svkqfdastpqsgsn
Gallus gallus	egkiisastpkndrs
Danio rerio	aisrlgsstpkavlv

Figure 31. Alignment of vertebrate PICH: threonine 1063 appeared to constitute a highly conserved, potential PBD binding/Cdk1 consensus site.

Mass spectrometric analysis by Dr Roman Körner (MPI of Biochemistry, Munich) of the Plk1-PICH complex isolated from mitotic cell lysates indeed identified threonine 1063 as a prominent phosphorylation site in PICH (Figure 32). This suggested that phosphorylation by Cdk1 might transform it into a PBD-binding site (Elia et al., 2003a).

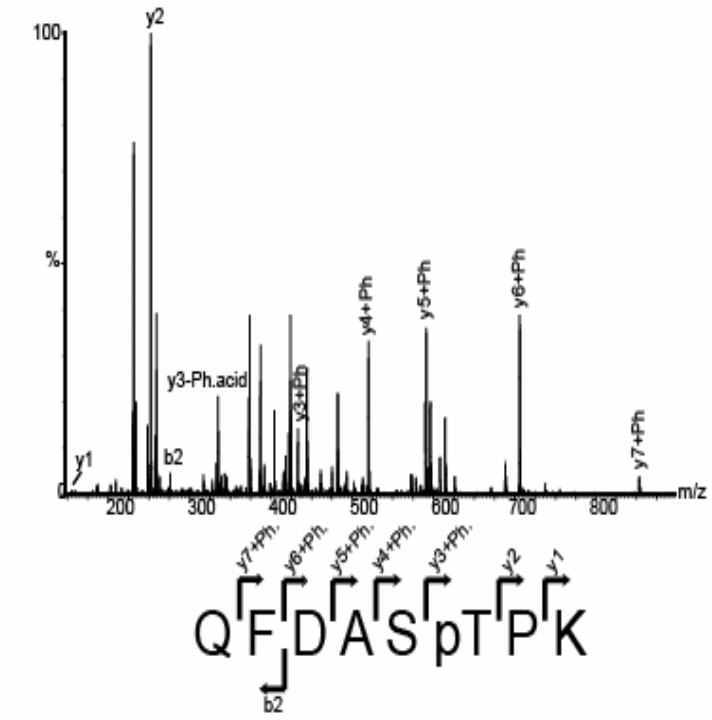

kindly provided by Dr Roman Körner

Figure 32. Collision induced dissociation (CID) mass spectrum of the ORF FLJ20105-derived phospho-peptide QFDASpTPK. C-terminal and N-terminal fragments are marked as y-ions and b-ions, respectively. pT denotes phosphothreonine, fragments containing the phosphate group are marked as "+Ph.", and the fragment showing a characteristic loss of phosphoric acid is labeled as "-Ph.acid".

Several further experiments were then performed to support the initial finding and explore the importance of PICH phosphorylation. First it was tested whether Cdk1 could phosphorylate PICH *in vitro*. When recombinant Cdk1 was used for kinase assays, it phosphorylated both wild-type (wt) and, to a lesser extent, a mutant PICH with threonine 1063 mutated to alanine (T1063A) (Figure 33, middle panel), indicating that T1063 is a Cdk1 phosphorylation site, albeit not the only one. Next, a Far Western ligand binding assay (Neef et al., 2003) was performed (shown below) to test the ability of recombinant GST-PBD to bind PICH, with or without

prior phosphorylation by Cdk1 (Figure 33, bottom panel). Whereas wt PICH and PICH T1063A showed virtually no PBD binding without pre-phosphorylation by Cdk1, strong PBD binding was seen after Cdk1-mediated phosphorylation. In the case of the T1063A mutant, PBD binding was strongly reduced, albeit not completely abolished, even after pre-phosphorylation by Cdk1. These results identify threonine 1063 as a major priming site for Plk1-PBD binding to PICH and suggest that the PICH-Plk1 interaction requires mitosis specific priming by Cdk1.

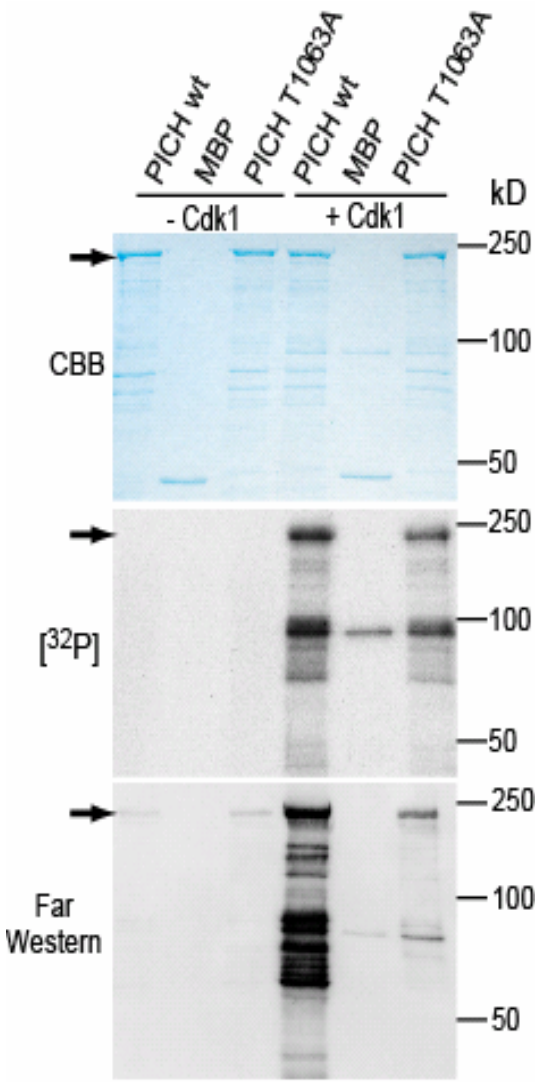

Figure 33. In vitro kinase assays were performed with Cdk1-Cyclin B (or buffer for control) and the indicated proteins as substrates, before samples were subjected to SDS-PAGE. Coomassie blue staining (CBB) and autoradiography shows protein loading (top panel) and phosphorylation ([^{32}P]; middle panel), respectively. The arrow marks MBP-PICH. In parallel, a Far Western ligand blotting assay was performed with GST-PBD (bottom panel), demonstrating that efficient PBD binding to PICH requires Cdk1 phosphorylation on threonine 1063.

We next investigated, whether the Cdk1-induced recruitment of Plk1 to PICH could convert PICH into a substrate of Plk1. Therefore, sequential kinase assays were performed (Figure 34). Recombinant wt PICH and T1063A PICH proteins were incubated with or without Cdk1 in the presence of unlabelled ATP for 1 hour.

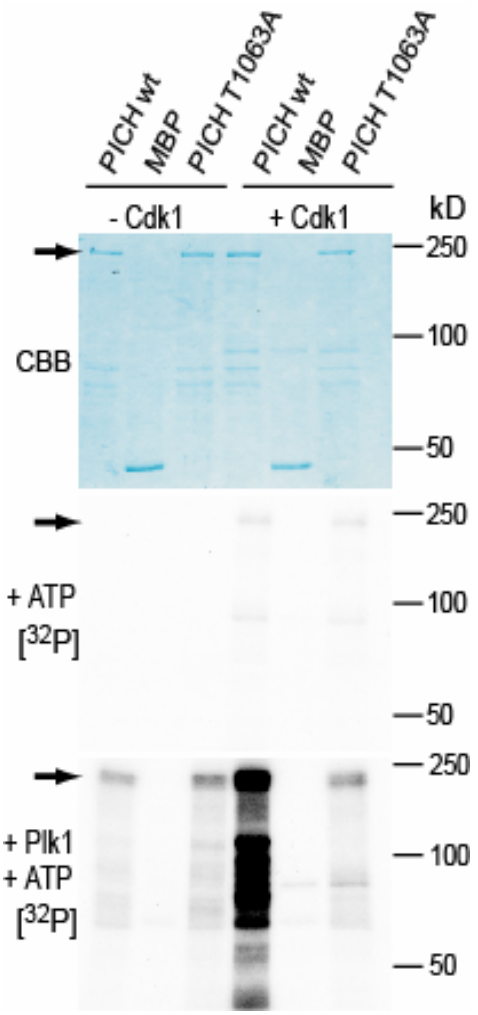

Figure 34. Sequential kinase assay. MBP-PICH-His wt or T1063A proteins (500ng) were pre-incubated for 1h at 30°C with or without Cdk1-Cyclin B, in the presence of unlabeled ATP. All samples were then split equally and incubated for 30min at 30°C with either γ-[^{32}P]-ATP alone (middle panel) or γ-[^{32}P]-ATP and Plk1 (bottom panel). Then, samples were resolved by 7.5 % SDS-PAGE and subjected to auto-radiography. Equal protein loading is shown by Coomassie blue staining (top panel). The arrow marks MBP-PICH.

Samples were then split and incubated with γ-[^{32}P]-ATP with or without Plk1. Phosphorylation of PICH incubated with only γ-[^{32}P]-ATP was minimal, presumably

reflecting residual Cdk1 activity (Figure 34, middle panel). Likewise, Plk1-dependent phosphorylation of both wt PICH and T1063A PICH was minimal in the absence of prior exposure to Cdk1 (Figure 34, bottom panel). In striking contrast, the sequential exposure of PICH to Cdk1 and then Plk1 resulted in strong phosphorylation of wt PICH, while still only a weak phosphorylation of the T1063A mutant (Figure 34, bottom panel). Therefore PICH is an excellent substrate of Plk1, provided that it has been primed for Plk1-PBD binding through phosphorylation at T1063.

PICH colocalizes with Plk1 at kinetochores

To investigate the subcellular localization of PICH in HeLa cells at different stages of the cell cycle, immunofluorescence microscopy was used. Anti-PICH antibodies produced weak, mostly cytoplasmic staining in interphase cells, but strong staining of the kinetochore region on mitotic chromosomes (Figure 35 and 36). Colocalization analysis of PICH with Hec1, a marker of the outer kinetochore (Ciferri et al., 2005), confirmed the kinetochore association of PICH in mitosis which could be abolished by siRNA mediated depletion of PICH, confirming both the specificity of the antibody and the kinetochore signal (Figure 36).

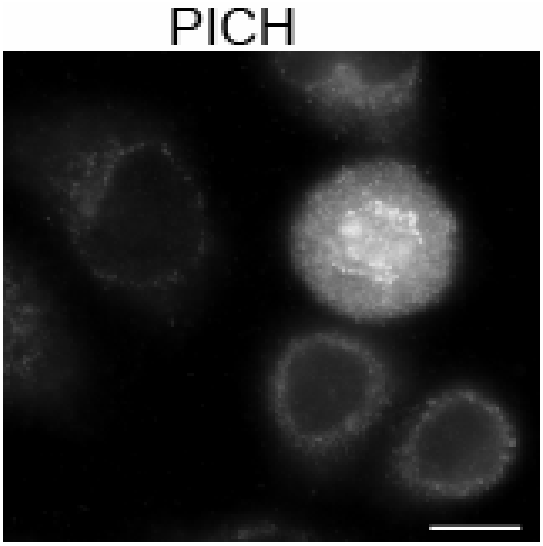

Figure 35. PICH localization in HeLa cells was determined by immunofluorescence microscopy. Cells were fixed with paraformaldehyde and permeabilized with Triton-X-100 before they were incubated with affinity-purified rabbit anti-PICH antibody (0.5 µg/ml), followed by secondary antibody. Bar, 10 µm).

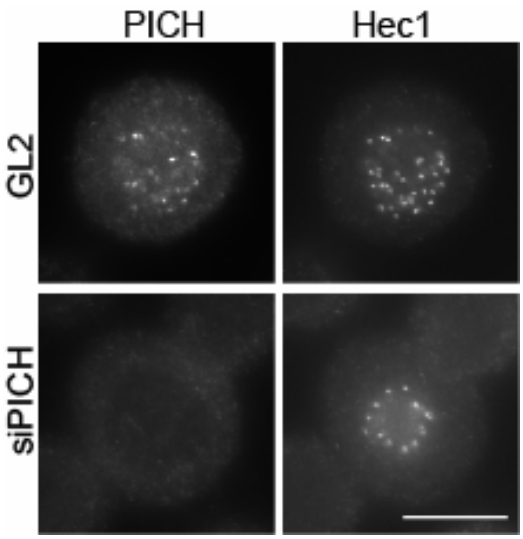

Figure 36. HeLa cells were treated with PICH siRNA or GL2 for control. Kinetochore localization of PICH was confirmed by colocalization with Hec1 and antibody specificity documented by siRNA-mediated depletion. Bar 10µm.

Next the subcellular localization of PICH and Plk1 was compared by immunofluorescence at different stages of mitosis (Figure 37). Beginning in prophase Plk1 localized to kinetochores, whereas PICH showed merely diffuse chromatin association, indicating that PICH is not required for the initial recruitment of Plk1 to kinetochores. In prometaphase PICH and Plk1 could be seen to colocalize at kinetochores, but only Plk1 was observed at centrosomes. PICH was still present at kinetochores in anaphase but not anymore in telophase, while Plk1 accumulated at the postmitotic bridge. Strikingly, strong association of PICH with novel “thread” structures could be detected in anaphase (arrow).

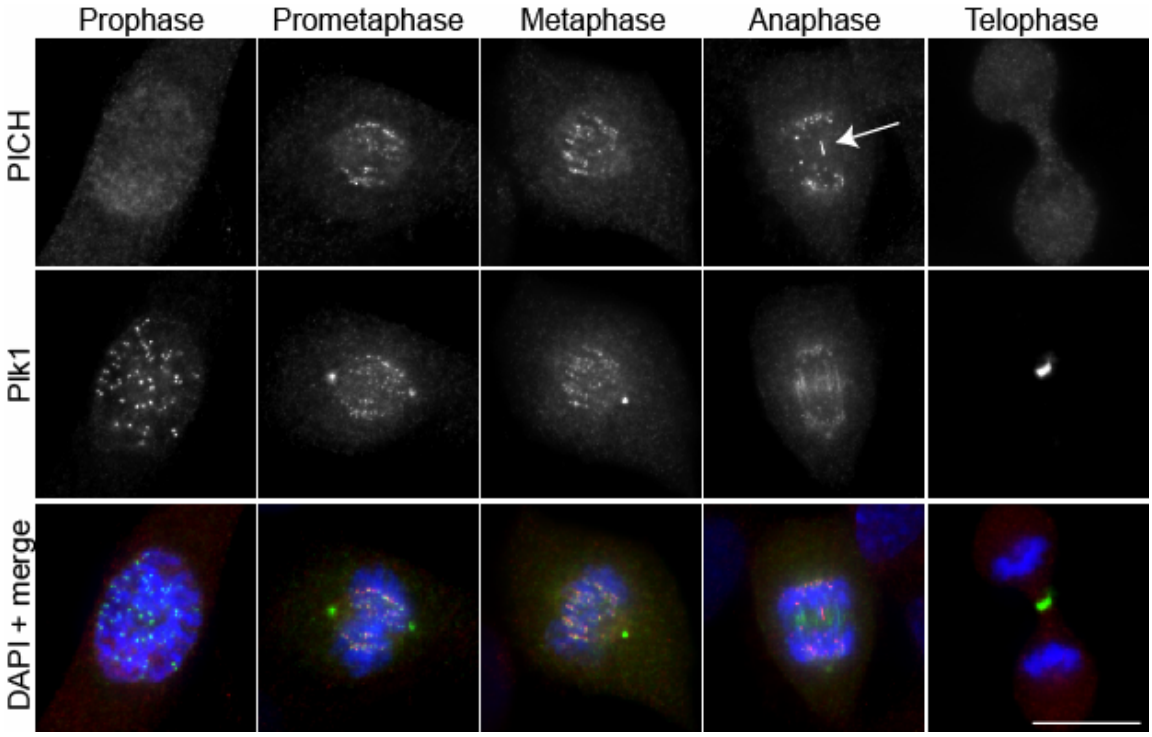

Figure 37. Double immunofluorescence microscopic analysis of asynchronously growing RPE-1 cells, comparing the localization of PICH and Plk1 at different mitotic stages. Merged images show Plk1 in green, PICH in red and DNA (DAPI staining) in blue. The arrow marks a typical PICH-positive thread in an anaphase cell. Bar, 10µm.

Plk1 phosphorylation removes PICH from chromatid arms

Given that PICH is a substrate of Plk1 it appeared obvious to ask whether Plk1 might be required to regulate PICH activity and/or localization. When Plk1 was depleted by siRNA (Figure 38A and 39), PICH staining spread from the kinetochore region to chromatid arms (compare Figures 38Ab and d), with similar results in all cell types analysed (HeLa, U2OS, MCF-7, RPE-1; data not shown). This suggested that either Plk1 might prevent PICH from association with chromatid arms, or that Plk1 is required to remove PICH from chromatin. Alternatively Plk1 could regulate PICH protein levels / degradation, resulting in increased PICH levels and arm distribution.

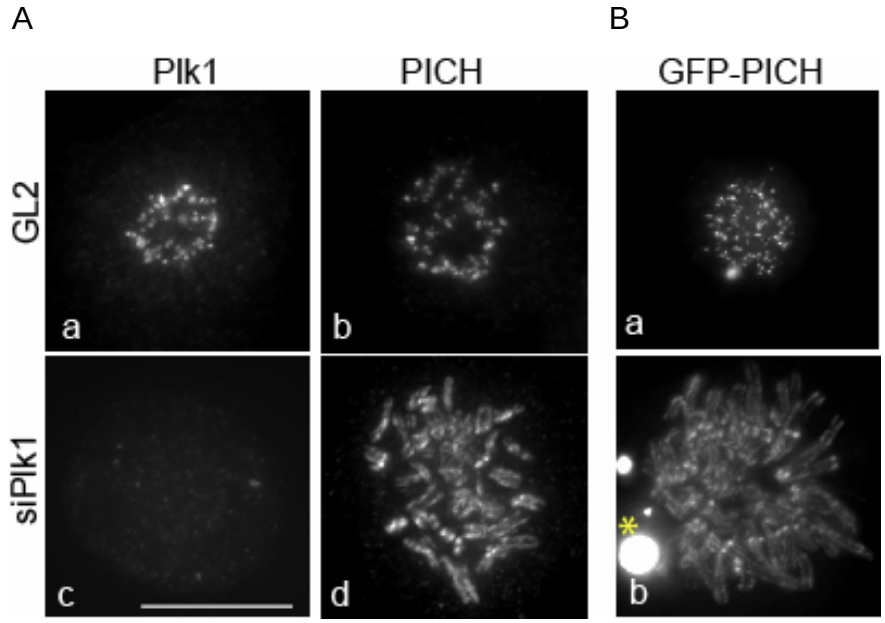

Figure 38. A) HeLa cells were treated with a siRNA duplex specific for Plk1 or GL2 for control before PICH and Plk1 were localized by immunofluorescence. Note spreading of PICH to chromatid arms in the absence of Plk1. Bar, 10µm. B) Overexpression of GFP-PICH in HeLa cells at low (a) and high (b) expression levels. Note spreading of excess PICH to chromatid arms. The asterisk denotes a GFP-PICH aggregate that was frequently observed in these transfections.

To further investigate PICH localization, GFP-tagged PICH was overexpressed in HeLa cells and its distribution observed under fluorescent light. Interestingly, when GFP-PICH was expressed at low levels it remained concentrated at kinetochores, similar to the distribution of the endogenous protein (Figure 38Ba). However, overexpression at higher levels resulted in the spreading of GFP-PICH to chromatid arms like in Plk1 depletion, suggesting that excess PICH could override a restraining influence of Plk1 (Figure 38Bb).

To rule out that Plk1 depletion caused an accumulation of PICH protein, PICH levels were compared in Plk1 depleted and nocodazole arrested cells, as well as in cells depleted of the kinesin-related motor Eg5 (which results in a similar mitotic arrest). As shown by Western blotting, Plk1 depletion did not cause an accumulation of PICH (Figure 39, right panel). Instead, the electrophoretic mobility shift of mitotic PICH was lost upon depletion of Plk1 (but not of Eg5), indicating that it depends on Plk1 activity. Thus Plk1 appeared to regulate the mitotic localization of PICH but not its abundance.

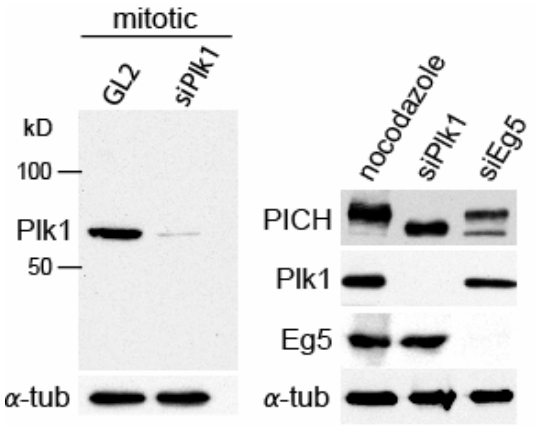

Figure 39. Left panel: Effective depletion of Plk1 from HeLa cells by 48 hrs siRNA treatment is shown by Western blotting. α-tubulin levels provide a loading control. Right panel: PICH mobility but not abundance is regulated by Plk1. Western blotting was used to compare levels and electrophoretic mobility of endogenous PICH protein in lysates of Plk1 or Eg5 depleted cells as well as nocodazole arrested cells (top row). Efficient depletion of Plk1 and Eg5 by siRNA is documented below and equal loading is shown by probing for α-tubulin (bottom row).

If PICH is a Cdk1 dependent substrate of Plk1 *in vitro*, it might be possible that the phosphorylation of PICH by Plk1 is required to regulate PICH chromatid arm localization *in vivo*. To answer this question, two types of co-transfection experiments were performed: First, the localization of PICH was analyzed in Plk1 rescue experiments using different Plk1 rescue constructs (Figure 40). Cells were depleted of Plk1 using a small hairpin plasmid (shRNA) and co-transfected with rescuing plasmids of Plk1wt, Plk1-PBD mutant (H538A, K540A), a Plk1 kinase mutant (K82R) and a fragment of the catalytic domain only (Hanisch et al., 2006).

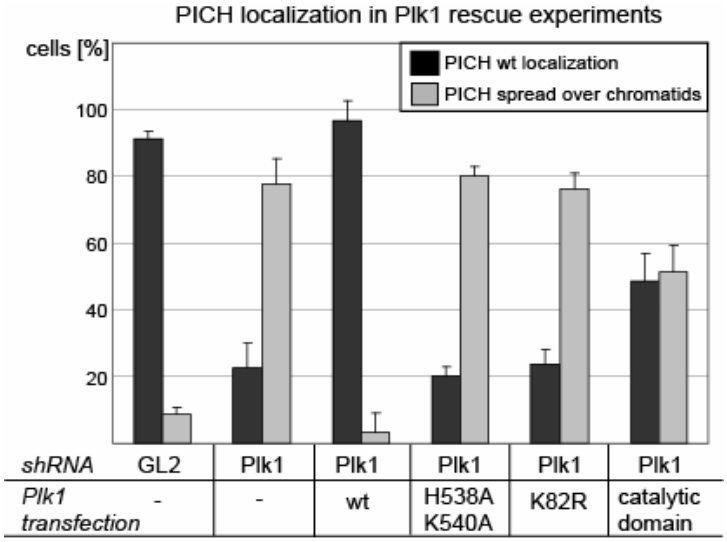

Figure 40. Rescue experiments confirm the role of Plk1 in determining PICH localization. HeLa cells were cotransfected with Plk1 or GL2 control shRNA Plasmids and the indicated myc-tagged Plk1 constructs. Cells were fixed after 48h and co-transfected cells were analyzed for PICH arm/kinetochore localization. Histogram summarizes the results of 3 independent experiments (n=150-170) and bars indicate standard deviations.

As summarized in Figure 40, only wt Plk1 was able to restore the typical concentration of endogenous PICH at kinetochores, whereas PBD and kinase mutants were unable to interfere with PICH arm localization. The catalytic domain alone produced an intermediary phenotype, suggesting that PICH could also be phosphorylated and regulated by an excess of unbound Plk1.

In a complementary experiment, wt or T1063A mutant GFP-PICH proteins were co-expressed in U2OS cells with either mycPlk1 T210D (constitutively active kinase) or mycPlk1 K82R (inactive kinase). Only the constitutively active Plk1 was able to prevent GFP-PICH from spreading to chromatid arms and this regulation required the presence of the PBD docking site on PICH (Figure 41). Collectively, these data demonstrate that the recruitment of Plk1 to PICH and the ensuing phosphorylation regulate the localization of PICH on mitotic chromosomes.

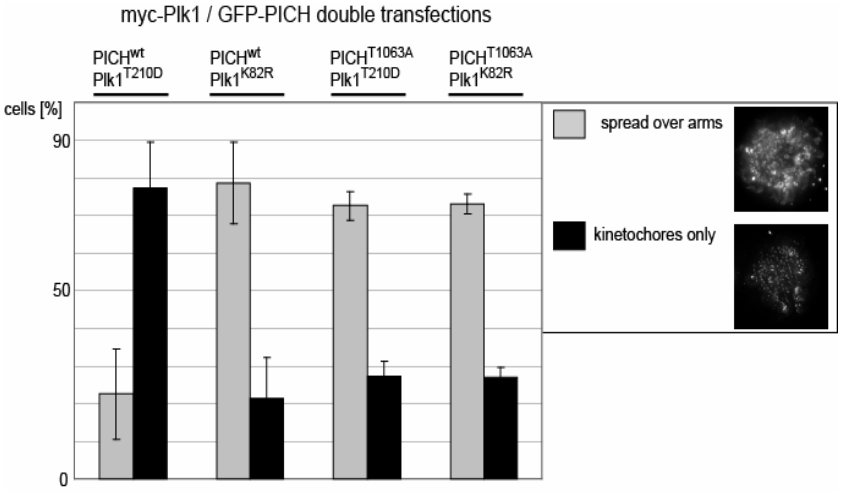

Figure 41. GFP-PICH^{wt} or GFP-PICH^{T1063A} were cotransfected for 48 hours with either myc-Plk1^{T210D} (constitutively active) or myc-Plk1^{K82R} (kinase dead) into U2OS cells. After fixation cells were stained with anti-myc antibodies and only double-transfected cells were analyzed for GFP-PICH staining over chromatid arms or kinetochores only (see insets below). Histogram summarizes results obtained from 3 independent experiments (n=75 for each experiment) and bars indicate standard deviations.

Interestingly, whenever PICH was present at chromatid arms, its localization was very reminiscent to that of Topoisomerase II, a marker of chromatid axes (Earnshaw et al., 1985; Gasser et al., 1986) (Figure 42), raising questions as to functional interaction of these proteins.

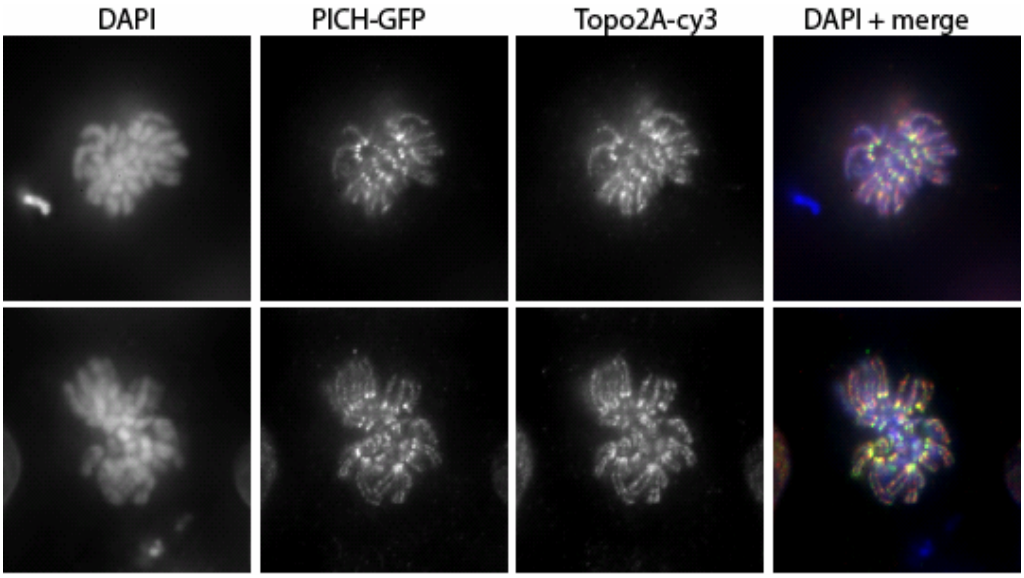

Figure 42. Two examples of GFP-PICH co-localization with Topoisomerase II in prometaphase.

Requirements for PICH localization

Next, further requirements for the localization of PICH were examined by expressing various GFP-tagged PICH fragments in U2OS cells (Figure 43) and analyzed for their localization. As shown above in HeLa cells, GFP-PICH wt was able to localize to both kinetochores and chromatin arms in U2OS cells.

A

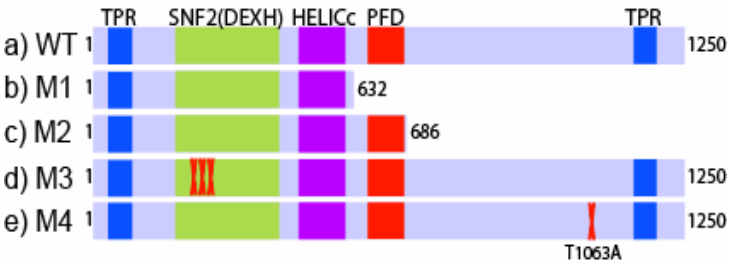

B

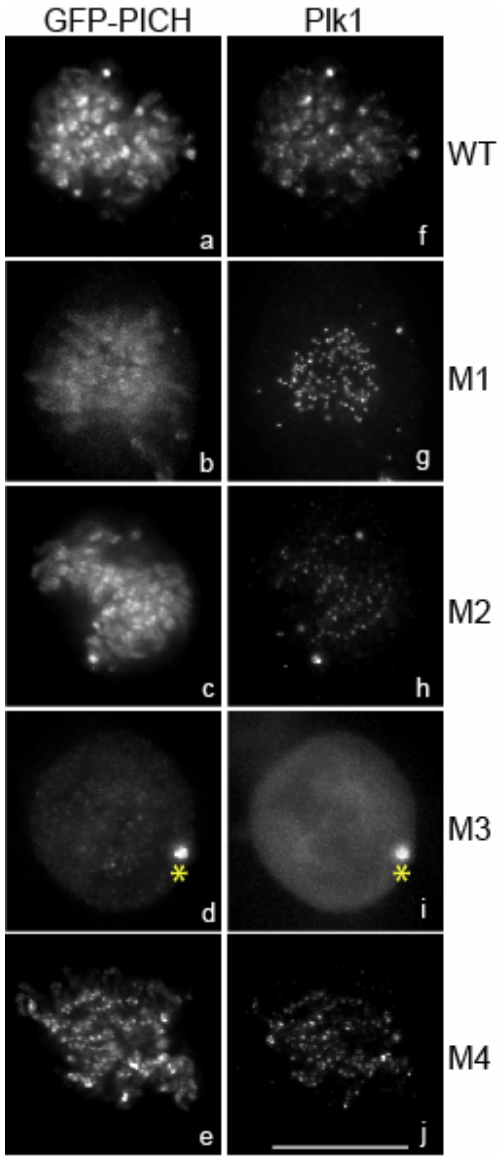

Figure 43. A) Schematic illustration of different GFP-PICH constructs analysed in B). M1-M4 refer to the same mutants in both panels. B) Wild-type and mutant GFP-PICH proteins were transfected into U2OS cells (left column) and these were counterstained with antibodies against Plk1 (right column, f-j). Asterisks in panels d and I point to a GFP-PICH aggregate, to which Plk1 is recruited. Bar, 10µm.

This localization could be observed also after overexpression of the N-terminal helicase domain alone (aa1-686). However, this wt localization required the presence of the PFD motif. In contrast, a fragment lacking the PFD helicase extension (aa1-632) associated with chromatin only in a diffuse manner. In agreement with an important role of the helicase domain in PICH chromatin localization, mutational inactivation of the Walker A nucleotide binding motif (GKT->AAA) completely abolished PICH localization. Overexpression of the T1063A mutant showed kinetochore and chromatid arm distribution comparable to wt PICH.

Examination of Plk1 localization by counter-staining of cells transfected with GFP-PICH constructs by anti-Plk1 antibodies revealed that Plk1 was recruited to wt PICH over chromatin arms (Figure 43f). Similarly, the Walker A mutant (GKT to AAA) caused extensive sequestration of Plk1 to both the cytoplasm and PICH aggregates (Figure 43i). Mutants lacking the C-terminal PBD-binding domain (M1 and M2) or carrying a mutation in T1063 (M4), however, were unable to significantly affect Plk1 localization (Figure 43g, h and j). These data demonstrate that an intact PICH 'helicase' domain including the extended PFD motif is critical for PICH localization and they further confirm that Plk1 interacts with PICH *in vivo*.

Further requirements for PICH localization might be (upstream) components of the centromere/kinetochore. To find proteins that are required for the localization of PICH, we depleted a variety of candidates by siRNA and tested for PICH localization in immunofluorescence. As PICH showed similar subcellular distribution to chromatid axes as Topoisomerase II when either PICH regulation by Plk1 was prevented or when PICH was overexpressed at higher levels (Figure 38 and 42), Topoisomerase II and Plk1 were also included in this siRNA analysis. Strikingly, siRNA depletion experiments of either Cdc14 or AuroraB resulted in the mislocalization of PICH and Topoisomerase II from kinetochores (table 4 and Figure 44). These data suggest that PICH and Topoisomerase II localization may, directly or indirectly, require coregulation by these enzymes. Moreover, the depletion of Hec1 resulted in a significant reduction of PICH signal from centromeres/kinetochores. Having shown that PICH kinetochore/centromere association requires an extended helicase domain comprising the PFD domain (Figure 43), this raises the question whether the specific PICH kinetochore and/or centromere recruitment might require protein-protein interactions between

PICH/the PFD and the Ndc80 complex or its downstream effectors. On the other side, long nocodazole treatment leads to reduced PICH centromere/kinetochore signals, which might be reflected in the Hec1 siRNA situation, where microtubule attachments are impaired (DeLuca et al., 2003).

	localization		
	Plk1	PICH	TopoIIa
siAuroraB	-	-	-
siHec1	-	-	
siPlk1	-	++	+
siCdc14		-	-
siPICH	+	-	-
siCenP-E	+	+	
siBub1	+	+	
siSgo1	-	+	+

Table 4. Summary of several siRNA experiments: the localization of Plk1, PICH and Topoisomerase II was analyzed in various siRNA depletion backgrounds. – indicates mislocalization, + indicates unaltered localization compared to GL2 control (wt), ++ stands for the PICH redistribution over chromatid arms.

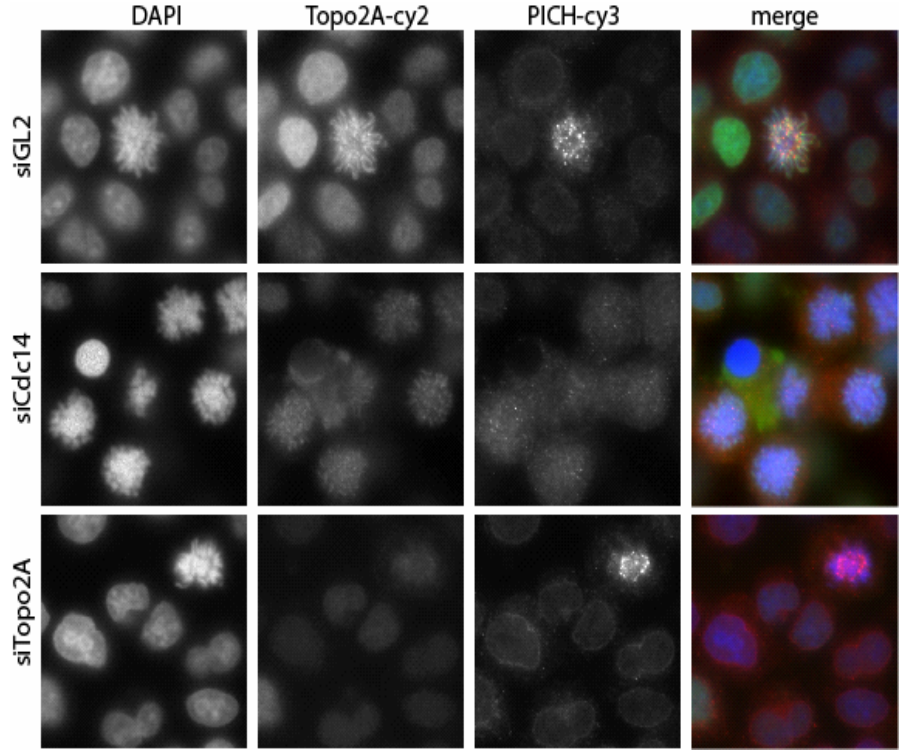

Figure 44. Immunofluorescence of Topoisomerase II (green) and PICH (red) in HeLa cells treated with siRNA targeting Cdc14, Topoisomerase II and GL2 control, respectively. DAPI is visualized in blue. Note that PICH and Topoisomerase chromatin localization is strongly reduced in siCdc14.

PICH reveals inter-kinetochore threads in anaphase

As mentioned above (Figure 36), anti-PICH antibodies stained conspicuous threads in mitotic cells. Shown in Figure 45, numerous but short PICH-positive threads could be seen already in metaphase cells where they connected Hec1-positive kinetochores of nearly all sister chromatids (a).

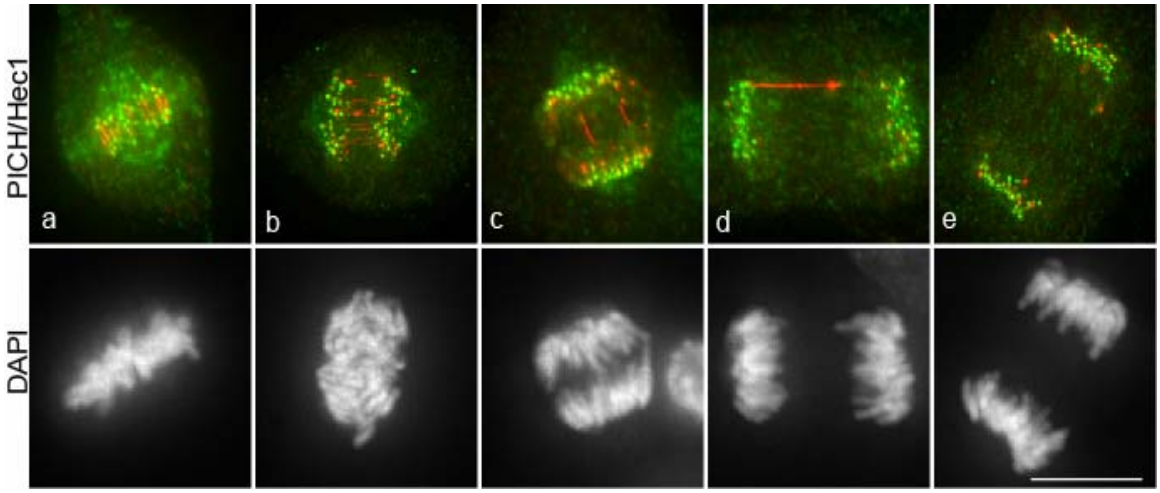

Figure 45. Immunofluorescent staining of PICH-positive threads (red) during mitotic progression, from left (prometaphase) to right (late anaphase/telophase), documenting progressive lengthening and concomitant loss of threads. Kinetochores are co-stained with antibodies against Hec1 (green). DAPI staining for DNA is shown below. Bar, 10µm.

Closer analysis of metaphase cells and co-localization studies with Hec1, a marker of the outer kinetochore plate (Ciferri et al., 2005; DeLuca et al., 2005), and Borealin, a marker of the inner centromere (Vagnarelli and Earnshaw, 2004), showed that PICH associates mostly with internal kinetochore structures and the centromeric region (Figure 46), often reminiscent of a “dumb bell”.

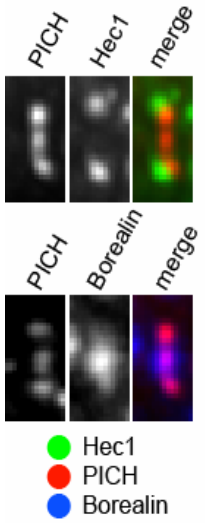

Figure 46. Metaphase HeLa cells were co-stained with the indicated antibodies to allow for a high resolution analysis of PICH localization (red) in comparison to Hec1 (a marker of the outer kinetochore plate; green) and Borealin (a marker for the inner centromere; blue).

When cells further progressed through anaphase (Figure 45b and c) the threads became progressively longer and, concomitantly, their number diminished, so that they were absent by telophase (Figure 45e). Occasionally, though, long threads could still be seen to connect Hec1-positive kinetochores in late anaphase cells (Figure 45d). Figure 47 shows a quantitative analysis of the length of these threads, along with their frequency, in cells at representative mitotic stages.

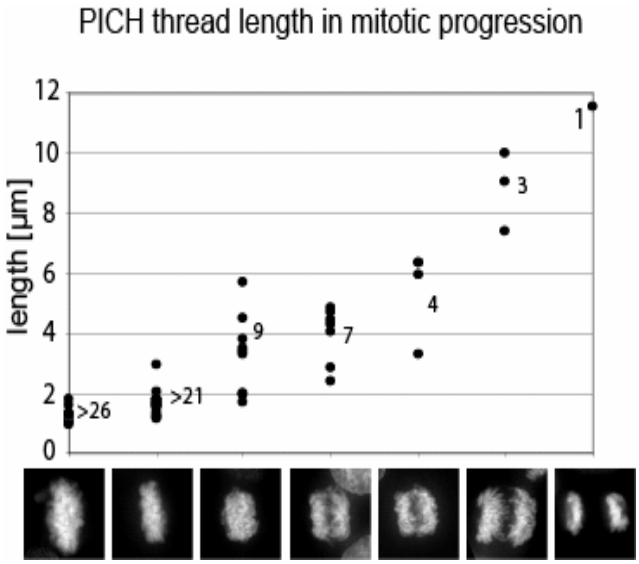

Figure 47. Quantification in U2OS cells confirms that PICH threads are progressively stretched and resolved during anaphase.

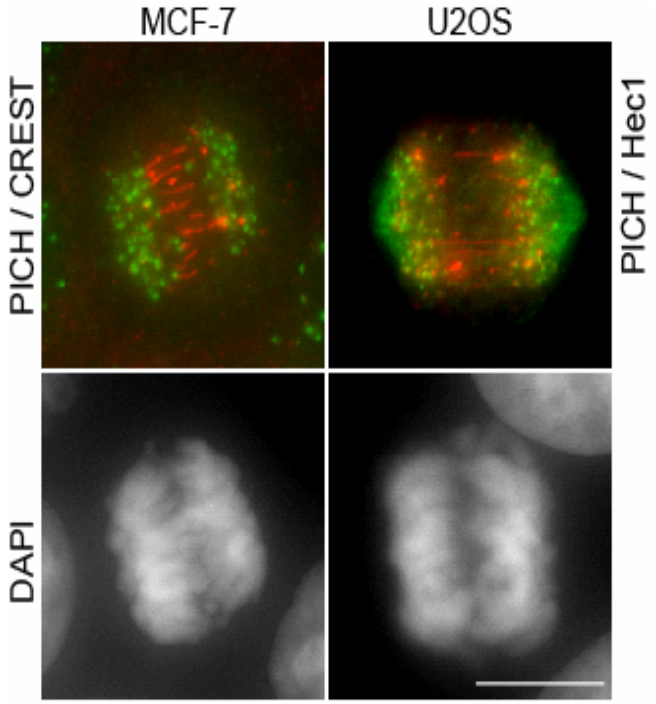

Figure 48. Anaphase cells in MCF-7 and U2OS populations were fixed and permeabilized using paraformaldehyde/Triton-X-100 (Stucke et al., 2002), before they were co-stained with rat anti-PICH antibodies (serum 1:1000; red) and CREST serum (green). DNA was stained with DAPI (blue).

As the appearance of PICH threads in anaphase is a suprising and new results, different cell lines were analyzed to exclude that this might be a HeLa specific artifact. However, PICH-positive threads were seen in all cells examined, both non-transformed (RPE-1)(Figure 45) and transformed (MCF7, U2OS, Cos-7, HeLa) (Figure 48), with all four different rat and rabbit anti-PICH antibodies (Figure 49).

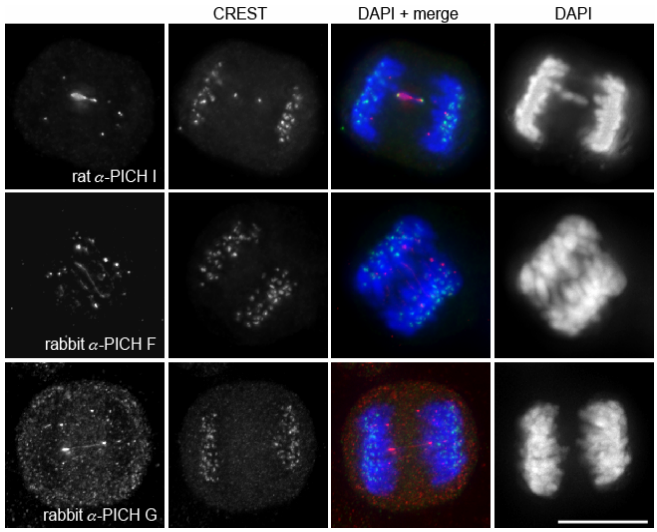

Figure 49. Visualization of PICH positive threads by three further polyclonal antibodies. Asynchronously growing HeLaS3 cells were fixed and stained for CREST (green), PICH (red) and DNA (blue; DAPI). Bar, 10µm.

The visualization of these PICH-positive threads did not require any deconvolution or data processing (Figure 48, pictures are neither deconvolved nor processed). Also, qualitatively identical results were obtained when using alternative fixation procedures (e.g. 3 % paraformaldehyde (10 min) followed by Triton-X-100 (0.5 %, 10 min) or methanol (10 min, -20^{o}C).

Further supporting evidence that these threads reflect real structures comes from GFP-PICH transient transfections in HeLa (Figure 50) and U2OS cells (data not shown). In these experiments GFP-PICH could be directly observed at sister kinetochore connecting threads in metaphase/anaphase, excluding that PICH threads are an artefact of antibody crossreactivity.

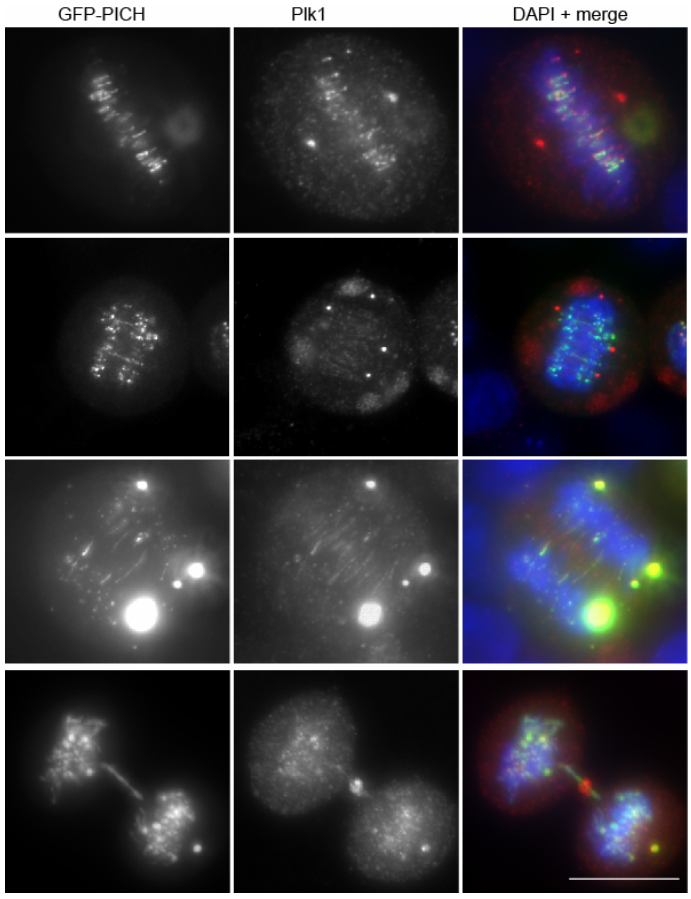

Figure 50. Visualization of PICH positive threads by GFP-PICH (green). HeLaL cells were transfected for 36h with an expression plasmid carrying GFP-PICH^{wt}. Cells were fixed and stained for Plk1 (red) and DNA (blue, DAPI). Bar, 10µm.

PICH positive threads are catenated, centromere-related, sister kinetochore connecting chromatin

The discovery of PICH threads required further analysis as to what specific structure they might reflect. Considering the helicase motif of PICH and that threads frequently connect sister kinetochores, the two most obvious models were explored further. a) PICH might associate with lagging chromosomes in anaphase, or b) PICH might associate with stretched centromeric chromatin forming at metaphase. To first examine a possible relationship between PICH-positive threads and lagging chromosomes, we increased the frequency of chromosome segregation errors by siRNA-mediated depletion of Mad2. This interference with spindle checkpoint function did not reveal any obvious relationship between PICH-positive threads and lagging chromosomes (Figure 51A). Next, we tested the

possibility that PICH-positive threads represent stretched chromatin extending between sister kinetochores. If this were the case, one would predict that the premature removal of centromeric cohesin should enhance thread formation. Indeed, when premature loss of centromere cohesion was induced by siRNA-mediated depletion of Sgo1 (Salic et al., 2004), a massive enhancement of PICH-positive threads was seen (Figure 51B). Further illsutration of the intriguing localization of PICH threads is shown in Figure 52, where images from Sgo1 depleted Hela cells were greatly magnified. In these photos threads reached lengths of several µm and often connected sister kinetochores (Figure 52), supporting the view that they represent stretched centromere-related chromatin.

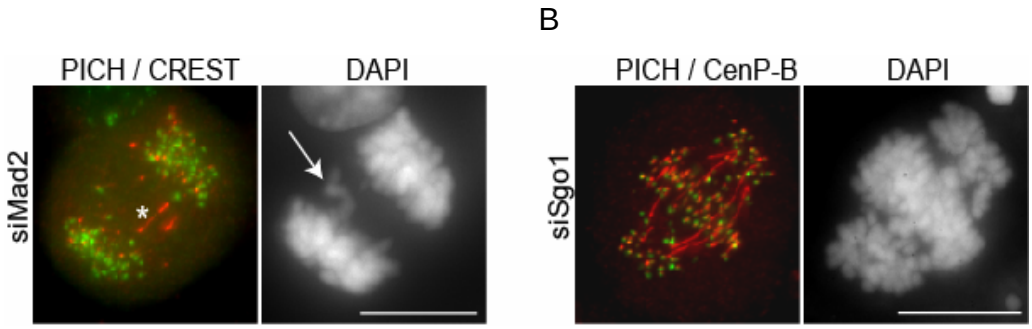

Figure 51. A) To induce lagging chromosomes, HeLa cells were subjected to Mad2 siRNA (36 h) before they were co-stained with anti-PICH antibodies (red) and CREST anti-Kinetochore serum (green). DNA in the same cell was stained by DAPI (right panel); notice lack of co-localization between PICH-positive thread (asterisk) and lagging chromosome (arrow). Bar, 10µm. B) To induce premature sister chromatid separation, HeLa cells were subjected to Sgo1 siRNA (48 h) and then stained with antibodies against PICH and CenP-B to visualize PICH-positive threads (red) and kinetochores (green), respectively. DNA was stained with DAPI (right panel). Bar, 10µm.

Furthermore, although PICH-positive threads could not reliably be counter-stained with DAPI over their entire lengths, DAPI staining could often be seen at their ends (e.g. Figure 45d).

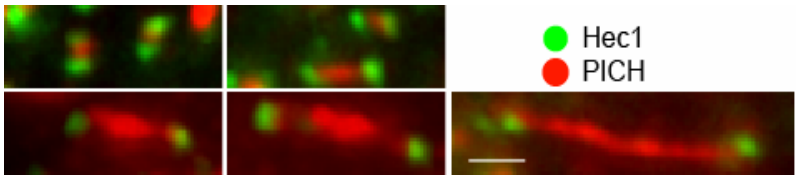

Figure 52. Sgo1-depleted HeLa cells (48 h) showing different degrees of sister chromatid separation were stained with antibodies against PICH and Hec1 to visualize PICH-positive threads (red) and kinetochores (green), respectively. Bar, 1µm.

In cooperation with Dr Valentin Nägerl (MPI of Neurobiology, Munich), 2 photon confocal microscopy on fixed, asynchronously growing U2OS cells was used to obtain high resolution images of PICH threads in colocalization with Hec1 at various stages of late mitosis. Shown below are three examples confirming previous results that PICH localizes to internal kinetochores and often decorates sister kinetochore connecting threads that disappear and stretch, beginning from early anaphase.

A) *Early anaphase*

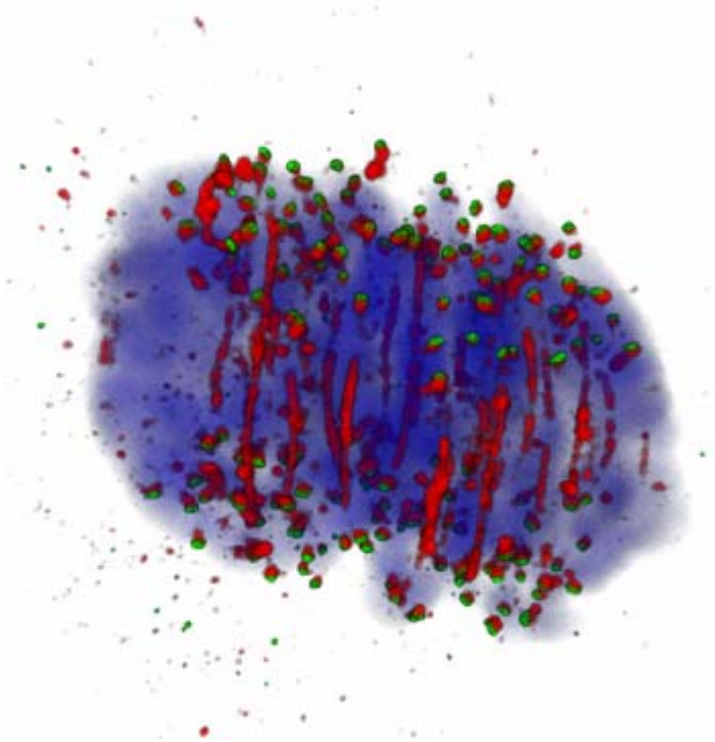

B) *Late anaphase*

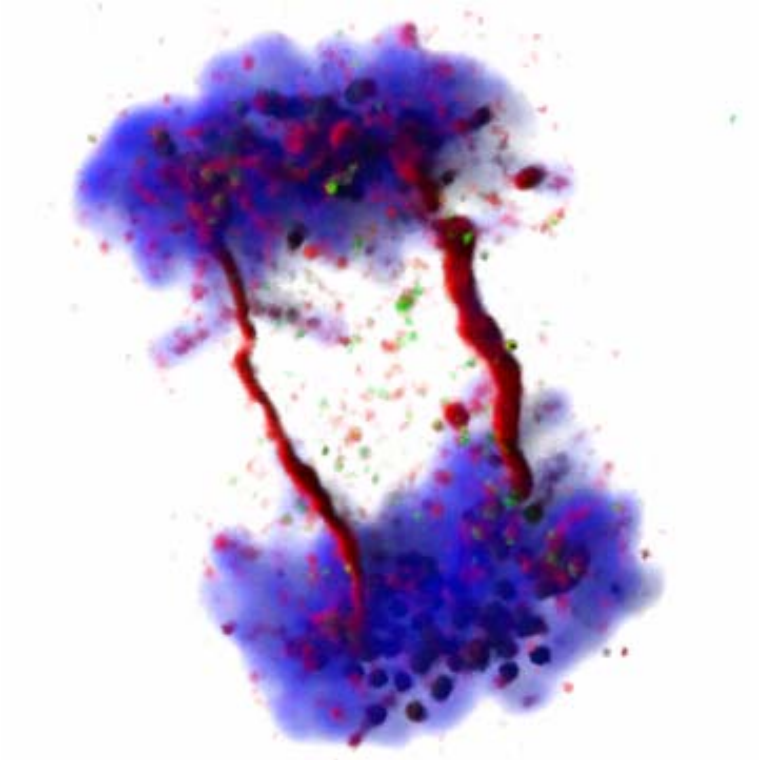

C) *Telophase*

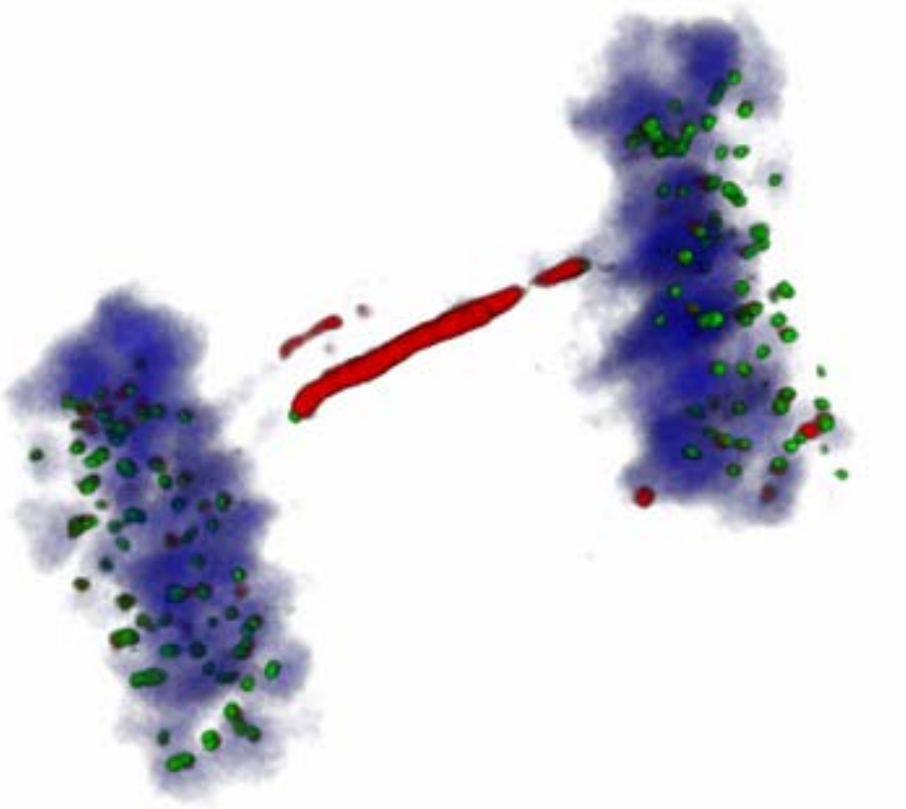

Figure 53 A-C) images were acquired with the help of Dr. Valentin Nägerl (MPI for Neurobiology) and show PICH-positive threads (red) in different stages between early anaphase and telophase. U2OS cell were counterstained for kinetochores (green) and DNA (blue). Confocal image stacks were acquired on a Leica SP2 and the images were processed and 3D rendered using the Imaris software package by Bitplane AG.

If PICH threads were to represent centromeric chromatin, they should be sensitive to DNAse treatment. Indeed, when HeLa cells - depleted of Sgo1 to induce PICH threads – were pre-permeabilized ten minutes prior to fixation and either control buffer, RNAse or DNAse was added, PICH threads rapidly disappeared from DNAse treated samples only (Figure 54), suggesting that they contain DNA.

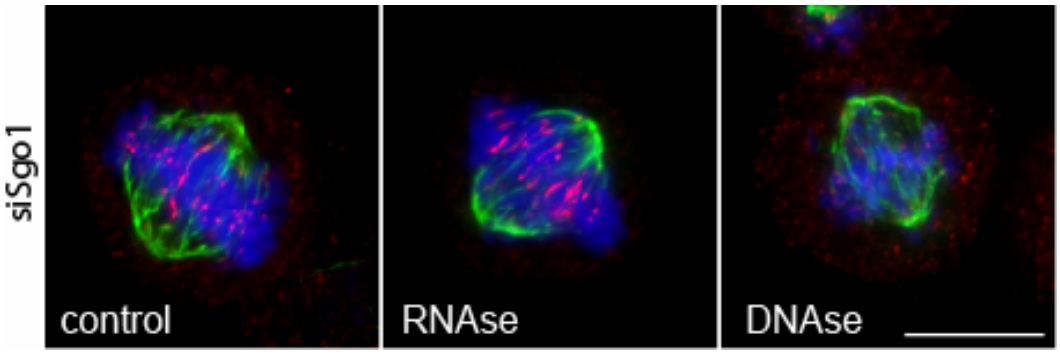

Figure 54. HeLa cells were treated for 24 h with Sgo1 siRNA, permeabilized and incubated for 12 min with buffer, RNAse or DNAase (5 μg/ml) prior to fixation. Then they were stained with antibodies against α-tubulin (green) and PICH (red). DNA was stained with DAPI (blue). Bar, 10μm.

In normal mitotic progression, PICH threads were visible in basically all post-prometaphase cells. Most striking, however, is the presence and length of threads in anaphase. Topoisomerase II is an enzyme required for the untangling of catenated DNA strands and hence is crucial for the decatenation of sister chromatids in early mitosis (Skoufias et al., 2004; Vagnarelli et al., 2004). Prompted by a previous study that Topoisomerase II is also required for sister chromatid separation during anaphase (Shamu and Murray, 1992), we asked whether the resolution of PICH-positive threads requires Topoisomerase II activity. To answer this question, indirect immunofluorescence experiments were performed in Mad2 depleted HeLa cells to avoid the early mitotic arrest typically induced by Topoisomerase II inhibition (Skoufias et al., 2004; Toyoda and Yanagida, 2006).

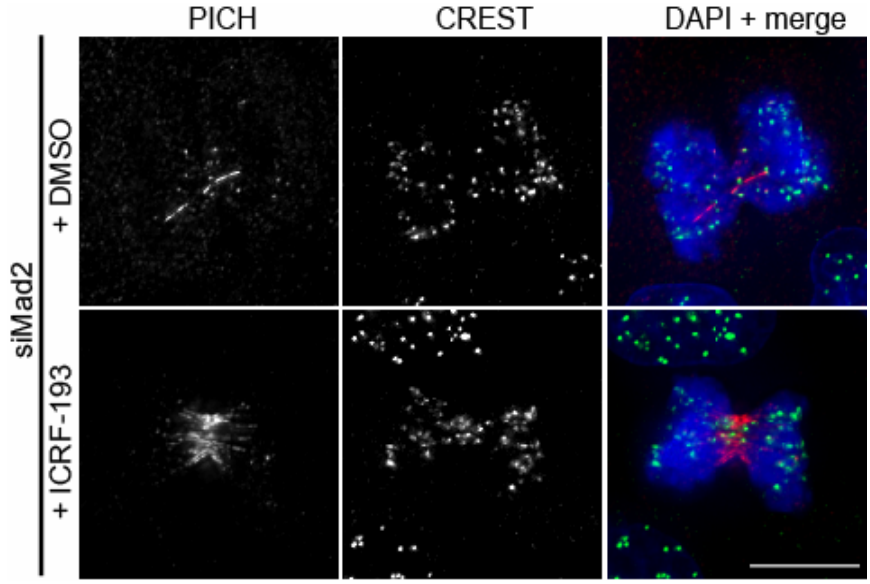

Figure 55. HeLa cells were treated for 36 h with Mad2 siRNA and, during the last three hours, the Topoisomerase II inhibitor ICRF-193 (20 µM) or DMSO were added. Then cells were fixed and stained with antibodies against CREST (green) and PICH (red). DAPI shows DNA (blue). Bar, 10µm.

Most remarkably, when DNA decatenation was inhibited by application of the Topoisomerase II inhibitor ICRF-193, PICH-positive threads became very prominent (Figure 55, and Figure 56) and persisted until cytokinesis (Figure 57). Costaining of PICH with CREST anti – centromere autoimmune serum suggested that kinetochores are mainly drawn polewards, whereas PICH threads accumulate in the area of the midzone / postmitotic bridge, suggesting that microtubules are pulling the kinetochores to the spindle poles, but the lagging and catenated DNA/threads can not be resolved.

Further colocalization analysis were carried out under the same experimental conditions with either Topoisomerase II to assess its localization under ICRF-193 inhibitor addition or with α-tubulin to confirm that PICH threads and tubulin do not colocalize.

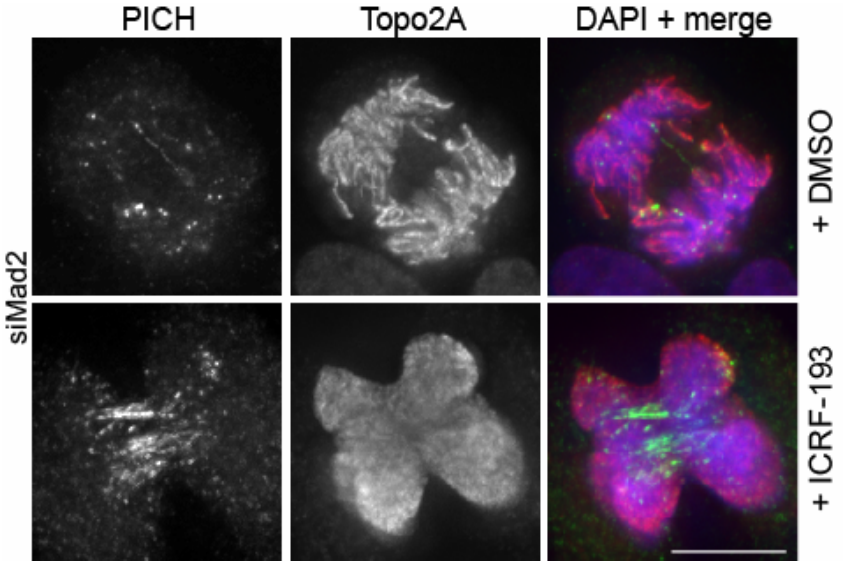

Figure 56. HeLa cells were treated for 36 h with Mad2 siRNA duplex and incubated for the last 3 h with the Topoisomerase II inhibitor ICRF-193 or solvent (DMSO). They were then fixed and co-stained with antibodies against Topoisomerase IIa (red) and PICH (green). DNA is stained with DAPI (blue). Bar, 10µm.

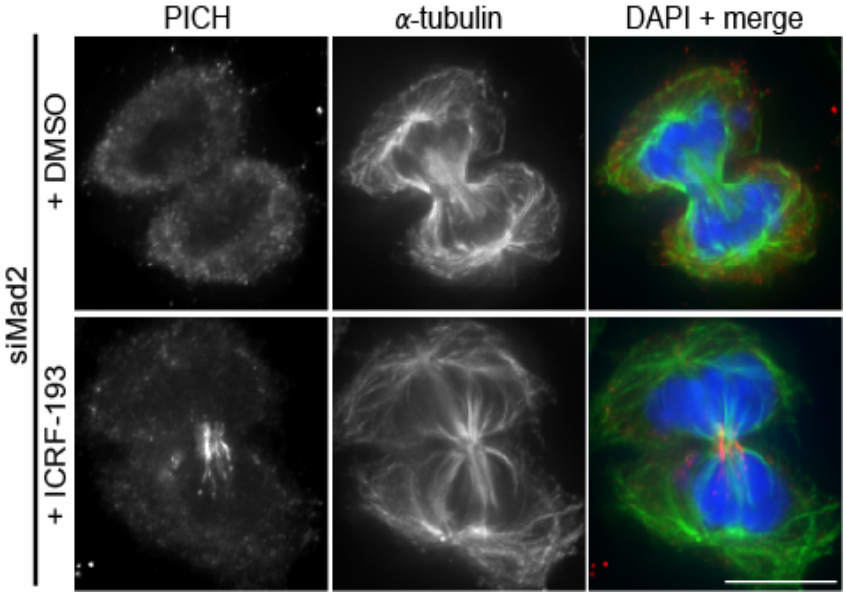

Figure 57. Cells were treated as described above, except that they were co-stained for PICH (red) and α-tubulin (green). DAPI shows DNA (blue). Bar, 10 µm.

Recent reports suggested that SNF2 type translocases depend in their mode of action and remodelling activity on the tension/torsion that is applied on their chromatin template (Lia et al., 2006; Zhang et al., 2006). This raises intriguing

questions as to the localization and action of PICH at these conspicuous threads and its dependence on thread conformation and tension status. To examine a possible influence of tension on PICH-positive threads, Sgo1 depleted cells were incubated with Taxol for 30min., an inhibitor of microtubule dynamics that is frequently used to decrease tension (Pinsky and Biggins, 2005). Under these conditions, PICH-positive threads disappeared rapidly (Figure 58), suggesting that thread formation and/or PICH recruitment to threads is sensitive to alterations in tension. These results lead to the interpretation that PICH associates with catenated centromere-related DNA that stretches under tension until decatenation by Topoisomerase II causes its resolution during anaphase.

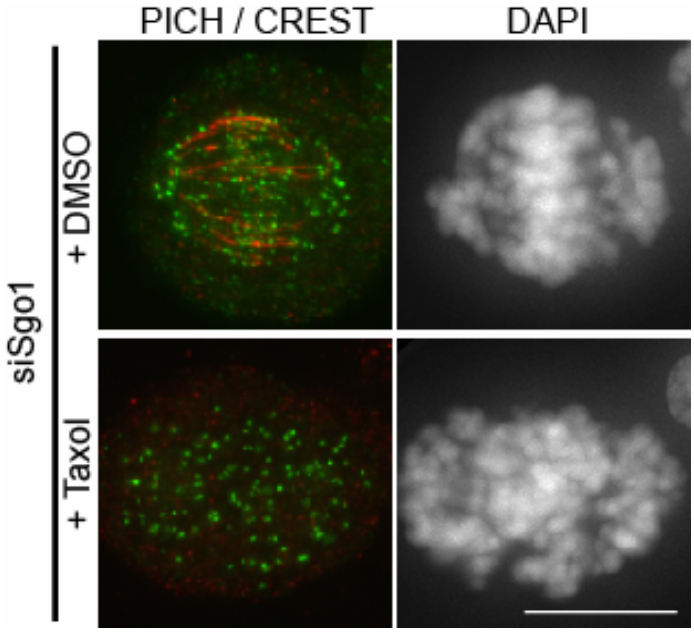

Figure 58. HeLa cells were treated for 36 hrs with Sgo1 siRNA. Then, cells were incubated for 30 min with either taxol (0.58 µM) or DMSO solvent before fixation and permeabilization. They were stained for CREST (green) and PICH (red). DNA was stained by DAPI (right panels). Note that PICH-positive threads disappeared in response to taxol. Bar, 10µm.

PICH is required for the spindle checkpoint

To explore the function of PICH, siRNA knockdown experiments were performed. Two distinct duplexes effectively depleted PICH (Figure 26) and produced virtually identical phenotypes. Compared to control treated HeLa cells (GL2), a 48 hour PICH knockdown resulted in aberrant division and extensive micronucleation, indicating that PICH is required for accurate chromosome segregation (Figure 59).

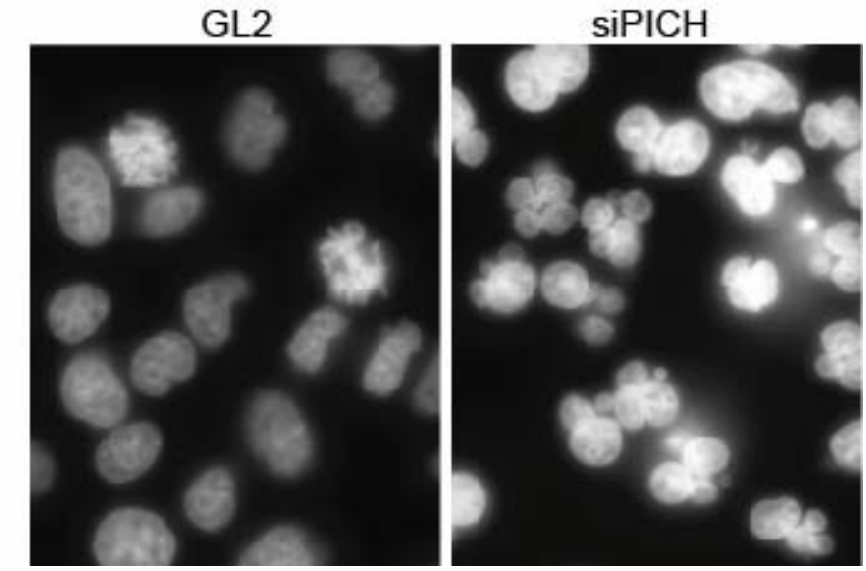

Figure 59. DAPI staining of HeLa cells treated for 48hrs with a siRNA duplex targeting PICH (right) or GL2 for control (left).

Even though unlikely due to the cytoplasmic localization of PICH in interphase (Figure 35), this SNF2 type ATPase could be involved in the establishment of cohesins in interphase which might result in a premature separation of sister chromatids and chromosome segregation defects. If PICH would be required for cohesin complex chromatin association, double depletion of PICH and Plk1 should result in a lack of sister chromatid cohesion, whereas depletion of Plk1 alone should confirm published results of persistent chromatid arm cohesion (Hanisch et al., 2006). To test this possibility, chromosome spreads were carried out in double-depleted HeLa cells with the following double siRNA treatments: PICH/GL2, Plk1/GL2, Mad2/GL2, Mad2/Plk1 and PICH/Plk1 for 48h with addition of the proteasome inhibitor MG132 for the last 3 hours to enrich for pre-anaphase mitotic cells. Inhibition of the proteasome by MG132 inhibits progression into anaphase, even if the APC/C is active, because the downstream targets CyclinB and Securin

can not be degraded by the proteasome. This results in a transient metaphase arrest before cells undergo cell death (Terret et al., 2003).

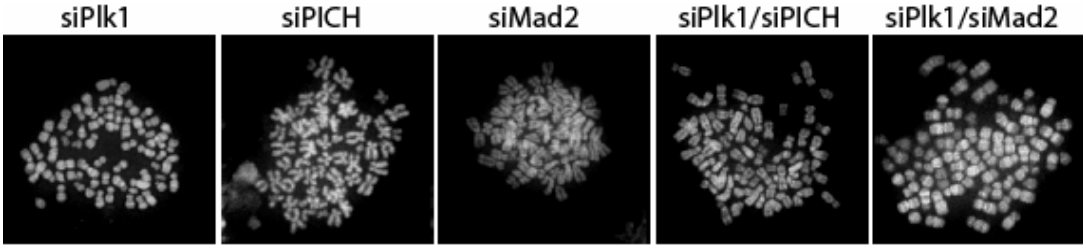

Figure 60. Chromosome spreads. HeLaL cells were treated with siRNA oligos as indicated for 48h. 3h prior to fixation MG132 was added to enrich for pre-anaphase cells. Note that siPlk1/siPICH double siRNA has mainly aligned chromatid arms, indicating that PICH is not required for the establishment of arm cohesins.

As shown in Figure 60, double depletion of Plk1 and PICH resulted in a Plk1-like phenotype with sister chromatids aligned at their arms and centromeres. The same result was obtained in a control where Plk1 and Mad2 were co-depleted. These data suggest that PICH is not required for the establishment of cohesions.

To analyse the siRNA phenotype in more detail, a HeLa cell line stably expressing GFP-tagged histone H2B was used for live cell imaging. Figure 61 shows stills from such movies, with pictures taken at the indicated time points after the start of chromosome condensation. Whereas control cells exhibited the expected congression of chromosomes to a metaphase plate, followed by the onset of anaphase (Figure 61, upper panel), PICH depleted cells separated their chromosomes without ever organizing them in a metaphase plate (Figure 61, lower panel). This could either be indicative of a defect in chromosome congression or in the inability to delay the onset of anaphase until efficient metaphase plate formation can be achieved. A disability to delay anaphase can be quantified, hence several time-lapse images of PICH and control depleted cells acquired by live cell imaging were analyzed for the time cells spent between chromosome condensation and the onset of anaphase. The average time elapsed was 33 min (range 22-90 min) for control cells but only 19 min (range 14-26 min) for PICH depleted cells (Figure 62).

This clearly suggests a defect of PICH depleted cells in mitotic timing. Because the timing of anaphase onset is controlled by the spindle assembly

checkpoint, the above results strongly suggested that PICH is required for spindle checkpoint function.

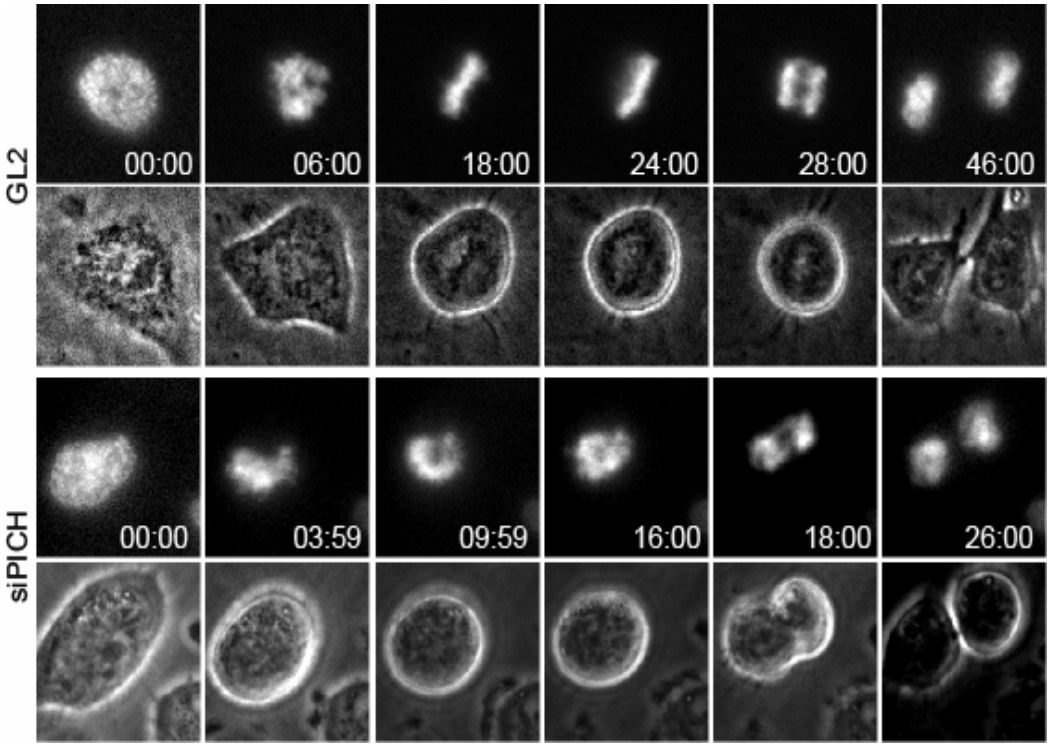

Figure 61. Representative stills illustrating mitotic progression in cells treated as described in B. Pictures were taken at the indicated time points after the onset of chromosome condensation.

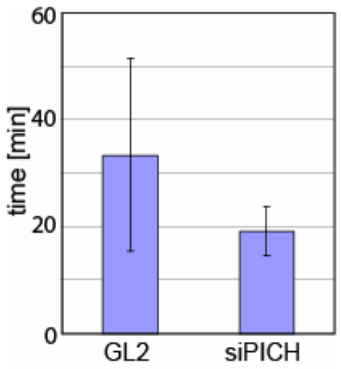

Figure 62. Histogram illustrating time elapsed between the beginning of chromosome condensation and the onset of anaphase in cells treated for approx. 36 hrs with GL2 or PICH siRNA duplexes. Data were collected by live cell imaging (N=36 cells; 5 different movies; bars indicate standard deviation).

Next a direct requirement for PICH in the spindle assembly checkpoint was tested. HeLa cells were depleted by siRNA specific for PICH or GL2 control, respectively, and treated with either nocodazole or monastrol for the last 12h. Both these compounds are commonly used to probe spindle checkpoint function in response to lack of microtubule attachment and/or tension (reviewed in (Pinsky and Biggins, 2005)). Fixed cells on coverslips were then quantified for the amount of mitotic, interphase or micronucleated cells. Strikingly, PICH depleted cells were unable to undergo a mitotic arrest in response to either drug, clearly suggesting a requirement of PICH in the spindle checkpoint, as summarized in Figure 63.

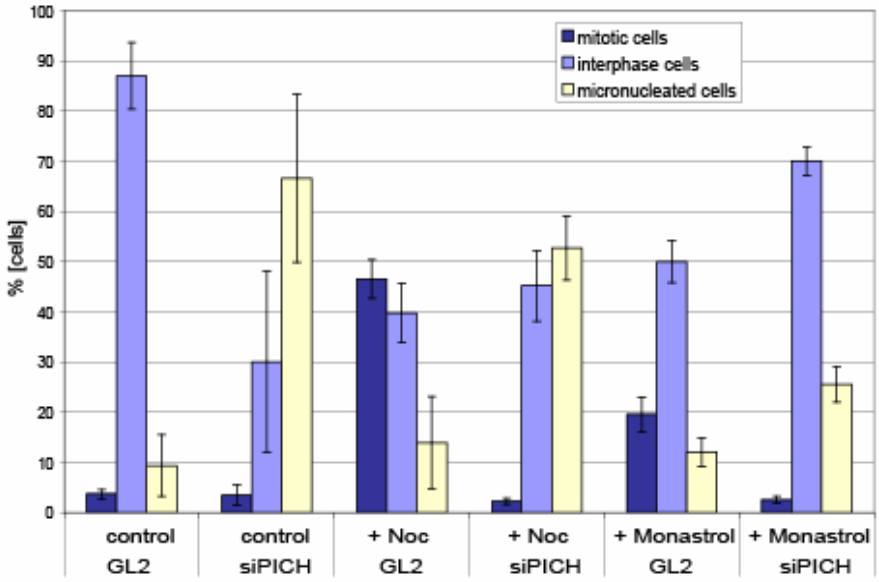

Figure 63. To study the SAC response of cells treated for 48 hrs with PICH or GL2 siRNA duplexes, nocodazole or monastrol were added during the last 12hrs of the incubation. DNA morphology was then analysed by DAPI staining and immunofluorescence microscopy and classified as interphase cells, mitotically arrested cells (indicative of a functional SAC) or micronucleated cells (indicative of checkpoint override). Histograms summarize the results of 3 independent experiments (with at least 250 cells counted for every column in each experiment) and bars indicate the standard deviation.

To corroborate our finding that PICH has a role in SAC signalling, PICH depleted cells were analyzed for possible effects on the most downstream effectors of the spindle assembly checkpoint by immunofluorescence. Of the well known spindle checkpoint proteins Mad1, Mad2 and BubR1, only Mad2 was selectively lost from

the kinetochores of PICH depleted cells (Figure 64). Interestingly Mad1, the binding partner of Mad2 at the kinetochores (Musacchio and Hardwick, 2002), was still present.

The loss of Mad2 from kinetochores in PICH depletion could be either due to a requirement for PICH in Mad2 recruitment or to PICH regulating the abundance of Mad2 protein in mitotic cells. However, Western blot analysis of siRNA depleted cells that were arrested in mitosis by addition of the proteasomal inhibitor MG132 for the last 3 hours, revealed that the abundance of Mad2 and Mad1 was not affected (Figure 65).

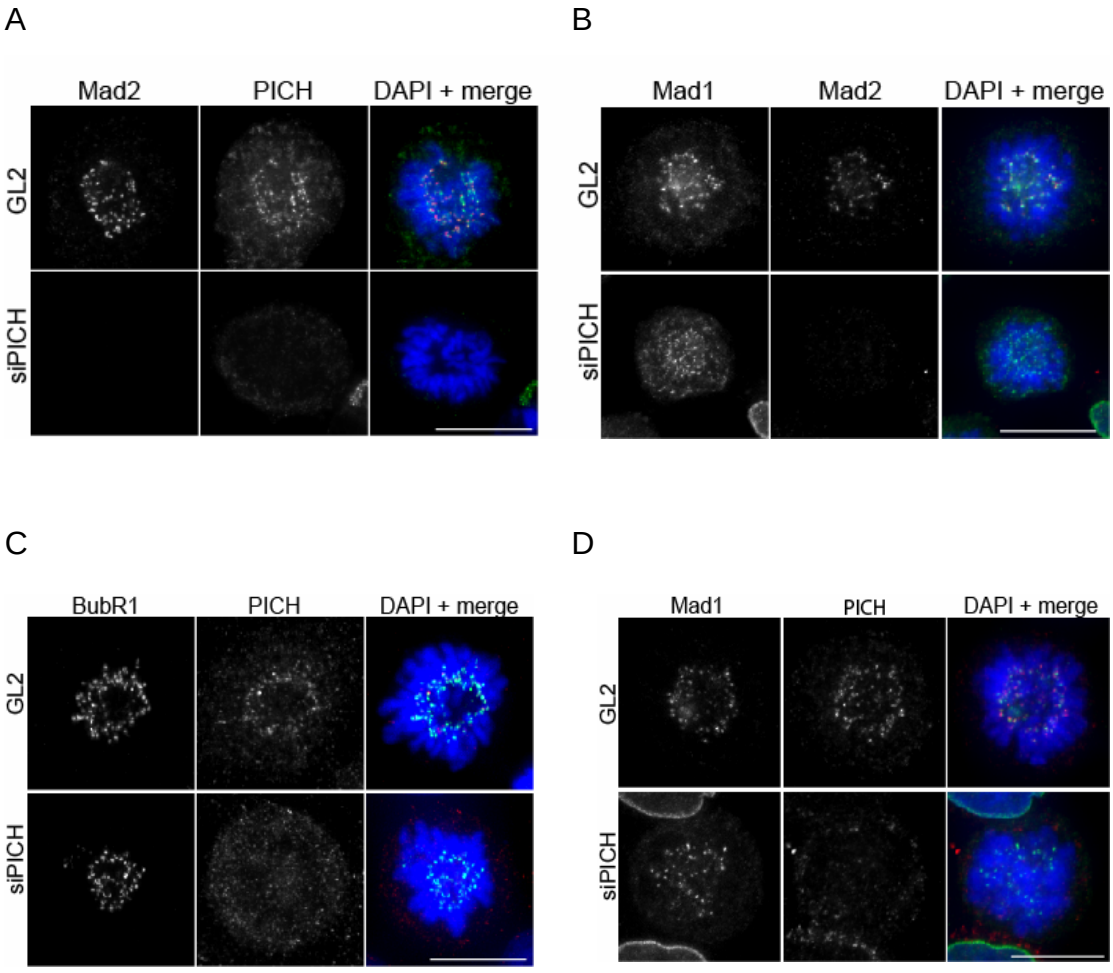

Figure 64. A-D: HeLa cells were treated for 48 hrs with PICH siRNA or GL2 control, before the localization of the Cdc20 inhibitors Mad2 and BubR1 or the Mad2 interactor Mad1 in PICH depleted prometaphase-like cells was examined by immunofluorescence microscopy. DNA is stained by DAPI (blue). Bar, 10µm. A,B,D) Mad2 is mislocalized from kinetochore in PICH depleted cells whereas Mad1 remains unaffected. C) PICH depletion has no effect on BubR1 localization. Bar, 10 µm.

To analyze whether Mad2 kinetochore localization directly requires the presence of PICH at kinetochores, siRNA depleted cells were treated with nocodazole for 30min. to depolymerize microtubules and subsequently induce recruitment of Mad2 to kinetochores (reviewed by (Pinsky and Biggins, 2005). Cells were arrested in mitosis by 3h MG132 treatment. Control cells but not PICH depleted cells (Figure 54) showed Mad2 kinetochore localization, confirming that PICH is required for the recruitment of Mad2 to kinetochores. Considering that Mad2 is a known interactor of Cdc20 and inhibitor of the APC/C (Fang et al., 1998; Mapelli et al., 2006; Yu, 2006) and that its loss from kinetochores often correlates with impaired spindle checkpoint function (Pinsky and Biggins, 2005), this protein plausibly constitutes one critical component (albeit perhaps not the only one) through which PICH exerts its specific effect on SAC signalling.

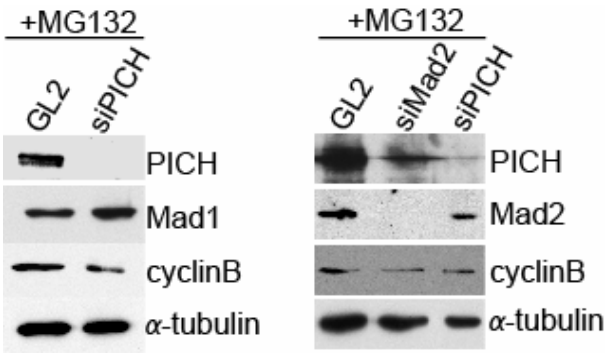

Figure 65. HeLa cells were treated for 42 hrs with PICH siRNA or for GL2 control and arrested in mitosis by addition of MG132 during the last 3 h. After shake off lysates were prepared and probed by Western blotting with the indicated antibodies.

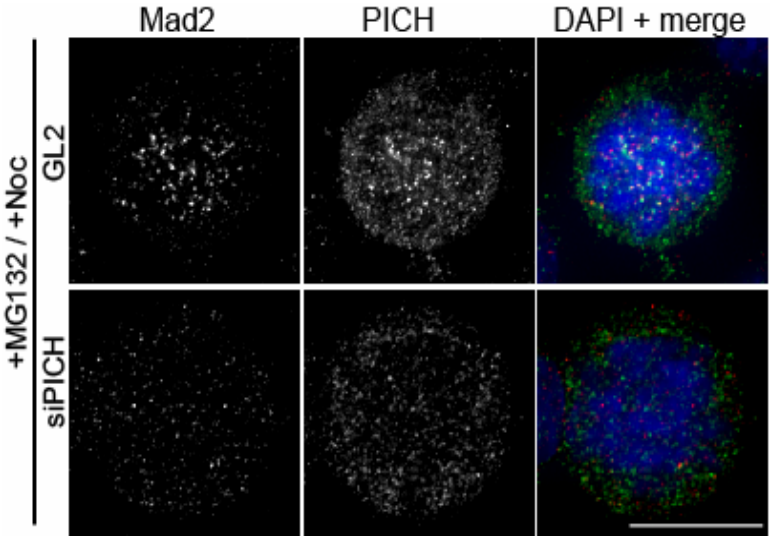

Figure 66. HeLa cells were treated as in A) but, prior to fixation, the proteasome inhibitor MG132 was added for 3h and nocodazole (100ng/ml) for the last 30 min. Then, cells were co-stained for PICH (green) and Mad2 (red). Bar, 10µm. Note that Mad2 does not return to kinetochores in the absence of PICH, even though microtubule attachment is prevented by nocodazole. (Mad2 levels in these cells are normal; data not shown, but see Figure 51).

PICH depleted cells have intact kinetochores and functional microtubule attachment

Because a loss of spindle checkpoint signalling together with the observed phenotype could also be due to a general disruption of kinetochore structure (Maiato et al., 2004; Vagnarelli and Earnshaw, 2004), we looked at the effect of PICH depletion in more detail. All together the mitotic localization of sixteen proteins representative of the outer corona, the kinetochore or the centromere were analyzed by immunofluorescence.

siPICH	Borealin	Aurora B	Incenp	Bub1	Hec1	Astrin	CenP-A	CenP-E	CenP-F	Cdc20	BubR1	Mad1	Mad2	hCap-E	Plk1	Topolla
	+	+	+	+	+	+	+	+	+	+	+	+	-	+	+	-/+

Table 5. Summary of results for all proteins analyzed as described in A: + : kinetochore staining indistinguishable from GL2 control; – : protein lost from kinetochores. -/+: Lost from kinetochores only

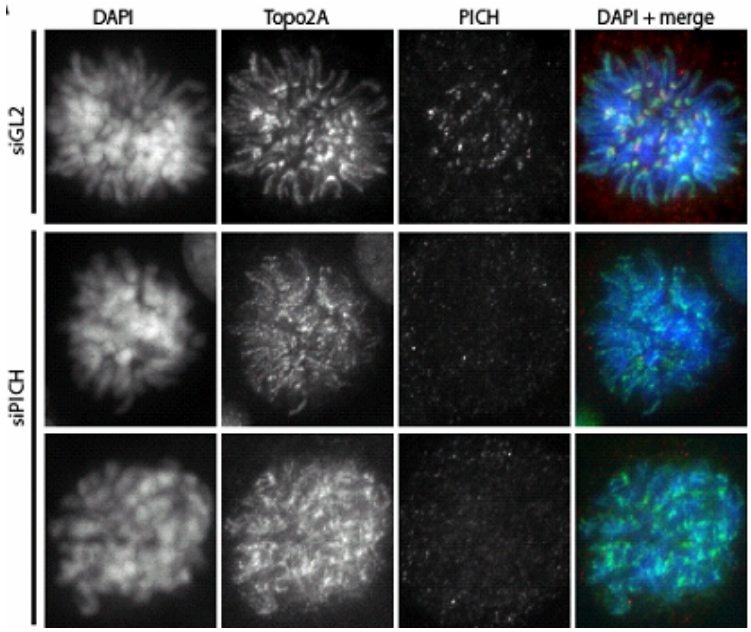

Figure 67. As summarized in table 5, the depletion of PICH (red) by siRNA from HeLa cells resulted in reduced kinetochore association and more diffuse localization of Topoisomerase II (green). DNA is visualized in blue (DAPI).

As summarized in Table 5, fourteen proteins showed wild type localization when PICH was depleted, strongly suggesting that kinetochores were intact. Quantitation of the kinetochore signals of representative proteins is shown in Table 6. As described above, only Mad2 localization was completely abolished (see Figures 64-66 and Table 5), but furthermore the depletion of PICH led to a loss of the prominent Topoisomerase II kinetochore staining in early mitosis, resulting in a readily diffuse localization over chromatids (Figure 67). This might provide further evidence for the interdependent requirement of PICH and Topoisomerase II in chromosome segregation and sister chromatid decatenation at centromeres.

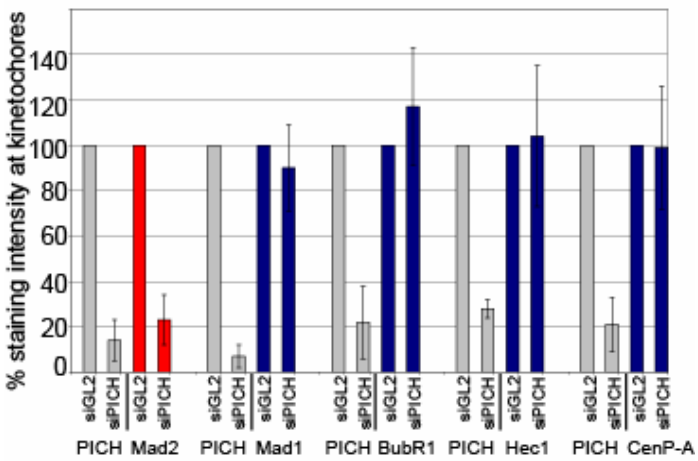

Table 6. Histograms show the kinetochore staining intensities for the 5 indicated proteins in PICH depleted cells relative to the GL2 samples (100 %), and bars indicate standard deviations. For each protein, 5 different mitotic cells were analyzed using metamorph software and intensity values in each cell were measured at 5 representative kinetochores (normalized against 5 random positions in the cytoplasm).

Additional evidence for the integrity of kinetochores and microtubule attachment could be obtained by depletion experiments under addition of the proteasome inhibitor MG132. If the inability of cells that have no PICH to build up a metaphase plate would be caused by impaired microtubule capture at kinetochores and disrupted kinetochore structure, than these cells should not be able to form metaphase plates upon addition of the proteasome inhibitor. However, like control depleted cells, MG132-arrested PICH depleted cells reacquired the ability to form metaphase plates, indicating that kinetochore-microtubule interactions were not significantly impaired (Figure 68). This result also suggests that the defects in chromosome segregation and spindle checkpoint signalling are caused by signalling components upstream of the APC/C rather than by cohesion mediating proteins.

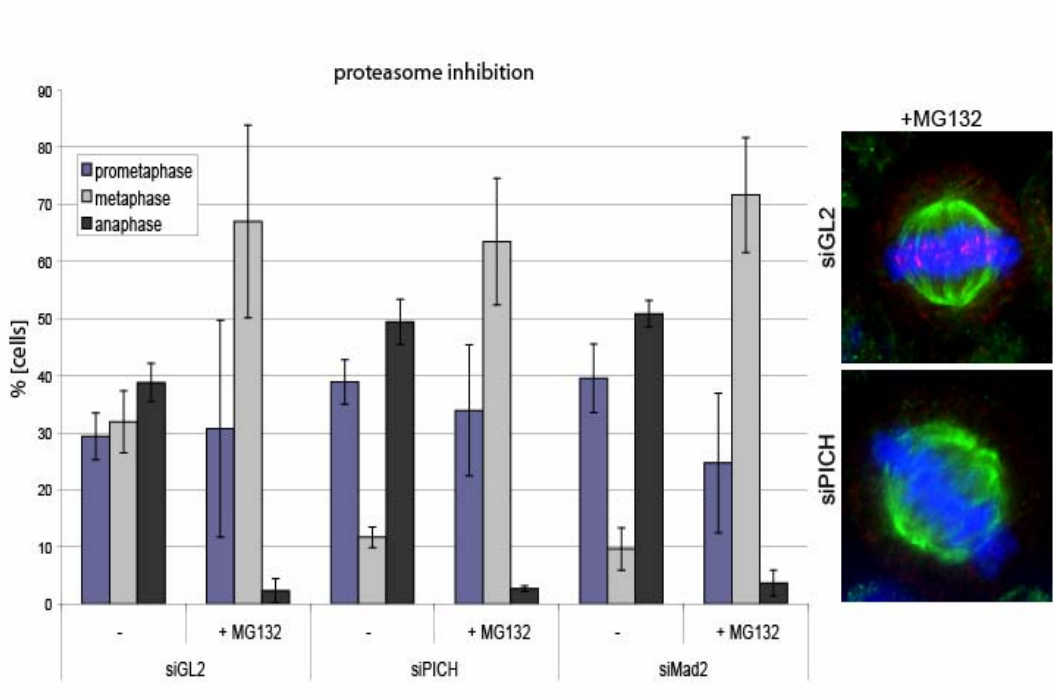

Figure 68. HeLa cells were treated for 48 hrs with siRNA duplexes targeting either PICH or Mad2, or with GL2 for control. Where indicated, the proteasome inhibitor MG132 was added during the last 3 hrs of the incubation, and the extent of restoration of metaphase plates was analyzed by immunofluorescence (DAPI staining).
Left panel: Histograms summarize the results of 3 independent experiments (for each column at least 150 cells were counted). Bars indicate standard deviations.
Right panel: Representative cells stained with DAPI and antibodies against PICH (red) and α-tubulin (green).

Conclusions II

In Plk1 immunoprecipitates we identified a novel interactor of Plk1, which we termed PICH. PICH belongs to the family of SNF2-type ATPases within the SF2 superfamily of helicases. We could identify a new motif conserved and present in PICH orthologs from plant to humans which we termed the PICH family domain (PFD). The Plk1-PICH interaction requires a priming phosphorylation by Cyclin dependent kinase 1 (Cdk1-CyclinB) at PICH threonine 1063, which converts this conserved STPK motif into a docking site for the C-terminal Polo-box domain of Plk1. Binding to Plk1 converts PICH into a strong substrate and phosphorylation of PICH by Plk1 negatively regulates the chromatin association of PICH. GFP-transfection experiments in U2OS cells showed that the N-terminal SNF2-type helicase domain, including the Walker A motif and the PFD are required and sufficient for PICH *wild type* localization. In all cell lines analyzed PICH can be observed at kinetochores and centromeres from prometaphase to anaphase. With the establishment of bipolarity and tension between sister kinetochores, PICH association with stretched centromeres becomes very prominent. When cells proceed into anaphase, PICH remains associated with threads that occasionally gain lengths of up to several µm. As cells proceed through anaphase PICH threads are progressively resolved and this action requires decatenation activity of Topoisomerase II. PICH threads are sensitive to DNAse treatment and disappear when tension is reduced, indicating that PICH associates with DNA in a tension dependent manner. We propose that these novel, thread-like structures are catenated, centromeric DNA that is resolved by Topoisomerase II after the onset of anaphase.

Depletion of PICH by siRNA resulted in severe chromosome segregation defects and micronucleation. Moreover, cells lacking PICH were not able to arrest in mitosis upon treatment with the compounds nocodazole or monastrol. Only Mad2 (and to some extent Topoisomerase II), but neither Mad1 nor any other of 15 proteins tested, was selectively lost from kinetochores of PICH depleted cells. Furthermore, the formation of metaphase plates could be restored in cells lacking PICH by addition of the proteasome inhibitor MG132, indicating that kinetochore structure and microtubule attachment are not disrupted in PICH depleted cells. We conclude that PICH is involved in Mad2 dependent spindle checkpoint signalling, possibly via regulation of the Mad1-Mad2 kinetochore interaction that is required

for the establishment of inhibitory Mad2 (DeAntoni et al., 2005; Yu, 2006). Moreover, Finally, the mitotic localization of PICH to stretched chromatin, its predicted SNF2 type translocase activity, its sensitivity to tension and its requirement for the spindle checkpoint lead us to propose that this enzyme might be ideally suited to monitor tension, thus possibly constituting the long sought tension sensor of the spindle checkpoint.

Discussion

The Ndc80 complex

The Ndc80 complex – consisting of its four subunits Hec1/Ndc80, Nuf2, Spc24 and Spc25 - has been reported previously to be required for microtubule attachment, chromosome congression and kinetochore assembly (DeLuca et al., 2005; DeLuca et al., 2003; Maiato et al., 2004; Martin-Lluesma et al., 2002; McCleland et al., 2003; McCleland et al., 2004). Using a directed Yeast-2-hybrid assay, we created an interaction model of the four complex components (Figure 15). In this model the N-terminus of Nuf2 (aa1-208) is sufficient to bind Hec1 residues 81-219. Moreover the small subunits Spc24 and Spc25 directly interact with each other and are linked to Hec1 via a direct Hec1-Spc25 interaction. These data support *in vitro* studies (summarized in Figure 69) where Hec1/Nuf2 or Spc24/Spc25 were co-expressed pairwise in bacteria and insect cells and exhibited subcomplex formation followed by whole complex assembly (Wei et al., 2005). Further studies described that the Hec1/Nuf2 dimer is directly involved in microtubule attachment (Cheeseman et al., 2006; Wei et al., 2007). Moreover, it has recently been suggested that phosphorylation of Hec1 by Aurora B might regulate merotelic attachment (Deluca et al., 2006), but further experimental evidences will be required to strengthen this hypothesis. Our approach of Nuf2 depletion by siRNA showed complex disruption and mislocalization of Hec1, resulting in disordered microtubules and failure in chromosome congression, supporting the requirement for Nuf2 and Hec1 in mitotic microtubule attachment and kinetochore structure.

To analyze the higher order complex formation around the Ndc80 proteins and to find novel interactors, two yeast-2-hybrid screens were carried out using $Nuf2^{1-208}$ and Spc25 as baits. Several interesting candidates were identified (Figures 16-18). None of these potential novel interactors was present in previous pull down experiments, where a higher order complex around Ndc80 was copurified from *C. elegans* and human lysates (Cheeseman et al., 2004). In this view it remains interesting to further study the most promising candidates (e.g. APC7, C10Orf94) obtained in our screens and their potential role at the kinetochore.

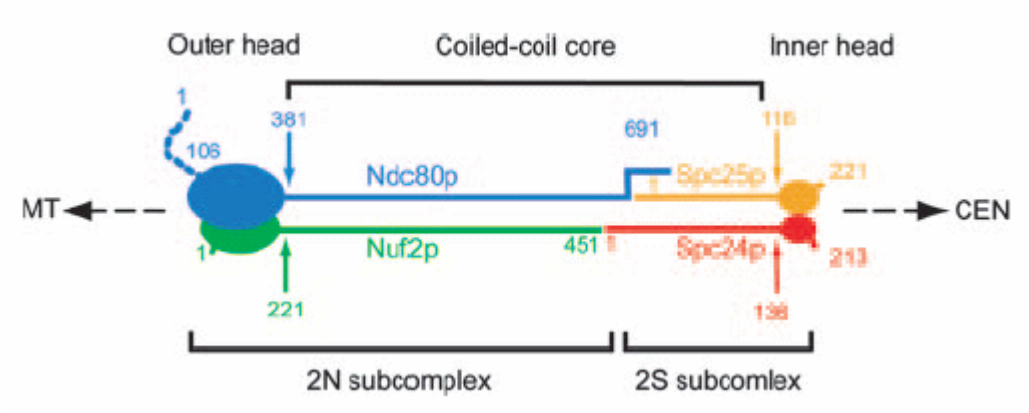

from Wei et al. PNAS 2005

Figure 69. Schematic model of the Ndc80 complex. Each subunit of the Ndc80 complex is represented by an oval (the globular domain) and a stick (the coiled-coil region). The dashed line indicates the N-terminal segment of Ndc80p that was deleted. Numbers label the approximate first and last residues of each protein segment. The coiled-coils of 2N and 2S form the coiled-coil core. The globular domains of 2N form the outer head (toward the microtubule); the globular domains of the 2S, the inner head (toward the centromere). MT, microtubule; CEN, centromere.

In Nuf2 siRNA depletion experiments the influence on known kinetochore and centromere proteins was analyzed (Table 2). Consistent with the finding that Hec1 depletion results in loss of the checkpoint proteins Mad1, Mad2, Mps1 and Cdc20 from kinetochores (Martin-Lluesma et al., 2002), we additionally observed that the kinetochore association of Polo-like kinase (Plk1) was selectively lost (Table 3). In general, this might open the possibility to separately observe Plk1 function when it is lost from kinetochores but remains at e.g. centrosomes. However, testing whether other centromere / kinetochore components might be required for the localization of Plk1 revealed the requirement for the chromosomal passenger protein Aurora B (see also (Goto et al., 2005) and Sgo1, indicating that Plk1 localization might underlie complex regulation by several proteins.

PICH – a novel mitotic target of Plk1

Polo-like kinase (Plk1) is an essential enzyme involved in the regulation of centrosome maturation and spindle assembly, the removal of cohesins from chromosome arms, the inactivation of APC/C inhibitors, and the regulation of

mitotic exit and cytokinesis (Barr et al., 2004). The distinct functions of Plk1 are reflected by its localization to centrosomes and spindle poles, kinetochores, the central spindle and the postmitotic bridge. Plk1 substrate binding depends on the C-terminal non-catalytic domain of Plk1 (Jang et al., 2002; Seong et al., 2002), the so-called Polo-box domain (PBD)(Elia et al., 2003b).

Human PICH was identified here as a novel interaction partner and substrate of Plk1. The PICH – Plk1 interaction requires a priming phosphorylation at threonine 1063, which creates a docking site for binding of Plk1`s Polo-box domain (PBD). Subsequently PICH becomes an efficient substrate of Plk1 (Figure 70).

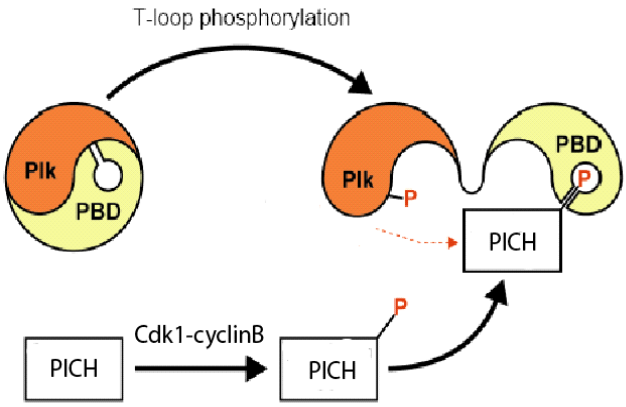

Figure 70. PICH is a Cdk1 dependent substrate of Plk1: Following a priming phosphorylation on threonine 1063 on PICH by Cdk1-CyclinB at the onset of mitosis, PICH is bound by Plk1 via its PBD (Polo-box domain). This turns PICH into an efficient substrate of Plk1. This mechanism follows exactly the model proposed by Yaffee and coworkers (see introduction Figure 8).

The Plk1-PICH mode of interaction fits exactly into the model of Plk1 substrate binding proposed by Yaffee and coworkers (Lowery et al., 2005). The identification of Cdk1-CyclinB as priming kinase points to a directed regulation of PICH in mitosis, even though this does not rule out further functions at other stages of the cell cycle. Our data indicate that Plk1 prevents the association of PICH with chromosome arms and restricts its localization to the kinetochore / centromere region by phosphorylation. This role of Plk1 in controlling PICH localization during

mitosis is highly reminiscent of the function of this kinase in removing cohesins from chromatid arms (Hauf et al., 2005; Losada et al., 2002; Sumara et al., 2002) and the protection of centromeric cohesins by Sgo1 and the phosphatase PP2A (Kitajima et al., 2006; Riedel et al., 2006; Tang et al., 2006)(Figure 71). The timely coordination in early mitosis between the removal of cohesins and PICH from chromatid arms raises questions as to possible connections between these events. In the future the identification of the Plk1 phosphorylation site(s) on PICH might help to understand the detailed function of the interaction between these enzymes.

It also remains to be understood why PICH is not removed from centromeres / kinetochores by Plk1. Preliminary results indicate that the Cdc14 phosphatase is required for *wild type* PICH localization and suggest that PICH could be protected from phosphorylation via the counteraction of a phosphatase that prevents dissociation (see also below). Hence Cdc14 phosphatase activity could be a strong candidate for protecting PICH at centromeres from Plk1 phosphorylation. It has previously been reported that the resolution of sister chromatid rDNA (ribosomal DNA) in yeast anaphase requires the activity of Cdc14 (Sullivan et al., 2004). Even though PICH localizes to centromeric DNA rather than to nucleoli, it is interesting to note, that PICH and Topoisomerase II localizations both depend on Cdc14 (Table 4).

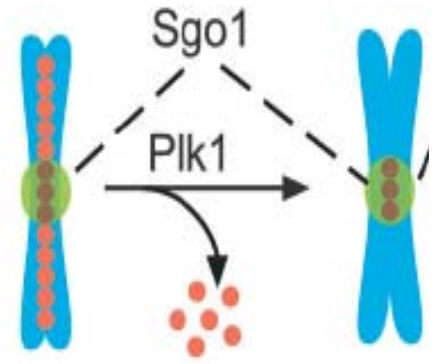

from McGuinness et al. PLOS Biology 2005

Figure 71. Plk1 removes cohesins from chromosome arms in prophase. Centromeric cohesin is protected from Plk1 activity by Sgo1 and the phosphatases PP2A until anaphase onset.

PICH defines a novel subclass of the SNF2 'helicase' family

PICH clearly belongs to the SNF2 family of ATPases, which share a catalytic core with the superfamily 2 of predicted 'helicases'. Rather than acting as processive helicases, members of this family utilize ATP hydrolysis to displace proteins from chromatin (Becker and Horz, 2002), translocate on double stranded DNA (Svejstrup, 2003), or generate superhelical torsion (Beerens et al., 2005; Havas et al., 2001; Lia et al., 2006), consistent with roles in chromatin remodeling, DNA recombination and DNA repair.

As shown above, mutation of the Walker A motif abolishes chromatin association, suggesting that PICH associates with DNA in an ATP-dependent fashion. Furthermore the N-terminal half of PICH, comprising the extended 'helicase' domain, is both necessary and sufficient for kinetochore / centromere localization, whereas deletion of the PFD domain resulted in diffuse chromatin association and to a significant loss of kinetochore staining. A potential role of the PFD in PICH kinetochore / centromere recruitment remains to be tested. Intriguing in the PICH domain structure are also the two TPR motifs in the very N- and C-termini of the protein. This could be a prerequisite for PICH oligomerization or hint at interactions with other TPR proteins. BubR1 and several members of the APC/C are TPR containing proteins (Passmore et al., 2005) and a recent study by the Pines lab (Acquaviva et al., 2004) established the localization of APC/C at centromeres.

Evidence for PICH localization to catenated centromeric DNA

In addition to its concentration at kinetochores and inner centromeres, endogenous PICH was found to localize to striking threads. These threads were difficult to visualize with DNA stains or antibodies against other proteins (including Topoisomerase II or the centromere-associated CENP-A or CENP-B, data not shown) and, to the best of our knowledge, no such threads have been reported in FISH experiments with centromeric DNA probes. Yet, PICH is predicted to bind DNA and several lines of evidence support the interpretation that these unusual PICH-positive threads represent stretched chromatin: firstly, they became visible when chromosomes underwent bipolar attachment during late prometaphase and connected most pairs of sister kinetochores in metaphase. Secondly, they

increased in length and concomitantly decreased in number during anaphase. Thirdly, they could be removed by DNAse treatment. Fourthly, they were exacerbated by depletion of Sgo1, indicating that premature release of centromeric cohesin caused their stretching. Finally, they persisted through telophase when Topoisomerase II activity was inhibited. Collectively, these data point to the conclusion that PICH-positive threads represent stretched and catenated centromere-related chromatin. The apparent persistence of catenated DNA into anaphase is unexpected, however a requirement for Topoisomerase II activity during anaphase has been reported previously (Shamu and Murray, 1992).

Decatenation of PICH threads in anaphase

Why would dividing cells maintain DNA catenation into anaphase, a leftover from DNA replication? The metaphase localization of PICH highlights that catenation between sister chromatids is only maintained at centromeric regions at this specific stage of mitosis. Presumably inter-centromeric threads are the last and only physical link where the cohesin ring complex can remain to maintain cohesion before the onset of anaphase. Therefore, the timely regulation of cohesion removal (at least at centromeres) could demand that Separase removes cohesins before the decatenation mediated by Topoisomerase II untangles centromeric DNA that has been freed from cohesins. It has been proposed that Cdc14 dependent resolution of rDNA in budding yeast anaphase requires previous activation by Separase, which might explain the surprising delay of centromere decatenation into mid-anaphase (Sullivan et al., 2004). As chromatin that is bound by PICH obviously exists into anaphase it will be interesting to test whether PICH – analogous to the role of cohesins – might stay at chromatin to prevent premature separation by constituting an inhibitor of decatenation. Thus removal of PICH from chromatid arms might be a requirement for timely progression through mitosis. In this view, the removal/clearance of PICH from chromosome arms in early mitosis might indeed reflect the necessity to remove an inhibitor of decatenation that counteracts Topoisomerase II activity. Moreover, it is tempting to speculate that in anaphase PICH associates with stretched chromatin threads that are under tension to stabilize them so they would resist tension/rupture and thus allow site directed decatenation by Topoisomerase II.

A regulatory network around PICH and Topoisomerase II

Overexpression of GFP-PICH shows a localization pattern on mitotic chromosomes very similar to that of Topoisomerase II. Both enzymes localize to chromatid axes and have strong kinetochore association in early mitosis. This intriguing codistribution might hint at a possible common role at kinetochores and centromeres and might further indicate that PICH and Topoisomerase II are specifically recruited to kinetochores, where they might be required to perform their checkpoint function(s). In PICH siRNA knockdown experiments, Topoisomerase II seemed selectively lost from centromeres but not from chromatid arms (Figure 67), suggesting that PICH might have a role to specifically target Topoisomerase II to the centromere (table 5). Moreover, PICH and Topoisomerase II seem to be co-regulated by several mitotic enzymes. Depletion of both Cdc14 and AuroraB mislocalizes PICH and Topoisomerase II from mitotic chromatin (Figure 72). In addition, Plk1 knockdown leads to redistribution of PICH over chromatid arms, resulting in colocalization with Topoisomerase II to chromatid axes. A possible interplay between PICH and Topoisomerase II in decatenation and their requirements for cohesin maintainance or cohesin removal remain to be unravelled. However, PICH might be ideally suited to provide a link between the needs of mitotic progression to resolve cohesion between sister chromatids through: a) decatenation and b) removal of cohesins. It is worth mentioning that mitotic arrests caused by either loss of cohesins induced by Sgo1 depletion or by Topoisomerase II inhibition using the compound ICRF-193 are mediated by Mad2 (McGuinness et al., 2005; Skoufias et al., 2004). This suggests that the mechanisms regulating cohesins and decatenation merge in the same downstream effector proteins, raising the question of where these two pathways come together.

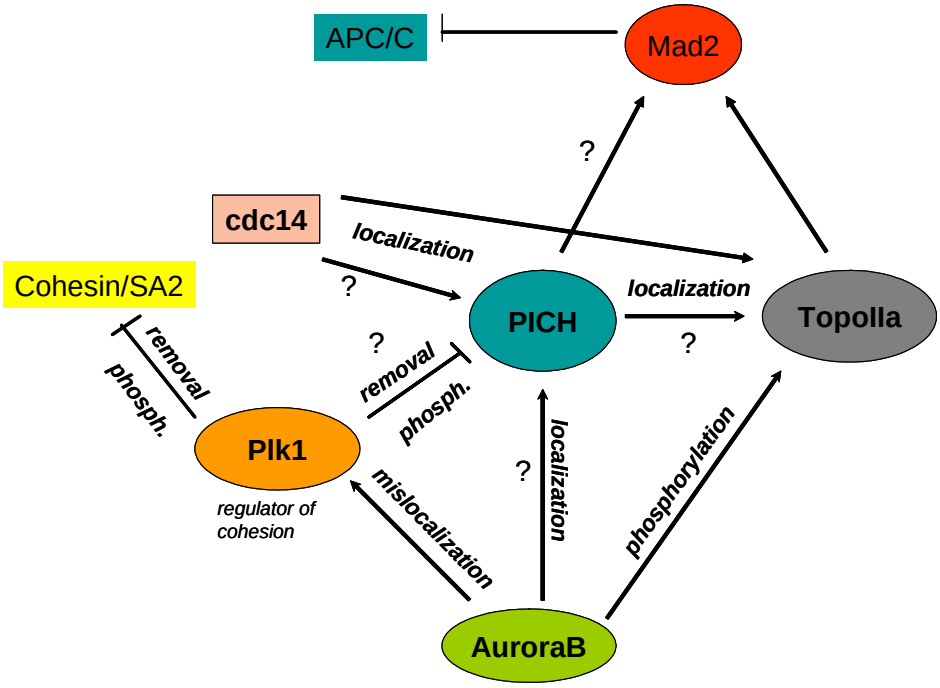

Figure 72. Model of PICH regulation. Cdc14 and AuroraB co-regulate the localization and function of PICH and Topoisomerase II. Plk1 is proposed as general regulator of cohesion, not only removing the cohesin ring complex but also PICH from chromatid arms. PICH also influences the kinetochore localization of Topoisomerase II. Both enzymes could have a common role in decatenation, which may be linked to the timely and physical regulation of cohesin removal. Furthermore, PICH regulates the onset of anaphase via Mad2 regulation.

Human PICH is an essential component of the SAC

As a consequence of PICH depletion, cells went through mitosis without awaiting chromosome congression. Moreover, they were unable to activate the spindle assembly checkpoint in response to either nocodazole or monastrol. Although rescue experiments proved unreliable because of extensive cell death induced by PICH overexpression (data not shown), we are confident that the inability of PICH depleted cells to mount a spindle checkpoint response reflects a direct role of PICH in checkpoint signaling. First, PICH was mostly cytoplasmic during interphase (Figure 36), arguing against an indirect mechanism due to a nuclear function related to transcription, replication, establishment of cohesion or chromatin remodelling. Second, the localization of many representative kinetochore/centromere proteins was not detectably affected by depletion of PICH, indicating that PICH is not required for generalized kinetochore assembly. Third,

PICH depleted cells were able to form metaphase plates when mitotic exit was blocked by MG132, demonstrating that microtubule attachment to kinetochores was not significantly impaired. Most importantly, PICH knock-down resulted in a specific loss of Mad2 from kinetochores, indicating that this Cdc20-inhibitor most likely represents a downstream mediator of PICH action. Interestingly, the kinetochore association of Mad1 was not detectably influenced, suggesting that PICH is required to regulate the Mad2-Mad1 interaction at kinetochores (either directly or indirectly). A crucial role in the spindle checkpoint has been proposed for the protein p31-Comet to turn off the checkpoint by competitive binding to Mad2 (Xia et al., 2004). Even though p31 has been found in vertebrates only, it presents an attractive way how to regulate spindle checkpoint status by interference with Mad2. There are further possibilities of Mad1-Mad2 interaction regulation, e.g. inhibitory phosphorylation of either Mad2 (Wassmann et al., 2003) or of Cdc20 by Bub1 (Tang et al., 2004). How PICH regulates Mad2 presence remains to be determined, but, with the examples given above it seems that there are several possible mechanisms and pathways to follow.

PICH in other organisms

It may appear surprising that no obvious orthologs of PICH could be identified in the genomes of yeast, *Drosophila* and *Caenorhabditis*. However, a PICH family member is clearly detectable in both *Dictyostelium, Ciona* and even *Arabidopsis* and rice (Figure 25), suggesting that functional homologs may be widespread amongst eukaryotes but escape detection by bioinformatics algorithms in lower order organisms. Considering that some 2 % of all *Saccharomyces cerevisiae* genes code for ‘helicase’-related proteins (Shiratori et al., 1999), there is no shortage for candidate PICH homologs in yeast and functional redundancy would readily explain why no PICH homologs were identified in the original screens for spindle checkpoint components (Hoyt et al., 1991; Li and Murray, 1991).

A working model for PICH function as tension sensor

According to current models, centromere-associated cohesins hold sister chromatids together until the extinction of the SAC results in Separase activation and cohesin cleavage (Haering and Nasmyth, 2003). Furthermore, the activity of the SAC is believed to be regulated through microtubule attachment and/or tension developing at the kinetochore-microtubule interface (Pinsky and Biggins, 2005; Sandall et al., 2006). Questions that remain largely unresolved concern the extent to which DNA catenation contributes to sister chromatid cohesion and the timing of Topoisomerase II action at centromeres (Shamu and Murray, 1992; Yanagida, 1995). The properties of the PICH protein described here lead us to envision a role for centromere-associated DNA in spindle checkpoint regulation. In analogy to the purported roles of other SNF2 family members, it seems plausible that PICH may induce changes in DNA topology or remodel centromeric chromatin. Additionally, PICH may respond to tension-dependent alterations in DNA topology.

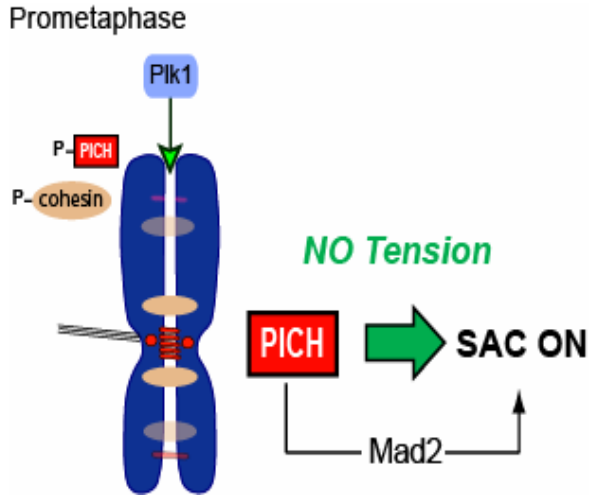

Figure 73. A model for PICH function at prometaphase

During prometaphase (Figure 73) PICH accumulates at kinetochores and inner centromeres similar to cohesins, reflecting its regulation by Plk1. At this stage, PICH is required to uphold conditions permissive for the production of Mad2

protein at kinetochores, so that the spindle checkpoint is on and the APC/C inhibited.

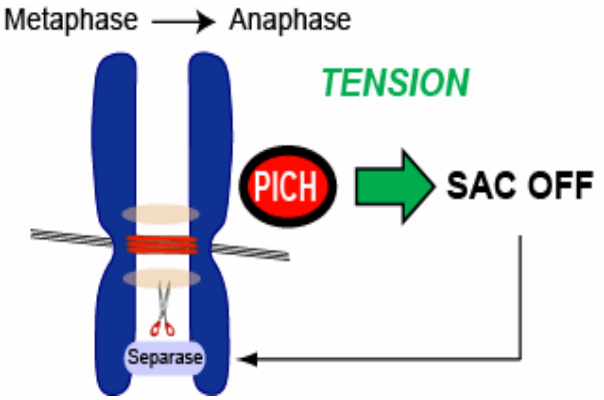

Figure 74. A model for PICH function at metaphase

In response to bipolar attachment (Figure 74), the catenated centromeric DNA is proposed to stretch under tension, resulting in the formation of PICH-positive threads connecting sister kinetochores. A tension-induced change in PICH activity (and/or the recruitment of PICH away from kinetochores) would then bring the production of inhibitory Mad2 protein to a halt, so that the SAC becomes extinct.

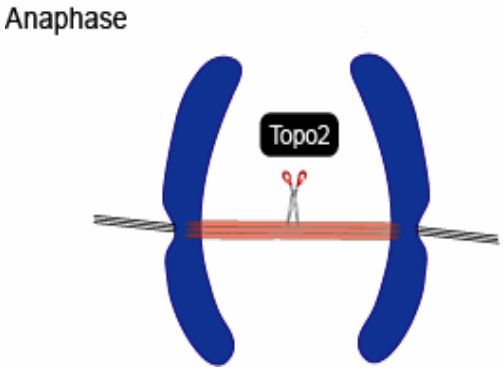

Figure 75. A model for PICH function at anaphase

Finally, during anaphase (Figure 75), PICH function is no longer coupled to SAC regulation but PICH remains associated with centromeric DNA threads until decatenation is completed by Topoisomerase II. At this stage, PICH may regulate

the access of Topoisomerase II and/or protect stretched DNA from non-specific rupture.

The key prediction is that catenated centromere-related DNA provides a structural continuity between sister kinetochores, thereby offering a platform for the monitoring of tension by a DNA-bound enzyme. The model further proposes PICH as a candidate tension sensor on chromatin, similar to the recent proposal that Sgo1 could function as a tension sensor at the kinetochore-microtubule interface (Indjeian et al., 2005). The two proposals are not mutually exclusive since spindle checkpoint signalling could conceivably originate from both catenated DNA and the kinetochore-microtubule interface. A mechanistic understanding of PICH function and concomitant testing of the above model will have to await studies on the enzymology of this predicted ATPase. However, the discovery of PICH provides new opportunities for elucidating the hitherto elusive connections between DNA catenation, sister chromatid cohesion and spindle checkpoint regulation. Considering that both SNF2-related proteins and spindle checkpoint components have been linked to human cancer (Kops et al., 2005b; Owen-Hughes, 2006), it will also be interesting to explore a possible relationship between PICH and the etiology of human disease.

Material and Methods

Chemicals and materials

All chemicals were purchased from Merck, Sigma-Aldrich Chemical Company (Sigma, St Louis, MO), Fluka-Biochemika, Switzerland, or Roth, unless otherwise stated. Components of growth media for E. coli and yeast were from Difco Laboratories or Merck. The Minigel system was purchased from Bio-Rad and the Hoefer SemiPHor Blotting system from Pharmacia-Biotech. Tabletop centrifuges were from Eppendorf.

Plasmids and antibodies

The complete ORF of PICH (corresponding exactly to FLJ20105; Acc. No. BC111486) was amplified by nested PCR, using a HeLa Marathon library (Clontech laboratories Inc.), and cloned into pEGFP-C1 vector (Clontech laboratories Inc.). The following primer pairs were used (see also list below):
primer pair 1:
AAG CTC CAG CTC CAA GCT CC and
TGC TTT TTG AGA TCT TTC TTG CC,
primer pair 2:
GACTCGAGCTATGGAGGCATCCCGAAGGTTTC and
GCCCGGGTCAATTGTTATTAAGTTGC.

These primers contain Xho1 and Xma1 sites, respectively, used for cloning. pEGFP-C1-PICH was the source for further PCR-mediated subcloning of PICH fragments. The T1063A and Walker A motif (GKT->AAA) mutants were produced by site directed mutagenesis, using Pfu turbo (Stratagene, La Jolla, CA) and the following primers (reverse primers correspond to the inverted sequence)
T1063A: CAATTTGATGCTTCAGCTCCCAAAAATGACATC;
AAA: GATGATATGGGATTAGCGGCGGCTGTTCAAATCATTGCT.
All plasmid constructs were confirmed by sequencing.
Coupled in vitro transcription-translations were carried out using the TNT T7 kit provided by Promega (Madison, WI, USA). Recombinant MBP-PICH protein was expressed in *E.Coli* (strain JM109-RIL) and purified under native conditions (QIAexpressionist system; Qiagen, Hilden, Germany). Antibodies against full

length MBP-PICH-His were raised in rabbits (Charles River laboratories (Romans, France) and rats (in-house animal facility, MPI of Biochemistry, Martinsried, Germany). All other antibodies were described previously or obtained commercially.

The monoclonal anti-Plk1 (Yamaguchi et al., 2005) and 9E10 anti-myc antibody (hybridoma tissue culture supernatant, (Evan et al., 1985) as well as the rabbit anti-Borealin antibody (Klein et al., 2006) have been described previously. Monoclonal anti-Hec1 (ab3613) and anti-CenP-A (Abcam, Cambridge, UK), anti-α-tubulin (DM1A) and anti-Flag M2 (Sigma, St Louis, MO); anti-Aurora B (AIM1),anti-Bub3 and anti-CenP-F (BD Biosciences Pharmingen, NJ USA), anti-BubR1 and anti-Cyclin B1 (Biomol, Plymouth meeting, USA), anti-CENP-E and anti-Cdc20 (Santa Cruz Biotechnology, Santa Cruz, CA), rabbit anti-Mad2 (Bethyl, Montgomery, Texas) were obtained commercially.

Hybridoma cells producing monoclonal anti-CENP-B antibodies were purchased from ATCC (Middlesex, UK), monoclonal antibodies against Bub1, INCENP and Plk1 were kindly provided by Andreas Uldschmidt (MPI for Biochemistry), and the rabbit anti-GST antibody was a kind gift from Dr U. Gruneberg. CREST human autoimmune serum was purchased from Immunovision (Springdale, AR) and mouse anti-Topoisomerase II antibodies was from Stressgen (Ann Arbor, MI). Primary antibodies were detected with cy2/cy3-conjugated donkey antibodies (Dianova, Hamburg, Germany) and Alexa Fluor 647-conjugated goat antibodies (Invitrogen, Carlsbad, CA), respectively.

name	tag	gene	insert	species	vector	comment
CB 1		APC7	wt	human	pCRTopoIIblunt	cloning vector
CB 2		APC7	wt	human	pCRTopoIIblunt	cloning vector
CB 3		APC7	wt	human	pCRTopoIIblunt	cloning vector
CB 4		APC7	wt	human	pAct2	Y2H
CB 5		APC7	wt	human	pFBT9	Y2H
CB 6	flag	APC7	wt	human	pcDNA3.1Aflag	mammalian expression
CB 7	GST	APC7	wt	human	pGEX6P-3	bacterial expression
CB 8	MYC	APC7	wt	human	pcDNA3.1Amyc	mammalian expression
CB 9		94	wt	human	pCRTopoIIblunt	cloning vector
CB 10		94	wt	human	pCRTopoIIblunt	cloning vector
CB 11		94	wt	human	pCRTopoIIblunt	cloning vector
CB 12		94	wt	human	pCRTopoIIblunt	cloning vector
CB 13		94	wt	human	pACT2	Y2H
CB 14		94	wt	human	pFBT9	Y2H
CB 15	myc	94	wt	human	pcDNA3.1Amyc	mammalian expression
CB 16	myc	Nek2B	wt	human	pcDNA3.1Amyc	mammalian expression
CB 17		Nek2B	wt	human	pFBT9	Y2H
CB 18		Nek2B	wt	human	pACT2	Y2H
CB 19	myc	ZWINT	wt	human	pcDNA3.1Amyc	mammalian expression
CB 20	flag	ZWINT	wt	human	pcDNA3.1Aflag	mammalian expression
CB 21	HIS	ZWINT	wt	human	pQE32	bacterial expression
CB 22		ZWINT	wt	human	pAct2	Y2H
CB 23		ZWINT	wt	human	pFBT9	Y2H
CB 24	His	Nuf2	1-208	human	pQE80	bacterial expression
CB 25	His	Nuf2	1-86	human	pQE80	bacterial expression
CB 26	His	Nuf2	wt	human	pQE80	bacterial expression
CB 27	His	Nuf2	83-464	human	pQE80	bacterial expression
CB 28	GST	Nuf2	wt	human	pGEX6P-3	bacterial expression
CB 29	MBP	Nuf2	1-208	human	pMalc2-x	bacterial expression
CB 30	His	Nuf2	202-464	human	pQE80	bacterial expression
CB 31	GST	Nuf2	83-464	human	pGEX6P-3	bacterial expression
CB 32	GST	Nuf2	202-464	human	pGEX6P-3	bacterial expression
CB 33	His	Hec1	wt	human	Com220	insect expression
CB 34	GST	Nuf2	wt	human	pACGHLT-B	insect expression
CB 35	myc	Nuf2	S244A	human	pcDNA3.1Amyc	mammalian expression
CB 36	myc	Nuf2	S244D	human	pcDNA3.1Amyc	mammalian expression
CB 37	myc	Nuf2	S244E	human	pcDNA3.1Amyc	mammalian expression
CB 38		Nuf2	wt	human	pAct2	Y2H
CB 39		Nuf2	wt	human	pFBT9	Y2H
CB 40		Nuf2	1-208	human	pAct2	Y2H
CB 41		Nuf2	1-208	human	pFBT9	Y2H
CB 42		Hec1	wt	human	pAct2	Y2H
CB 43		Hec1	wt	human	pFBT9	Y2H
CB 44		Hec1	1-250	human	pAct2	Y2H
CB 45		Hec1	1-250	human	pFBT9	Y2H
CB 46		Spc24	wt	human	pAct2	Y2H
CB 47		Spc24	wt	human	pFBT9	Y2H
CB 48	His	Spc24	wt	human	pQE32	bacterial expression
CB 49	myc	Spc24	wt	human	pcDNA3.1myc	mammalian expression
CB 50	flag	Spc24	wt	human	pcDNA3.1flag	mammalian expression
CB 51		Spc25	wt	human	pAct2	Y2H
CB 52		Spc25	wt	human	pFBT9	Y2H
CB 53	myc	Spc25	wt	human	pcDNA3.1myc	mammalian expression
CB 54	flag	Spc25	wt	human	pcDNA3.1flag	mammalian expression

CB 55	myc	PICH	wt	human	pcDNA3.1myc	mammalian expression
CB 56	FLAG	PICH	wt	human	pcDNA3.1flag	mammalian expression
CB 57		PICH	wt	human	pAct2	Y2H
CB 59		PICH	wt	human	pFBT9	Y2H
CB 60	MBP-HIS	PICH	wt	human	pMaltFN-His	bacterial expression
CB 61	GST	PICH	wt	human	pGEX4T-1	bacterial expression
CB 62	GFP	PICH	wt	human	pEGFP-C1	mammalian expression
CB 63	MBP-HIS	PICH	T1063A	human	pEGFP-C1	mammalian expression
CB 64	His	PICH	wt	human	pQE32	bacterial expression
CB 65	GFP	PICH	T1063A	human	pEGFP-C1	mammalian expression
CB 66	GFP	PICH	full length	human	peGFPC1	mutation
CB 67	GFP	PICH	full length	human	peGFPC1	AAA mutant
CB 68	GFP	PICH	full length	human	peGFPC1	PICH oligo1
CB 69	GFP	PICH	full length	human	peGFPC1	PICH oligo 1
CB 70	GFP	PICH	full length	human	peGFPC1	construct for PICH oligo 1
CB 71	GFP	PICH	full length	human	peGFPC1	construct for PICH oligo 1
CB 72		PICH	shRNA PICH oligo1	human	pTer+	
CB73	GFP	PICH	1-632 (SNF2 domain)	human	peGFP-C1	mammalian expression
CB74	GFP	PICH	1-686 (SNF2 + PFD domain)	human	peGFP-C1	mammalian expression
CB75	GFP	PICH	DEAH->DQAH	human	peGFP-C1	mammalian expression
CB76	GFP	PICH	GKT->GAT	human	peGFP-C1	mammalian expression
CB77	myc	Mps1	Mps1wt S389	human	pcDNA3.1Amyc	transfection vector/IVT
CB78	myc	Mps1	Mps1kd S389	human	pcDNA3.1Amyc	transfection vector/IVT

Table 7. List of all Plasmids cloned during this work with aliquots deposited in the lab`s -80°C stock (Department of Cell Biology, MPI of Biochemistry, Martinsried, Munich). Gene name 94 corresponds to C10Orf94.

To generate monoclonal antibodies against hNuf2, recombinant His6-hNuf2 was expressed in JM109 bacteria. Recombinant proteins were purified on Ni2+-columns as described. For the production of mAbs, Balb/c mice were immunized by repeated subcutaneous injections of 100-150µg of His6-hNuf2, using either Freund´s (Sigma-Aldrich) or Alu-Gel-8 (SERVA Electrophoresis GmbH) as an adjuvant. Spleen cells were fused with PAIB3Ag81 mouse myeloma cells using polyethylene glycol medium (PEG 4000;Merck) as described by Kohler and Milstein (Kohler and Milstein, 1975). Fused cells were initially selected for two weeks in HAT-medium (hypoxanthine/aminopterin/thymidine-medium) followed by selection in HT-medium (hypoxanthine/thymidine-medium) for the cloning procedure. Supernatant screening was performed by indirect ELISA using His6-hNuf2 as an antigen, by dot blot assays and by Western blotting on total HeLa cell

extracts. mAb isotyping was performed by dot blot analysis using Mouse Monoclonal Antibody Isotyping Reagents (Sigma-Aldrich) as described by the supplier and revealed that 28-37-1/3 and 27-123-1 are all IgG1.

name	purpose	comment	sequence
M3246	site directed mut	GKT-AAA Walker mut	GATGATATGGGATTAGCGGCGGCTGTTCAAATCATTGCT
M3247	site directed mut	GKT-AAA Walker mut	AGCAATGATTTGAACAGCCGCCGCTAATCCCATATCATC
M3254	site directed mut	GKT-GRT Walker mut	GATGATATGGGATTAGGGAGGACTGTTCAAATCATTGCT
M3255	site directed mut	GKT-GRT Walker mut	AGCAATGATTTGAACAGTCCTCCCTAATCCCATATCATC
M3298	site directed mut	T1063A	CAATTTGATGCTTCAGCTCCCAAAAATGACATC
M3299	site directed mut	T1063A	GATGTCATTTTTGGGAGCTGAAGCATCAAATTG
M3387	sequencing	5` 600	TATGTAGTGATAATAACACC
M3388	sequencing	5` 350	TCTTCCATCCCTATACAGGC
M2765	amplification	FLJ90238 up2	TTCCTTTGCTGAATCCGATTGAGG
M2766	amplification	FLJ90238 up1	TTGGCCCCTAAAGCTTGAAAGTTG
M3344	site directed mut	rescue PICH oligo 1	GAGGGTGAGAAACAAGACTTATCCAGTATAAAGGTG
M3345	site directed mut	rescue PICH oligo 1	CACCTTTATACTGGATAAGTCTTGTTTCTCACCCTC
M2854	sequencing	397down	ATTGCTTTCCTTTCCGGTATG
M2855	sequencing	801down	ATGGTCCCTATTTGATTTTGC
M2856	sequencing	1195down	TCACCTTTGGCTGAGCTAG
M2857	sequencing	1613down	TAGGTGGTGTCGGTTTAAC
M2858	sequencing	2103down	TCAGAAAGCTCAATTCCTCG
M2859	sequencing	2564down	AGGCACTGCAAGAGGATCC
M2860	sequencing	2978down	TGCATAGCAAAACATGTCTC
M2861	sequencing	3424down	ACAGAAGAGGATCCTTCCG
M2862	sequencing	3823down	TTCTTTGGGAACATGAAGC
M2952	cloning	eGFP Xma1 up	GCCCGGGTCAATTGTTATTAAGTTGC
M2955	cloning	Xma1 Y2Hd100	CTCCCGGGCATGAATCCAGATGTTGATGCC
M2961	cloning	Kpn1down100	CGGGTACCTATGAATCCAGATGTTGATGCC
M2828	cloning	Xma1down full length Y2H	CTCCCGGGCATGGAGGCATCCCGAAGGTTTC
M2829	cloning	Kpn1downmyc	CGGGTACCTATGGAGGCATCCCGAAGGTTTC
M2830	cloning	Kpn1downpQE	CGGGTACCCAATGGAGGCATCCCGAAGGTTTC
M3092	cloning	Kpn1dmyc270	CGGGTACCTATGCGAGAACTGCACAACCAACTC
M3093	cloning	Xho1mycup1300	GCTCGAGTCATCCAGATTCTTCCATCAATGTG
M3094	cloning	Xho1mycup2000	GCTCGAGTCAAGCAGCATGCAAAGACTGAAGC
M3095	cloning	Xho1mycup2600	GCTCGAGTCACCAAGGATTGCAATGACG
M3096	cloning	Xho1mycup3000	GCTCGAGTCAATCTTCATCTTCGCCATCTG
M3097	cloning	Xho1GFPdown270	GACTCGAGCTATGCGAGAACTGCACAACCAACTC
M3098	cloning	Xho1GFPdown3000	GACTCGAGCTATGTGTGGCTCTGCACCTAATTCC
M3099	cloning	Xho1GFPdown2000	GACTCGAGCTATGGCCTACCTGCAGTCTTTGG
M3101	cloning	Xho1GFPdown1000	GACTCGAGCTATGAATCCAGATGTTGATGCC
M3102	cloning	Xma1GFPup1300	GCCCGGGTCATCCAGATTCTTCCATCAATGTG
M3103	cloning	XmaGFPup2000	GCCCGGGTCAAGCAGCATGCAAAGACTGAAGC
M3104	cloning	XmaGFPup2600	GCCCGGGTCACCAAGGATTGCAATGACG
M3105	cloning	XmaGFPup3000	GCCCGGGTCAATCTTCATCTTCGCCATCTG
M2922	Nested PCR	down	ATGGAGGCATCCCGAAGGTTTCC
M2923	Nested PCR	down-60	AAGCTCCAGCTCCAAGCTCC
M2951	cloning	eGFPC1Xho1down	GACTCGAGCTATGGAGGCATCCCGAAGGTTTC
M2953	cloning	XmaY2Hd3000	CTCCCGGGCATGTGTGGCTCTGCACCTAATTCC
M2954	cloning	XmaY2Hd2000	CTCCCGGGCATGGCCTACCTGCAGTCTTTGG
M2956	cloning	Kpn1pQE3000	CGGGTACCCAATGTGTGGCTCTGCACCTAATTCC
M2957	cloning	Kpn1pQE2000	CGGGGTACCCAATGGCCTACCTGCAGTCTTTGG
M2958	cloning	Kpn1pQE1000	CGGGTACCCAATGAATCCAGATGTTGATGCC
M2959	cloning	Kpn1downmyc3000	CGGGTACCTATGTGTGGCTCTGCACCTAATTCC
M2960	cloning	Kpn1downmyc2000	CGGGTACCTATGGCCTACCTGCAGTCTTTGG
M3058	cloning	pMalHisTEVXho1up	GCCTCGAGATTGTTATTAAGTTGCTT
M3059	cloning	pMalHisTEVNot1down	GGCGGCCGCAATGGAGGCATCCCGAAGGTTTCC
M2821	Nested PCR	FLJ31932NestedDown	ACAACCAACTCTTTGAGCACCAG
M2822	Nested PCR	FLJ31932Nestedup	TGCTTTTTGAGATCTTTCTTGCC
M2823	cloning	FLJ31932Xma1down	CTCCCGGGCATGGGATTAGGGAAGACTGTTC
M2824	cloning	FLJ31932Xho1up	GCCTCGAGTCAATTGTTATTAAGTTGC
M2825	cloning	FLJ31932Xho1up	GCCTCGAGCTATTCACCAGACAAAGGCTC
M2826	cloning	FLJ31932Kpn1downMYC	CGGGTACCTATGGGATTAGGGAAGACTGTTC
M2827	cloning	FLJ31932Kpn1downPQE	CGGGTACCCAATGGGATTAGGGAAGACTGTTC
M2849	cloning	FLJaa228BamH1	CGGGATCCCAAGAAGGATTGTTTCAGATGGCG
M3657	cloning	GFPXma1upfromaa632 no PFD	ccccccgggtcaatcctcgattgtaaagagctc
M3658	cloning	GFPXma1upfromaa686 incl PFD	ccccccgggtcactcttctttaacagacagatc
M3659	cloning	GFPXma1upfrom1060	ccccccgggtcaatcaaattgtttcacagatga
M3666	siRNA vector pTER	PICH1siRNAforw	gatcccCAAGATCTCTCCAGTATAATtcaagagaTTATACTGGAGAGATCTTGtttttggaaa
M3667	siRNA vector pTER	PICH1siRNArev	agcttttccaaaaaCAAGATCTCTCCAGTATAAtctcttgaaTTATACTGGAGAGATCTTGgg

Table 8. List of primers used for the cloning of PICH constructs.

Immunofluorescence microscopy and live cell imaging

Immunofluorescence microscopy was performed using a Zeiss Axioplan II microscope (Carl Zeiss, Jena, Germany) equipped with an Apochromat 63x oil immersion objective, and images were acquired using a Micromax charge coupled device (CCD) camera (model CCD-1300-Y; Princeton Instruments, Trenton, NJ) and MetaView software (Visitron Systems, Puchheim, Germany) (data shown in Figures 2C, 6A and S2D). Alternatively (all other Figures), a Deltavision microscope on a Nikon Eclipse TE200 base (Applied Precision, Issaquah, WA) equipped with an Apo 60_/1.4 oil immersion objective and a CoolSnap HQ camera (Photometrics) was used for collecting 0.15-µm distanced optical sections in the *z*-axis. Images at single focal planes were processed with a deconvolution algorithm (Nikon_60x_140_12601.otf or Olympus_60x_140_10602.otf, depending on the objective used). Settings were conservative, with noise filtering set to low or medium and 3 or 4 deconvolution cycles. The number of z-stacks collected was variable (between 8 and 18), depending on the height of the individual cell. Images were projected into one picture using the Softworx software (Applied Precision). Exposure times and settings for image processing (deconvolution) were constant for all samples to be compared within any given experiment. Images were opened in Adobe Photoshop CS and then sized and placed in figures using Adobe Illustrator CS (Adobe Systems, Mountain View, CA).

For the quantification shown in Figure 45, asynchronously growing U2OS cells were fixed and stained for PICH and CREST. Cells at representative states of mitosis from early metaphase to telophase (shown by DAPI staining below) were analyzed and the number and length of PICH threads was quantified using Softworx imaging software.

To digest nucleic acids, cells grown on coverslips were incubated for 12 min with 5 µg/ml of DNAse or RNAse (Sigma, St Louis, MO) in 0.2 % Triton-X-100, 20 mM Pipes pH 6.8, 1 mM $MgCl_2$, before they were fixed by the addition of formaldehyde and EGTA (to 4 % and 10 mM final concentration, respectively).

For live-cell imaging, a HeLa S3 cell line stably expressing histone H2B-GFP was used. Following siRNA treatment, cells were placed into CO_2-independent medium and onto a heated stage (37°C). Live-cell imaging was performed using a Zeiss Axiovert-2 microscope equipped with a Plan Neofluar 60x objective. Metaview software (Visitron Systems GmbH, Puchheim, Germany) was

used to collect and process data. Images were captured with 50 millisecond exposure times with 2 minutes intervals for 16 hours.

Transient transfections and siRNA

Plasmid transfections were performed using FuGENE6 reagent (Roche Diagnostics, Indianapolis, IN, USA) according to the manufacturer's instructions. SiRNA duplexes were transfected using Oligofectamine (Invitrogen, Carlsbad, CA, USA). PICH was depleted using duplexes (Qiagen, Hilden, Germany) targeting 2 different sequences, with identical results. In siRNA experiments, Plk1, Mad2 and Sgo1 were depleted using previously published duplexes (Hanisch et al., 2006; McGuinness et al., 2005; Stucke et al., 2004) and the GL2 duplex (Elbashir et al., 2001) was used for control. Target sequences for Eg5 and PICH were:

Eg5 siRNA: 5'-CTAGATGGCTTTCTCAGTA-3'

PICH siRNA oligo 1: 5'-CAAGATCTCTCCAGTATAA-3'

PICH siRNA oligo 2: 5'-GGACCATATTGATCAAGTA-3'

Depletion of PICH with both siRNA nucleotides had identical results.

Biochemical assays

In vitro phosphorylation of PICH by Cdk1 was carried out in a total volume of 20 µl BRB80 kinase buffer (Stucke et al., 2004) for 30 min at 30°C, using 200ng PICH, 100ng Cdk1/Cyclin B (Upstate, Charlottesville, VA, USA), 1mM ATP, 0.1 µl γ-[^{32}P]-ATP, 3000 Ci/mmol, and 10 mCi/ml. After stopping the kinase reactions by addition of gel sample buffer, samples were resolved by 7.5% SDS-PAGE and subjected to either autoradiography or transferred to HybondC-extra membranes (Amersham Biosciences, England) for Far Western blotting. Kinase reactions used in Far Western analyses were performed under identical conditions except that γ-[^{32}P]-ATP was omitted. Far Western assays were performed using GST-tagged PBD (1µg/ml) for 6h at 4°C, followed by detection of bound protein with affinity-purified rabbit anti-GST antibodies (Neef et al., 2003).

Yeast two-hybrid screens were performed according to the yeast protocol handbook (Clontech). For the directed interaction screening, yeast colonies were selected by pACT2 and pFBT9 selection markers (Leu$^-$/Trp$^-$) for plasmid uptake.

The GAL4 binding domain (BD) – activation domain (AD) interaction and subsequent expression of markers (His^-/Ade^-) were monitored by streaking yeasts out on QDO selective plates (Quadruple Drop Out: $Leu^-/Trp^-/His^-/Ade^-$). Every single construct was additionally tested in the same assay for self activation by cotransfection with an empty vector. Self activating plasmids were $Hec1^{1-250}$-pFBT9 and Spc24-pFBT9.

For chromosome spreads mitotic cells were collected by mitotic shake off, centrifuged for 4 min at 1000 rpm and resuspended in diluted DMEM culture medium (40% DMEM without antibiotics and 60 % deionised H_2O). Cells were swelled at RT for 5 min before spinning and resuspending them in fixation solution (3:1 methanol:acetic acid). The fixed cells were incubated at 4°C for at least 20 min, washed three more times with the fixation solution and, finally, 10 µl of each cell solution were dropped on a -20°C HCl-treated cover slip, which had been moistened before by breathing on to it. After drying of the cover slip on a wet Kleenex tissue over a 60°C heating block, spreads were stained for 5 min with 0,4 µg/ml DAPI and mounted.

Co-immunoprecipitations

For co-immunoprecipitations, mitotic HeLa cells were harvested by mitotic shake off after 16h nocodazole treatment. Lysates were prepared using RIPA buffer (10mM Tris-HCL pH7.5, 150mM NaCl, 0.5% Triton, 1% sodium deoxycholate, complete mini protease inhibitor tablets (1/10ml) (Roche Diagnostics, Indianapolis, IN, USA), DNAse 20µg/ml, 100nM Okadaic Acid) and 250µl aliquots were incubated for 2h at 4°C with either one of two monoclonal anti-Plk1 antibodies or 9E10 anti-myc antibodies for control. In each case, 10µg antibody was coupled to 20µl Sepharose-G beads (Pierce, Rockford, IL, USA). After protein capture, beads were washed 4x with RIPA buffer and 2x with PBS, resuspended in gel sample loading buffer and resolved by 7.5% PAGE. Gels were either processed for Western blotting or analysis by mass spectrometry.

Miscellaneous reagents

The HeLa S3 cell line stably expressing GFP-histone H2B was constructed and kindly provided by Dr. Herman Silljé (Sillje et al., 2006). Calf intestine phosphatases (CIP) was purchased from New England Biolabs (Ipswich, MA), the proteasome inhibitor MG132 was from Calbiochem (San Diego, CA, USA), Taxol, Nocodazole and Aphidicoline were from Sigma (St Louis, MO, USA). The Topoisomerase II inhibitor ICRF-193 was purchased from Biomol (Plymouth Meeting, PA, USA).

Abbreviations

All units are abbreviated according to the International Unit System.

AA: amino acid
ATP: adenosine 5´-triphosphate
BSA: bovine serum albumin
CDK: Cyclin-dependent kinase
DAPI: 4´,6-diamidino-2-phenylindole
DTT: dithiothreitol
ECL: enhanced chemiluminescence
EDTA: ethylenedinitrilotetraacetic acid
ELISA: enzyme linked immunosorbent assay
FCS: fetal calf serum
GFP: green fluorescent protein
GST: glutathione S-transferase
HCl: hydrochloric acid
Ig: Immunglobulin
IP: immunoprecipitation
mAb: monoclonal antibody
Mad: mitotic arrest deficient
MBP: maltose binding protein
MS: mass spectrometry
ORF: open reading frame
PBD: Polo-box domain
PBS: phosphate-buffered saline
PCR: polymerase chain reaction
PFD: PICH family domain
PICH: Plk1 interacting checkpoint helicase
PIPES: 1,4-Piperazinediethanesulfonic acid
PMSF: phenylmethylsulfonyl fluoride
PTEMF: Pipes, Triton, EGTA, $MgCl_2$, Formaldehyde
RACE: rapid amplification of cDNA ends

RNA: ribonucleic acid

RT: room temperature

SDS-PAGE: sodium dodecylsulfate polyacrylamid gelelectrophoresis

SF: helicase superfamily

siRNA: small interference ribonucleic acid

SNF2: sucrose non-fermenting

T1063: threonine at position 1063

Topo: Topoisomerase

TPR: tetratricopeptide repeats

WT: wild-type

References

Abdel-Monem, M., Durwald, H. and Hoffmann-Berling, H. (1976) Enzymic unwinding of DNA. 2. Chain separation by an ATP-dependent DNA unwinding enzyme. *Eur J Biochem*, **65**, 441-449.

Abdel-Monem, M. and Hoffmann-Berling, H. (1976) Enzymic unwinding of DNA. 1. Purification and characterization of a DNA-dependent ATPase from Escherichia coli. *Eur J Biochem*, **65**, 431-440.

Abrieu, A., Kahana, J.A., Wood, K.W. and Cleveland, D.W. (2000) CENP-E as an essential component of the mitotic checkpoint in vitro. *Cell*, **102**, 817-826.

Acquaviva, C., Herzog, F., Kraft, C. and Pines, J. (2004) The anaphase promoting complex/cyclosome is recruited to centromeres by the spindle assembly checkpoint. *Nat Cell Biol*, **6**, 892-898.

Ahonen, L.J., Kallio, M.J., Daum, J.R., Bolton, M., Manke, I.A., Yaffe, M.B., Stukenberg, P.T. and Gorbsky, G.J. (2005) Polo-like kinase 1 creates the tension-sensing 3F3/2 phosphoepitope and modulates the association of spindle-checkpoint proteins at kinetochores. *Curr Biol*, **15**, 1078-1089.

Bachant, J., Alcasabas, A., Blat, Y., Kleckner, N. and Elledge, S.J. (2002) The SUMO-1 isopeptidase Smt4 is linked to centromeric cohesion through SUMO-1 modification of DNA topoisomerase II. *Mol Cell*, **9**, 1169-1182.

Barr, F.A., Sillje, H.H. and Nigg, E.A. (2004) Polo-like kinases and the orchestration of cell division. *Nat Rev Mol Cell Biol*, **5**, 429-440.

Becker, P.B. and Horz, W. (2002) ATP-dependent nucleosome remodeling. *Annu Rev Biochem*, **71**, 247-273.

Beerens, N., Hoeijmakers, J.H., Kanaar, R., Vermeulen, W. and Wyman, C. (2005) The CSB protein actively wraps DNA. *J Biol Chem*, **280**, 4722-4729.

Bharadwaj, R., Qi, W. and Yu, H. (2004) Identification of two novel components of the human NDC80 kinetochore complex. *J Biol Chem*, **279**, 13076-13085.

Cheeseman, I.M., Chappie, J.S., Wilson-Kubalek, E.M. and Desai, A. (2006) The conserved KMN network constitutes the core microtubule-binding site of the kinetochore. *Cell*, **127**, 983-997.

Cheeseman, I.M., Niessen, S., Anderson, S., Hyndman, F., Yates, J.R., 3rd, Oegema, K. and Desai, A. (2004) A conserved protein network controls assembly of the outer kinetochore and its ability to sustain tension. *Genes Dev*, **18**, 2255-2268.

Christensen, M.O., Larsen, M.K., Barthelmes, H.U., Hock, R., Andersen, C.L., Kjeldsen, E., Knudsen, B.R., Westergaard, O., Boege, F. and Mielke, C. (2002) Dynamics of human DNA topoisomerases IIalpha and IIbeta in living cells. *J Cell Biol*, **157**, 31-44.

Ciferri, C., De Luca, J., Monzani, S., Ferrari, K.J., Ristic, D., Wyman, C., Stark, H., Kilmartin, J., Salmon, E.D. and Musacchio, A. (2005) Architecture of the human ndc80-hec1 complex, a critical constituent of the outer kinetochore. *J Biol Chem*, **280**, 29088-29095.

Cleveland, D.W., Mao, Y. and Sullivan, K.F. (2003) Centromeres and kinetochores: from epigenetics to mitotic checkpoint signaling. *Cell*, **112**, 407-421.

Cozzarelli, N.R. (1980) DNA gyrase and the supercoiling of DNA. *Science*, **207**, 953-960.

DeAntoni, A., Sala, V. and Musacchio, A. (2005) Explaining the oligomerization properties of the spindle assembly checkpoint protein Mad2. *Philos Trans R Soc Lond B Biol Sci*, **360**, 637-647, discussion 447-638.

DeLuca, J.G., Dong, Y., Hergert, P., Strauss, J., Hickey, J.M., Salmon, E.D. and McEwen, B.F. (2005) Hec1 and nuf2 are core components of the

kinetochore outer plate essential for organizing microtubule attachment sites. *Mol Biol Cell*, **16**, 519-531.

Deluca, J.G., Gall, W.E., Ciferri, C., Cimini, D., Musacchio, A. and Salmon, E.D. (2006) Kinetochore microtubule dynamics and attachment stability are regulated by hec1. *Cell*, **127**, 969-982.

DeLuca, J.G., Howell, B.J., Canman, J.C., Hickey, J.M., Fang, G. and Salmon, E.D. (2003) Nuf2 and Hec1 are required for retention of the checkpoint proteins Mad1 and Mad2 to kinetochores. *Curr Biol*, **13**, 2103-2109.

Ditchfield, C., Johnson, V.L., Tighe, A., Ellston, R., Haworth, C., Johnson, T., Mortlock, A., Keen, N. and Taylor, S.S. (2003) Aurora B couples chromosome alignment with anaphase by targeting BubR1, Mad2, and Cenp-E to kinetochores. *J Cell Biol*, **161**, 267-280.

Downes, C.S., Mullinger, A.M. and Johnson, R.T. (1991) Inhibitors of DNA topoisomerase II prevent chromatid separation in mammalian cells but do not prevent exit from mitosis. *Proc Natl Acad Sci U S A*, **88**, 8895-8899.

Durr, H., Flaus, A., Owen-Hughes, T. and Hopfner, K.P. (2006) Snf2 family ATPases and DExx box helicases: differences and unifying concepts from high-resolution crystal structures. *Nucleic Acids Res*, **34**, 4160-4167.

Earnshaw, W.C., Halligan, B., Cooke, C.A., Heck, M.M. and Liu, L.F. (1985) Topoisomerase II is a structural component of mitotic chromosome scaffolds. *J Cell Biol*, **100**, 1706-1715.

Eisen, J.A., Sweder, K.S. and Hanawalt, P.C. (1995) Evolution of the SNF2 family of proteins: subfamilies with distinct sequences and functions. *Nucleic Acids Res*, **23**, 2715-2723.

Elbashir, S.M., Harborth, J., Lendeckel, W., Yalcin, A., Weber, K. and Tuschl, T. (2001) Duplexes of 21-nucleotide RNAs mediate RNA interference in cultured mammalian cells. *Nature*, **411**, 494-498.

Elia, A.E., Cantley, L.C. and Yaffe, M.B. (2003a) Proteomic screen finds pSer/pThr-binding domain localizing Plk1 to mitotic substrates. *Science*, **299**, 1228-1231.

Elia, A.E., Rellos, P., Haire, L.F., Chao, J.W., Ivins, F.J., Hoepker, K., Mohammad, D., Cantley, L.C., Smerdon, S.J. and Yaffe, M.B. (2003b) The molecular basis for phosphodependent substrate targeting and regulation of Plks by the Polo-box domain. *Cell*, **115**, 83-95.

Evan, G.I., Lewis, G.K., Ramsay, G. and Bishop, J.M. (1985) Isolation of monoclonal antibodies specific for human c-myc proto-oncogene product. *Mol Cell Biol*, **5**, 3610-3616.

Fabbro, M., Zhou, B.B., Takahashi, M., Sarcevic, B., Lal, P., Graham, M.E., Gabrielli, B.G., Robinson, P.J., Nigg, E.A., Ono, Y. and Khanna, K.K. (2005) Cdk1/Erk2- and Plk1-dependent phosphorylation of a centrosome protein, Cep55, is required for its recruitment to midbody and cytokinesis. *Dev Cell*, **9**, 477-488.

Fang, G., Yu, H. and Kirschner, M.W. (1998) The checkpoint protein MAD2 and the mitotic regulator CDC20 form a ternary complex with the anaphase-promoting complex to control anaphase initiation. *Genes Dev*, **12**, 1871-1883.

Flaus, A., Martin, D.M., Barton, G.J. and Owen-Hughes, T. (2006) Identification of multiple distinct Snf2 subfamilies with conserved structural motifs. *Nucleic Acids Res*, **34**, 2887-2905.

Floridia, G., Zatterale, A., Zuffardi, O. and Tyler-Smith, C. (2000) Mapping of a human centromere onto the DNA by topoisomerase II cleavage. *EMBO Rep*, **1**, 489-493.

Foltz, D.R., Jansen, L.E., Black, B.E., Bailey, A.O., Yates, J.R., 3rd and Cleveland, D.W. (2006) The human CENP-A centromeric nucleosome-associated complex. *Nat Cell Biol*, **8**, 458-469.

Gasser, S.M., Laroche, T., Falquet, J., Boy de la Tour, E. and Laemmli, U.K. (1986) Metaphase chromosome structure. Involvement of topoisomerase II. *J Mol Biol*, **188**, 613-629.

Gorbsky, G.J. (1994) Cell cycle progression and chromosome segregation in mammalian cells cultured in the presence of the topoisomerase II inhibitors ICRF-187 [(+)-1,2-bis(3,5-dioxopiperazinyl-1-yl)propane; ADR-529] and ICRF-159 (Razoxane). *Cancer Res*, **54**, 1042-1048.

Goto, H., Kiyono, T., Tomono, Y., Kawajiri, A., Urano, T., Furukawa, K., Nigg, E.A. and Inagaki, M. (2005) Complex formation of Plk1 and INCENP required for metaphase-anaphase transition. *Nat Cell Biol*.

Haering, C.H. and Nasmyth, K. (2003) Building and breaking bridges between sister chromatids. *Bioessays*, **25**, 1178-1191.

Hanisch, A., Wehner, A., Nigg, E.A. and Sillje, H.H. (2006) Different Plk1 Functions Show Distinct Dependencies on Polo-Box Domain-mediated Targeting. *Mol Biol Cell*, **17**, 448-459.

Hauf, S., Roitinger, E., Koch, B., Dittrich, C.M., Mechtler, K. and Peters, J.M. (2005) Dissociation of cohesin from chromosome arms and loss of arm cohesion during early mitosis depends on phosphorylation of SA2. *PLoS Biol*, **3**, e69.

Havas, K., Whitehouse, I. and Owen-Hughes, T. (2001) ATP-dependent chromatin remodeling activities. *Cell Mol Life Sci*, **58**, 673-682.

Hirano, T. (2000) Chromosome cohesion, condensation, and separation. *Annu Rev Biochem*, **69**, 115-144.

Holm, C., Goto, T., Wang, J.C. and Botstein, D. (1985) DNA topoisomerase II is required at the time of mitosis in yeast. *Cell*, **41**, 553-563.

Hoyt, M.A., Totis, L. and Roberts, B.T. (1991) S. cerevisiae genes required for cell cycle arrest in response to loss of microtubule function. *Cell*, **66**, 507-517.

Indjeian, V.B., Stern, B.M. and Murray, A.W. (2005) The centromeric protein Sgo1 is required to sense lack of tension on mitotic chromosomes. *Science*, **307**, 130-133.

Jang, Y.J., Lin, C.Y., Ma, S. and Erikson, R.L. (2002) Functional studies on the role of the C-terminal domain of mammalian polo-like kinase. *Proc Natl Acad Sci U S A*, **99**, 1984-1989.

Kang, Y.H., Park, J.E., Yu, L.R., Soung, N.K., Yun, S.M., Bang, J.K., Seong, Y.S., Yu, H., Garfield, S., Veenstra, T.D. and Lee, K.S. (2006) Self-regulated Plk1 recruitment to kinetochores by the Plk1-PBIP1 interaction is critical for proper chromosome segregation. *Mol Cell*, **24**, 409-422.

Kitajima, T.S., Sakuno, T., Ishiguro, K., Iemura, S., Natsume, T., Kawashima, S.A. and Watanabe, Y. (2006) Shugoshin collaborates with protein phosphatase 2A to protect cohesin. *Nature*, **441**, 46-52.

Klein, U.R., Nigg, E.A. and Gruneberg, U. (2006) Centromere targeting of the chromosomal passenger complex requires a ternary subcomplex of Borealin, Survivin, and the N-terminal domain of INCENP. *Mol Biol Cell*, **17**, 2547-2558.

Kohler, G. and Milstein, C. (1975) Continuous cultures of fused cells secreting antibody of predefined specificity. *Nature*, **256**, 495-497.

Kops, G.J., Kim, Y., Weaver, B.A., Mao, Y., McLeod, I., Yates, J.R., 3rd, Tagaya, M. and Cleveland, D.W. (2005a) ZW10 links mitotic checkpoint signaling to the structural kinetochore. *J Cell Biol*, **169**, 49-60.

Kops, G.J., Weaver, B.A. and Cleveland, D.W. (2005b) On the road to cancer: aneuploidy and the mitotic checkpoint. *Nat Rev Cancer*, **5**, 773-785.

Kozak, M. (1987) At least six nucleotides preceding the AUG initiator codon enhance translation in mammalian cells. *J Mol Biol*, **196**, 947-950.

Lamb, J.R., Tugendreich, S. and Hieter, P. (1995) Tetratrico peptide repeat interactions: to TPR or not to TPR? *Trends Biochem Sci*, **20**, 257-259.

Li, R. and Murray, A.W. (1991) Feedback control of mitosis in budding yeast. *Cell*, **66**, 519-531.

Li, X. and Nicklas, R.B. (1995) Mitotic forces control a cell-cycle checkpoint. *Nature*, **373**, 630-632.

Lia, G., Praly, E., Ferreira, H., Stockdale, C., Tse-Dinh, Y.C., Dunlap, D., Croquette, V., Bensimon, D. and Owen-Hughes, T. (2006) Direct observation of DNA distortion by the RSC complex. *Mol Cell*, **21**, 417-425.

Lin, Y.T., Chen, Y., Wu, G. and Lee, W.H. (2006) Hec1 sequentially recruits Zwint-1 and ZW10 to kinetochores for faithful chromosome segregation and spindle checkpoint control. *Oncogene*, **25**, 6901-6914.

Liu, R., Liu, H., Chen, X., Kirby, M., Brown, P.O. and Zhao, K. (2001) Regulation of CSF1 promoter by the SWI/SNF-like BAF complex. *Cell*, **106**, 309-318.

Losada, A., Hirano, M. and Hirano, T. (2002) Cohesin release is required for sister chromatid resolution, but not for condensin-mediated compaction, at the onset of mitosis. *Genes Dev*, **16**, 3004-3016.

Lowery, D.M., Lim, D. and Yaffe, M.B. (2005) Structure and function of Polo-like kinases. *Oncogene*, **24**, 248-259.

Maiato, H., DeLuca, J., Salmon, E.D. and Earnshaw, W.C. (2004) The dynamic kinetochore-microtubule interface. *J Cell Sci*, **117**, 5461-5477.

Mapelli, M., Filipp, F.V., Rancati, G., Massimiliano, L., Nezi, L., Stier, G., Hagan, R.S., Confalonieri, S., Piatti, S., Sattler, M. and Musacchio, A. (2006) Determinants of conformational dimerization of Mad2 and its inhibition by p31comet. *Embo J*, **25**, 1273-1284.

Martin-Lluesma, S., Stucke, V.M. and Nigg, E.A. (2002) Role of Hec1 in spindle checkpoint signaling and kinetochore recruitment of Mad1/Mad2. *Science*, **297**, 2267-2270.

McCleland, M.L., Gardner, R.D., Kallio, M.J., Daum, J.R., Gorbsky, G.J., Burke, D.J. and Stukenberg, P.T. (2003) The highly conserved Ndc80 complex is required for kinetochore assembly, chromosome congression, and spindle checkpoint activity. *Genes Dev*, **17**, 101-114.

McCleland, M.L., Kallio, M.J., Barrett-Wilt, G.A., Kestner, C.A., Shabanowitz, J., Hunt, D.F., Gorbsky, G.J. and Stukenberg, P.T. (2004) The vertebrate Ndc80 complex contains Spc24 and Spc25 homologs, which are required to establish and maintain kinetochore-microtubule attachment. *Curr Biol*, **14**, 131-137.

McGuinness, B.E., Hirota, T., Kudo, N.R., Peters, J.M. and Nasmyth, K. (2005) Shugoshin prevents dissociation of cohesin from centromeres during mitosis in vertebrate cells. *PLoS Biol*, **3**, e86.

Musacchio, A. and Hardwick, K.G. (2002) The spindle checkpoint: structural insights into dynamic signalling. *Nat Rev Mol Cell Biol*, **3**, 731-741.

Neef, R., Preisinger, C., Sutcliffe, J., Kopajtich, R., Nigg, E.A., Mayer, T.U. and Barr, F.A. (2003) Phosphorylation of mitotic kinesin-like protein 2 by polo-like kinase 1 is required for cytokinesis. *J Cell Biol*, **162**, 863-875.

Nicklas, R.B., Ward, S.C. and Gorbsky, G.J. (1995) Kinetochore chemistry is sensitive to tension and may link mitotic forces to a cell cycle checkpoint. *J Cell Biol*, **130**, 929-939.

Nigg, E.A. (2001) Mitotic kinases as regulators of cell division and its checkpoints. *Nat Rev Mol Cell Biol*, **2**, 21-32.

Nishino, M., Kurasawa, Y., Evans, R., Lin, S.H., Brinkley, B.R. and Yu-Lee, L.Y. (2006) NudC is required for Plk1 targeting to the kinetochore and chromosome congression. *Curr Biol*, **16**, 1414-1421.

Owen-Hughes, T. (2006) The role of Snf2-related proteins in cancer. *Ernst Schering Res Found Workshop*, 47-59.

Passmore, L.A., Booth, C.R., Venien-Bryan, C., Ludtke, S.J., Fioretto, C., Johnson, L.N., Chiu, W. and Barford, D. (2005) Structural analysis of the anaphase-promoting complex reveals multiple active sites and insights into polyubiquitylation. *Mol Cell*, **20**, 855-866.

Peters, J.M. (2002) The anaphase-promoting complex: proteolysis in mitosis and beyond. *Mol Cell*, **9**, 931-943.

Pines, J. (2006) Mitosis: a matter of getting rid of the right protein at the right time. *Trends Cell Biol*, **16**, 55-63.

Pinsky, B.A. and Biggins, S. (2005) The spindle checkpoint: tension versus attachment. *Trends Cell Biol*, **15**, 486-493.

Qi, W., Tang, Z. and Yu, H. (2006) Phosphorylation- and polo-box-dependent binding of Plk1 to Bub1 is required for the kinetochore localization of Plk1. *Mol Biol Cell*, **17**, 3705-3716.

Rattner, J.B., Hendzel, M.J., Furbee, C.S., Muller, M.T. and Bazett-Jones, D.P. (1996) Topoisomerase II alpha is associated with the mammalian centromere in a cell cycle- and species-specific manner and is required for proper centromere/kinetochore structure. *J Cell Biol*, **134**, 1097-1107.

Rauh, N.R., Schmidt, A., Bormann, J., Nigg, E.A. and Mayer, T.U. (2005) Calcium triggers exit from meiosis II by targeting the APC/C inhibitor XErp1 for degradation. *Nature*, **437**, 1048-1052.

Riedel, C.G., Katis, V.L., Katou, Y., Mori, S., Itoh, T., Helmhart, W., Galova, M., Petronczki, M., Gregan, J., Cetin, B., Mudrak, I., Ogris, E., Mechtler, K.,

Pelletier, L., Buchholz, F., Shirahige, K. and Nasmyth, K. (2006) Protein phosphatase 2A protects centromeric sister chromatid cohesion during meiosis I. *Nature*, **441**, 53-61.

Rieder, C.L., Cole, R.W., Khodjakov, A. and Sluder, G. (1995) The checkpoint delaying anaphase in response to chromosome monoorientation is mediated by an inhibitory signal produced by unattached kinetochores. *J Cell Biol*, **130**, 941-948.

Rieder, C.L., Schultz, A., Cole, R. and Sluder, G. (1994) Anaphase onset in vertebrate somatic cells is controlled by a checkpoint that monitors sister kinetochore attachment to the spindle. *J Cell Biol*, **127**, 1301-1310.

Saha, A., Wittmeyer, J. and Cairns, B.R. (2002) Chromatin remodeling by RSC involves ATP-dependent DNA translocation. *Genes Dev*, **16**, 2120-2134.

Salic, A., Waters, J.C. and Mitchison, T.J. (2004) Vertebrate shugoshin links sister centromere cohesion and kinetochore microtubule stability in mitosis. *Cell*, **118**, 567-578.

Sandall, S., Severin, F., McLeod, I.X., Yates, J.R., 3rd, Oegema, K., Hyman, A. and Desai, A. (2006) A Bir1-Sli15 complex connects centromeres to microtubules and is required to sense kinetochore tension. *Cell*, **127**, 1179-1191.

Seong, Y.S., Kamijo, K., Lee, J.S., Fernandez, E., Kuriyama, R., Miki, T. and Lee, K.S. (2002) A spindle checkpoint arrest and a cytokinesis failure by the dominant-negative polo-box domain of Plk1 in U-2 OS cells. *J Biol Chem*, **277**, 32282-32293.

Shamu, C.E. and Murray, A.W. (1992) Sister chromatid separation in frog egg extracts requires DNA topoisomerase II activity during anaphase. *J Cell Biol*, **117**, 921-934.

Shiratori, A., Shibata, T., Arisawa, M., Hanaoka, F., Murakami, Y. and Eki, T. (1999) Systematic identification, classification, and characterization of the open reading frames which encode novel helicase-related proteins in Saccharomyces cerevisiae by gene disruption and Northern analysis. *Yeast*, **15**, 219-253.

Sillje, H.H., Nagel, S., Korner, R. and Nigg, E.A. (2006) HURP is a Ran-importin beta-regulated protein that stabilizes kinetochore microtubules in the vicinity of chromosomes. *Curr Biol*, **16**, 731-742.

Singleton, M.R. and Wigley, D.B. (2002) Modularity and specialization in superfamily 1 and 2 helicases. *J Bacteriol*, **184**, 1819-1826.

Singleton, M.R. and Wigley, D.B. (2003) Multiple roles for ATP hydrolysis in nucleic acid modifying enzymes. *Embo J*, **22**, 4579-4583.

Skoufias, D.A., Lacroix, F.B., Andreassen, P.R., Wilson, L. and Margolis, R.L. (2004) Inhibition of DNA decatenation, but not DNA damage, arrests cells at metaphase. *Mol Cell*, **15**, 977-990.

Spence, J.M., Critcher, R., Ebersole, T.A., Valdivia, M.M., Earnshaw, W.C., Fukagawa, T. and Farr, C.J. (2002) Co-localization of centromere activity, proteins and topoisomerase II within a subdomain of the major human X alpha-satellite array. *Embo J*, **21**, 5269-5280.

Starr, D.A., Saffery, R., Li, Z., Simpson, A.E., Choo, K.H., Yen, T.J. and Goldberg, M.L. (2000) HZwint-1, a novel human kinetochore component that interacts with HZW10. *J Cell Sci*, **113 (Pt 11)**, 1939-1950.

Stern, B.M. and Murray, A.W. (2001) Lack of tension at kinetochores activates the spindle checkpoint in budding yeast. *Curr Biol*, **11**, 1462-1467.

Stucke, V.M., Baumann, C. and Nigg, E.A. (2004) Kinetochore localization and microtubule interaction of the human spindle checkpoint kinase Mps1. *Chromosoma*, **113**, 1-15.

Stucke, V.M., Sillje, H.H., Arnaud, L. and Nigg, E.A. (2002) Human Mps1 kinase is required for the spindle assembly checkpoint but not for centrosome duplication. *Embo J*, **21**, 1723-1732.

Subramanya, H.S., Bird, L.E., Brannigan, J.A. and Wigley, D.B. (1996) Crystal structure of a DExx box DNA helicase. *Nature*, **384**, 379-383.

Sullivan, B.A. and Karpen, G.H. (2004) Centromeric chromatin exhibits a histone modification pattern that is distinct from both euchromatin and heterochromatin. *Nat Struct Mol Biol*, **11**, 1076-1083.

Sullivan, M., Higuchi, T., Katis, V.L. and Uhlmann, F. (2004) Cdc14 phosphatase induces rDNA condensation and resolves cohesin-independent cohesion during budding yeast anaphase. *Cell*, **117**, 471-482.

Sumara, I., Vorlaufer, E., Stukenberg, P.T., Kelm, O., Redemann, N., Nigg, E.A. and Peters, J.M. (2002) The dissociation of cohesin from chromosomes in prophase is regulated by Polo-like kinase. *Mol Cell*, **9**, 515-525.

Svejstrup, J.Q. (2003) Rescue of arrested RNA polymerase II complexes. *J Cell Sci*, **116**, 447-451.

Taagepera, S., Rao, P.N., Drake, F.H. and Gorbsky, G.J. (1993) DNA topoisomerase II alpha is the major chromosome protein recognized by the mitotic phosphoprotein antibody MPM-2. *Proc Natl Acad Sci U S A*, **90**, 8407-8411.

Tang, Z., Shu, H., Oncel, D., Chen, S. and Yu, H. (2004) Phosphorylation of Cdc20 by Bub1 provides a catalytic mechanism for APC/C inhibition by the spindle checkpoint. *Mol Cell*, **16**, 387-397.

Tang, Z., Shu, H., Qi, W., Mahmood, N.A., Mumby, M.C. and Yu, H. (2006) PP2A Is Required for Centromeric Localization of Sgo1 and Proper Chromosome Segregation. *Dev Cell*, **10**, 575-585.

Terret, M.E., Wassmann, K., Waizenegger, I., Maro, B., Peters, J.M. and Verlhac, M.H. (2003) The meiosis I-to-meiosis II transition in mouse oocytes requires separase activity. *Curr Biol*, **13**, 1797-1802.

Toyoda, Y. and Yanagida, M. (2006) Coordinated requirements of human topo II and cohesin for metaphase centromere alignment under Mad2-dependent spindle checkpoint surveillance. *Mol Biol Cell*, **17**, 2287-2302.

Twomey, C., Wattam, S.L., Pillai, M.R., Rapley, J., Baxter, J.E. and Fry, A.M. (2004) Nek2B stimulates zygotic centrosome assembly in Xenopus laevis in a kinase-independent manner. *Dev Biol*, **265**, 384-398.

Uemura, T., Ohkura, H., Adachi, Y., Morino, K., Shiozaki, K. and Yanagida, M. (1987) DNA topoisomerase II is required for condensation and separation of mitotic chromosomes in S. pombe. *Cell*, **50**, 917-925.

Uhlmann, F., Wernic, D., Poupart, M.A., Koonin, E.V. and Nasmyth, K. (2000) Cleavage of cohesin by the CD clan protease separin triggers anaphase in yeast. *Cell*, **103**, 375-386.

Vagnarelli, P. and Earnshaw, W.C. (2004) Chromosomal passengers: the four-dimensional regulation of mitotic events. *Chromosoma*, **113**, 211-222.

Vagnarelli, P., Morrison, C., Dodson, H., Sonoda, E., Takeda, S. and Earnshaw, W.C. (2004) Analysis of Scc1-deficient cells defines a key metaphase role of vertebrate cohesin in linking sister kinetochores. *EMBO Rep*, **5**, 167-171.

Vigneron, S., Prieto, S., Bernis, C., Labbe, J.C., Castro, A. and Lorca, T. (2004) Kinetochore localization of spindle checkpoint proteins: who controls whom? *Mol Biol Cell*, **15**, 4584-4596.

Vos, L.J., Famulski, J.K. and Chan, G.K. (2006) How to build a centromere: from centromeric and pericentromeric chromatin to kinetochore assembly. *Biochem Cell Biol*, **84**, 619-639.

Wassmann, K., Liberal, V. and Benezra, R. (2003) Mad2 phosphorylation regulates its association with Mad1 and the APC/C. *Embo J*, **22**, 797-806.

Wei, R.R., Al-Bassam, J. and Harrison, S.C. (2007) The Ndc80/HEC1 complex is a contact point for kinetochore-microtubule attachment. *Nat Struct Mol Biol*, **14**, 54-59.

Wei, R.R., Sorger, P.K. and Harrison, S.C. (2005) Molecular organization of the Ndc80 complex, an essential kinetochore component. *Proc Natl Acad Sci U S A*, **102**, 5363-5367.

Xia, G., Luo, X., Habu, T., Rizo, J., Matsumoto, T. and Yu, H. (2004) Conformation-specific binding of p31(comet) antagonizes the function of Mad2 in the spindle checkpoint. *Embo J*, **23**, 3133-3143.

Yamaguchi, T., Goto, H., Yokoyama, T., Sillje, H., Hanisch, A., Uldschmid, A., Takai, Y., Oguri, T., Nigg, E.A. and Inagaki, M. (2005) Phosphorylation by Cdk1 induces Plk1-mediated vimentin phosphorylation during mitosis. *J Cell Biol*, **171**, 431-436.

Yanagida, M. (1995) Frontier questions about sister chromatid separation in anaphase. *Bioessays*, **17**, 519-526.

Yu, H. (2006) Structural activation of Mad2 in the mitotic spindle checkpoint: the two-state Mad2 model versus the Mad2 template model. *J Cell Biol*, **173**, 153-157.

Zhang, Y., Smith, C.L., Saha, A., Grill, S.W., Mihardja, S., Smith, S.B., Cairns, B.R., Peterson, C.L. and Bustamante, C. (2006) DNA translocation and loop formation mechanism of chromatin remodeling by SWI/SNF and RSC. *Mol Cell*, **24**, 559-568.

Publications

Parts of this study are published in

Baumann, C., Korner, R., Hofmann, K. and Nigg, E.A. (2007) PICH, a Centromere-Associated SNF2 Family ATPase, Is Regulated by Plk1 and Required for the Spindle Checkpoint. *Cell*, **128**, 101-114.

Stucke, V.M., **Baumann, C.** and Nigg, E.A. (2004) Kinetochore localization and microtubule interaction of the human spindle checkpoint kinase Mps1. *Chromosoma*, **113**, 1-15.

Posters

ELSO meeting in Dresden (2005): **Baumann, C**. and Nigg, E.A. A role for Nuf2 at the kinetochore.

Oral presentation

Cold Spring Harbour Meeting “Cell Cycle” (2006): A centromeric ATPase is regulated by Plk1 and required for the spindle checkpoint.

Awards

Max-Planck Institute of Biochemistry (MPIB) junior research award 2007

Curriculum Vitae

Christoph Baumann
Date and place of birth: 29.01.76, Augsburg

Education

12/02 – 12/06 **PhD thesis** in the Department of Cell Biology at the Max-Planck Institute (MPI) of Biochemistry in Munich. Title: “PICH, a centromere-associated SNF2 family ATPase is regulated by Plk1 and required for the spindle checkpoint.” Supervisor: Prof. Erich Nigg.

08/02 – 11/02 **Internship** at the Institute for Molecular Biology and Tumor Research Marburg (IMT). Investigation of shuttling and RNA-binding proteins in budding yeast (supervisor: Dr Heike Krebber).

05/02 – 07/02 **Internship** at the MPI for Terrestrial Microbiology in Marburg. Sumoylation and ubiquitination of the yeast proteins POL30 and SRS2 (supervisor: Prof. Regine Kahmann).

08/01 – 04/02 **Diploma thesis** in the Department of Microbiology and Immunology, University of California, San Francisco, Title: “Proteins that bind to the switch region Sμ.” Supervisor: Prof. Matthias Wabl.

09/96 – 07/01 **Study in Biology** at the Ludwig–Maximilians University of Munich (LMU), with major in Genetics, Human Genetics, Biochemistry and Molecular Biology.

08/95 – 08/96 **Alternative Community Service** at the Welfare Centre Herrenbach, Augsburg.

09/85 – 06/95 **High School** St.Stephan, Augsburg.

Relevant Work Experience

12/02 – 12/06 **PhD thesis** at the MPI Munich: methods of cell biology and biochemistry to analyze the role of several proteins in human mitosis: microscopy (confocal and deconvolution, live cell imaging), human tissue culture, transient transfections, siRNA/shRNA, immunoprecipitation, immunofluorescence, (far) western blotting, cloning, site directed mutagenesis, protein purification from insect cells and bacteria, yeast-2-hybrid library screens and directed interaction screening, sample preparation for mass spectrometry (LC-MS/MS), radioactive work (P32 and S35); data processing with Adobe Photoshop, Illustrator and Acrobat; Excel, Word, Access, Clonemanager/SEcentral, softworx and metamorph.

08/02 – 11/02 **Practical work** at the IMT Marburg, lab of Dr. Krebber: microscopy, immunofluorescence analysis, RNA export assay, recombinant yeast work.

05/02 – 07/02 **Internship** at the MPI for Terrestrial Microbiology, Marburg: methods of protein purification in yeast, western blot, immunoprecipitation, tetrad dissection, Biacore 1st level course with certificate, FACS analysis.

08/01 – 05/02 **Diploma thesis**: yeast-one-hybrid assay with the human and murine immunoglobulin switch region Sμ; amplification (PCR, M13 phage DNA isolation) and cloning of the murine and human bait sequence, multiple screening with three cDNA libraries, and sequence analysis.

03/00 – 09/00 **Practical work** in the lab of Prof. Muskhelishvili, Institute of Genetics, LMU Munich: study of transcriptional regulation of the E. coli gyrB promoter (lacZ assays, primer extensions, DNA footprints).

05/98 – 08/99 **Practical work** in the lab of Prof. Svante Pääbo, Institute of Zoology, LMU Munich: comparative sequence analysis of human and primate chromosome regions (DNA purification, PCR techniques, shotgun sequencing and sequence analysis).

08/96 – 10/96 **Practical work** at the Analytisch-Biologisches Forschungslabor, Munich. Screening for nicotine and cotinine derivates from hair and urine probes of smokers and non-smokers.